INVESTIGATION OF INTEGRATED CONTROL OF ARTICULATED HEAVY VEHICLE USING SCALED MULTI-BODY DYNAMIC MODEL

BY

Mohamed Magdy Ibrahim Hafez

A thesis submitted to the College of Engineering and Physical Sciences of the University of Birmingham for the degree of DOCTOR OF PHILOSOPHY

Department of Mechanical Engineering

School of Engineering

College of Engineering and Physical Sciences

University of Birmingham

September 2020

ABSTRACT

Heavy vehicle handling control systems have proven to be an efficient way of reducing road accidents and improving road traffic safety. Testing these control systems on heavy vehicles can be expensive and unsafe. Meanwhile, the scaled model has proven a secure and inexpensive way of designing and deploying vehicle dynamics control. However, the scaled model's mathematical modelling has been mainly limited to the bicycle model, reducing the scope of exploring the handling dynamics. This study presents an innovative way of modelling a scaled tractor semi-trailer using multi-body dynamics software and testing control systems through co-simulation to help develop new control systems safely and inexpensively for improving road traffic safety. In this research, modelling the scaled model of an articulated vehicle was simulated on MSC ADAMS/View, which extends the mathematical model to 168 degrees of freedom. A 1/14 physical model was used to validate the simulation model and co-simulation has been established between MSC ADAMS/View and MATLAB to investigate the control of a scaled model built on MSC ADAMS/View with a developed control system built on MATLAB/Simulink.

The scaled model is a 1/14 Scania R620 articulated lorry manufactured by TAMIYA. Different parameters of the scaled model have been measured and used as inputs to the simulation model. MSC ADAMS/View was used to model the vehicle and to capture its response. The results were validated through physical tests, so a microcontroller was added to the physical model with different accelerometers to control and record the vehicle's motion instead of the existing radio control. Co-simulation has been implemented using two different control schemes, which have been built and compared against each other. The first control scheme is the electronic stability control system only. The second one is an integrated control system which combines

the active front steering with the electronic stability control scheme. The main target of the developed control systems is to stabilise the vehicle through manoeuvres using the Fuzzy logic methodology.

The study's main findings are that the experimental results show reasonable similarity to the simulation results, although there are minor differences. The physical validation of the simulation model indicates that it is possible to model a scaled model using multi-body dynamics software with specific considerations. Also, the results give a good understanding of the performance of heavy vehicles. Finally, using the co-simulation implemented using two different control schemes proves that the control can be developed using the scaled model. The proposed control method has been shown to be useful in developing the stability of the vehicle. It enhances the yaw rate for both tractor-trailer by around 25% and the lateral acceleration by around 20% at manoeuvres. Also, the control can be tuned easily using MATLAB. Meanwhile, the electronic stability control scheme gives better performance than the combined active front steering and electronic stability control scheme.

Acknowledgement

I would like to thank Allah for enlightening my way throughout my research. Also, I would like to show my deepest gratitude, honour and appreciation to **Dr Oluremi Olatunbosun** for his guidance, assistance and encouragement throughout this study. I am lucky to be supervised by him. He is a great adviser and is so patient in showing me the right way and widening my research through various aspects—besides **Dr Marco Castellani** and **Prof. Karl Dearn** for their helpful comments, encouragement and support.

Special thanks and appreciation are dedicated to my wife, **Mrs Hager Abdelshafy,** for her patience, care and support.

I am deeply grateful to my family, especially my parents, **Magda Sanan** and **Magdy Hafez**, and my brother **Mostafa** and my Sisters **Mona** and **Marwa**, for their support.

Furthermore, I could not ignore the potential effort of the technicians, **MR. Suyil Miah, Mr Lee Gauntlett, Mr peter Thornton, Mr Mark Wager, Mr Kevan Charlesworth, Mr Jack Garrod** for their generous help in finishing my experimental work.

Many thanks to **Eng Eslam Rizk** for his advice through working on MSC ADAMS, **Dr Tamer el Sayed** and **Eng Abdallah Aly** for their support when I had some problems dealing with the Arduino. Moreover, thanks to **Dr Wael Saber** and **Dr Mahmoud Omar** for having fruitful discussions with them and their guidance to choose the appropriate control system. Furthermore, **Dr Ramy Abdallah, Dr Hamad Eldhufairi, Dr Harith Alayoobi and Dr Mohamed Elsherif** helped me test the scaled model at the tennis court and parking area.

Many thanks to **Eng Ali Muhammad Ali** for his videos in productivity and management on his YouTube channel.

Many thanks to **Dr Ahmed Eltaweel** for his intensive support, encouragement, time, effort and advice.

Many thanks to **Prof Ibrahim Musad,** who provide me with information about non-linear models.

Also, I would like to thank my friends, **Dr Mohamed Noshy, Dr Said Elshayeb, Dr Abdullah Alqahtani, Dr Anam Hashmi, Kamil Hashmi, Dr Ali Abdelhafeez, Dr Tawfik Badawy, Dr Raya Eldadah, Dr Hassan Hemida, Prof Moataz Attallah, Dr Mohamed Ali, Dr Ahmed Wael.**

Finally, I am deeply grateful to my country Egypt, especially my engineering faculty at Mattaria, Helwan University, who funded my study.

Table of contents

Contents

List of Figures

list of Tables

Nomenclature

Abbreviations	Description
CAPMAS	Central Agency for Public Mobilisation and Statistics
UK	United Kingdom
GVA	Gross Value Added
US	United States
UNECE	United Nations Economic Commission for Europe
RC	Radio-Controlled
IMU	Inertial Measurement Unit
ESC	Electronic Stability Control
AFS	Active Front Steering
TCS	Traction Control System
ESP	Electronic Stability Programme
EHB	Electrohydraulic Brake System
EMB	Electromechanical Brake System
PD	Proportional derivative
PI	Proportional integration
PID	Proportional integration derivative
ADAS	The advanced driving assistance system

Chapter 1: Introduction

1.1 Background

Currently, automobiles are significant in the transportation sector and play a vital role in the world's economy. Thus, this industry has been one of the most important areas of investments for different companies worldwide. Although the automotive sector is beneficial for companies, it has undesirable effects on societies, such as environmental pollution and road accidents. Therefore, there is a significant need for companies and organisations to solve these problems by researching.

One of these problems is road accidents. About 54 million people were seriously injured in road accidents in 2013, according to the global mortality cause report [1] and 1.4 million people deaths in that year. The low-income countries have the highest percentage of road accidents per capita, especially in Africa (24.1 per 100,000 people)[2]. In Egypt, which is in the northeast of Africa, road accidents resulted in many losses. According to the report published in 2014 from the Egyptian Central Agency for Public Mobilisation and Statistics (CAPMAS), the annual rate of death of people per 100,000 vehicles was 71.4 persons while the number of injuries per day was 66.2 persons. The percentage of the contribution of heavy vehicles to these accidents was 27.9%[3].

The percentage contribution of heavy vehicles to road accidents in the United Kingdom (UK) is 20%[4]. Furthermore, looking from the economic perspective, the UK automotive sector is key to the UK economy and a crucial part of UK industrial policy. It produced £14.5 billion in Gross Value Added (GVA) in 2016 (0.8 per cent of total UK GVA)[5], which

emphasises the importance of running the vehicles in a safe condition. Thus, there is a need to study and research vehicle motion and its relation to road accidents.

Commercial vehicles dynamics have been divided into three main research areas. The first one is the deployment of the powertrain in the active safety system to control the vehicle dynamics. It concentrates on the engine and driveline and how it can help achieve stability of the vehicle, such as integrating the Traction control system with the Anti-lock brake system to achieve whole vehicle stability through turns. The second area focuses on ride behaviour and riding comfort for the driver and passengers and safely transporting goods. The third one is handling, which is the main area concerned with studying stability and avoiding road accidents[6]. The primary target is to reduce the number of road accidents involving heavy vehicles. This study focuses on heavy vehicle handling and safety.

Studying handling can be divided into two different categories; the whole vehicle or vehicle sub-systems. Scientific journals have published many papers on modelling heavy vehicles sub-systems and their effect on actual vehicle dynamics. These papers aim to achieve better performance by redesigning these sub-systems in different ways and using various control methods to enhance vehicle performance. It is essential to identify the purpose of the model while modelling the whole vehicle. Some researchers predict the vehicle's performance by modelling sub-systems alone, as these sub-systems need to be modelled and tested separately, then the results placed in the whole vehicle model.

It is a challenge for a researcher to model all the internal and external parameters in one model. However, by doing so, the designing of a robust control will become more achievable. Due to the high cost of experimental work, researchers develop computer programs to help them with modelling and virtual testing of the vehicle, especially for any newly invented

system. It allows them to define the characteristics of the vehicle and its motion before any prototype is built. Furthermore, the development in electronics and control systems has been used in vehicle dynamics, which controls many systems.

The most common types of heavy vehicle accidents are the Roll-over, Jack-Knifing, and Trailer -Swing. A study by K. Rumar about United States (US) and UK road accidents states that more than 50% of road accidents are caused by human factors[7]; also, he stated that the other elements are the vehicle itself and the roadway. Human behaviour is the highest cause of these accidents; many researchers nowadays try to overcome driver mistakes by developing new systems to control vehicle motion. For example; The United Nations Economic Commission for Europe (UNECE) endorsed that all commercial vehicles and coaches must be provided with autonomous emergency braking[8]. This system that is fitted to the truck operates the brakes in place of the driver if the system detects a possible collision and the driver does not press the brake pedal at the right time.

Vehicle handling dynamics is an essential aspect determining how the vehicle responds to the driver on the road; it can also provide a good understanding of each sub-system separately and interact with the other sub-systems. The development that has taken place in the previous years, most of the passive systems in the vehicle have been changed to active systems. So, these passive systems can be controlled to enhance the handling of the vehicle. Nowadays, control systems have been developed to eliminate or reduce the tractor semi-trailer Roll-over and Jack-Knifing occurrence.

Using the study of vehicle dynamics to develop new control systems requires testing these systems before launching them. There are several ways to test new systems; one of these ways is a simulation. However, the problem in simulation is the validation of the mathematical

model that is used in it. Unfortunately, validating the control in a full vehicle model through physical testing requires many safety considerations, and it is costly. Thus, a relatively inexpensive and safe way to create, develop and test heavy vehicles control systems is required.

The scaled model has proved a useful way of predicting the Full-scale model handling dynamics[9]. Most researchers have used the Buckingham Theorem [10] to correlate the full and scaled model dynamics. They also used scaled models to develop control methods. Most scaled models studies were on passenger cars, but trucks or tractor semi-trailer have been used [11]. Tuning and developing the control systems may need changes in the design parameters and operating conditions because commercial vehicles work with different trailers configurations and different loading conditions. Therefore, it is necessary to develop a simulating scaled model of a tractor semi-trailer using a multi-body dynamics programme and control systems to study the effects of changing the different design parameters and operating conditions.

MSC ADAMS is one of the multi-body dynamic programmes that facilitate modelling and simulating the motions of vehicles. MSC ADAMS has different packages such as ADAMS/car, ADAMS/truck that models various vehicle types. Also, it separates motions (ride and handling) in most operating conditions. Moreover, it allows for running control over the system. It gives the effect of a particular action (forces and moments) in terms of the reaction (displacement, velocity, and acceleration) on various parts of the vehicle and the vehicle sub-systems. However, simulating a scaled model using multi-body dynamics software and controlling it have not been addressed before. Thus, using MSC ADAMS in simulating a scaled model and controlling it need to be examined.

1.2 Aims and objectives

1.2.1 Overall aim

The main aim of this research is to determine the fidelity of modelling a scaled model of a tractor semi-trailer using multi-body dynamics software and applying it in developing a control system for enhancing heavy vehicle stability by co-simulation of vehicle dynamics **model** and control system. Figure 1-1 shows a schematic of the complete process of using a scaled model to develop vehicle dynamics control systems for a heavy vehicle. The research concentrates on the dashed area's part and the impact of vehicle operating conditions on tuning the control systems.

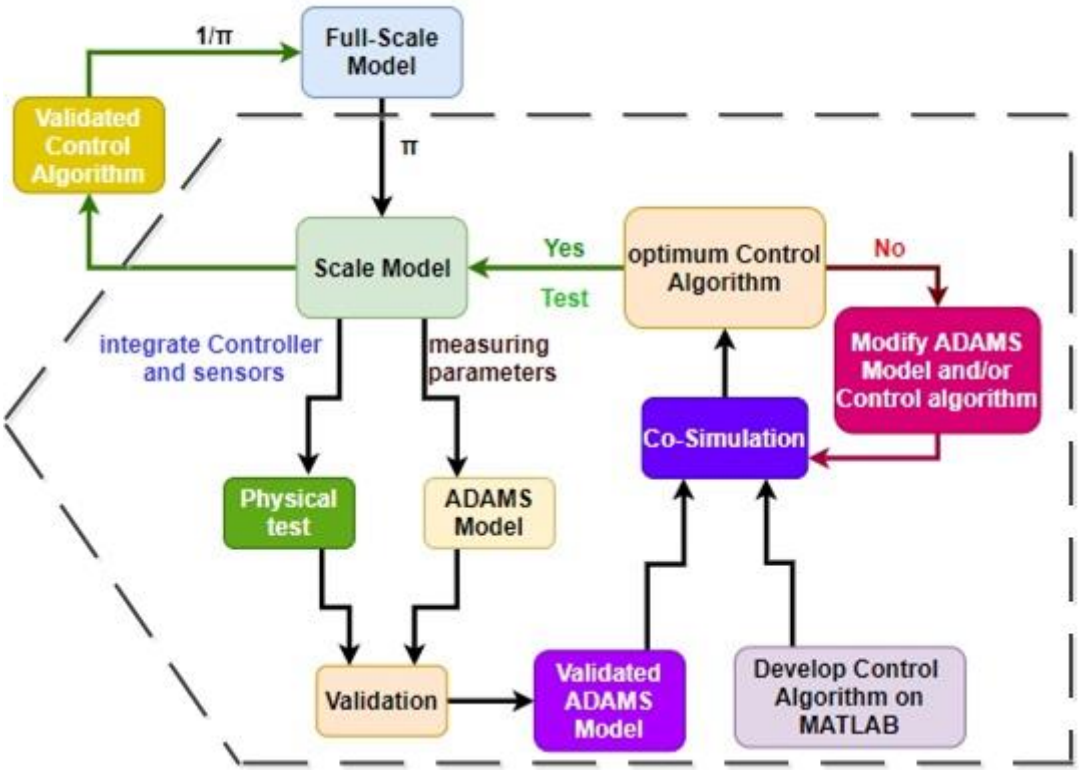

Figure 1-1: Whole system composition

1.2.2 Objectives

The main objectives that allow the aim of the study to be achieved can be summarised through the following points:

- Study heavy vehicle dynamics using a scaled model by developing a detailed, complete vehicle handling model of a 1/14 scaled model of a tractor semi-trailer using computer software (MSC ADAMS/View) and validate that model experimentally.
- Develop a new control system that can be used for stabilising the vehicle through maneuverers.
- Investigate the performance of heavy vehicle scaled model handling dynamics when it is equipped with control systems through co-simulation of the vehicle dynamics model and the control system.
- Investigate the performance of newly introduced integrated control systems to merge chassis control systems.

1.3 Scope and limitations

A scaled tractor semi-trailer with six axles is modelled with a rigid frame and passive suspension system on MSC ADAMS/View. The physical 1/14 Radio-Controlled (RC) model is modified and programmed to move autonomously and perform specific tests to validate the simulation model. An Inertial Measurement Unit (IMU) is installed with a microcontroller to record the vehicle's six degrees of freedom motion to be used for the validation. Furthermore, two control algorithms (electronic stability control, integrated control) are developed in MATLAB/Simulink and compared to explore its fidelity and enhance the scaled model's stability, primarily through manoeuvres.

The following assumptions have been considered to simplify the modelling technique in the present thesis:

- The effects of aerodynamic resistance are ignored as the vehicle moves at low speed, so there is no effect of aerodynamic forces on the vehicle.
- The engine and driveline are not simulated as the vehicle's motion is effected through torque applied on the tractor rear axle hub. The engine and driveline's absence is because adding an electric motor to the scaled model will increase the mathematical model's degrees of freedom. The study focuses on handling behaviour, not the performance from the vehicle powertrain or even the output torque coming from the engine, so putting a torque at the wheel's hub instead of the whole engine and driveline system will be more suitable.
- The braking system is not simulated, and the brake torque is implemented as a negative torque applied to the vehicle at the wheels. Since the scaled model has no brake system, putting a brake torque at wheels will be more effective than building tiny parts to represent the brake system and increasing the degrees of freedom of the mathematical model.
- The vehicle tyres stay in contact with the road surface profile. Meanwhile, the road surface used is a smooth road, so this will not generate any force that will push the tyre out of the road profile through the whole simulation.
- The engine's effects, power line vibrations, and tyres unbalance on the vehicle handling are neglected as the scaled model's frequency is low due to low speed.

1.4 Thesis outline

The thesis consists of six chapters, and the chapters are divided as follows:

Chapter 1: Introduction

Chapter1 is an Introduction about the study background illustrating the main objectives and limitations.

Chapter 2 reviews the previously published works on vehicle handling dynamics relevant to this research and an overall discussion of state of the art in subject.

Chapter 3 introduces the simulation of the 1/14 scaled tractor semi-trailer model and how the model is validated.

Chapter 4 develops the equations of motion for the reference model while applying the electronic stability control with the Fuzzy control methodology and presents the results and discussion from the Fuzzy control of electronic stability control (ESC) and the effect of load changing.

Chapter 5 presents the active front steering system (AFS) and the integration of the electronic stability control (ESC) with the active front steering (AFS) using the Fuzzy control methodology and compares it with electronic stability control (ESC).

Chapter 6 summarises the present study's findings, presents the conclusion that was reached, and provides suggestions for future work.

Chapter 2: Literature review

2.1 Introduction

Studying vehicle dynamics and developing new control systems requires testing those vehicles to investigate the actual performance and verify any newly developed method. Testing physical systems, heavy vehicles, entails high safety precautions; free test road, qualified driver, fitting large stabiliser mechanisms to avoid roll-over, etc. Also, there is a need to provide the vehicle with different sensors and actuators to test and measure the heavy vehicles' performance with the newly developed systems. Moreover, the newly developed system requires tuning, such as changing trailer configurations and changing loading conditions. As a result, the Full-scale model's physical test will consume much time and be expensive.

A solution to this problem was proposed by S. Brennan and Alleyne [12] when they used Buckingham’s theorem and applied a dimensionless analysis. They built a scaled roadway for vehicle dynamics control equipped with a scaled vehicle. Brennan and his colleague called it Illinois Roadway Simulator (IRS). They measured the parameters for three different cars and compared them with average values for four Full-scale vehicles. Their study concluded that the scaled model could present a good understanding of vehicle performance on the road. In line with the aim and objectives of this study, this chapter contains a review of the heavy vehicle handling models starting with conventional modelling techniques, then moving to the modern ones, especially scaled models, then a review of different control systems.

In the beginning, the leading causes of vehicle accidents are reviewed. After this, a study of the vehicle's handling performance is carried out from two perspectives: conventional handling models and tyre models. Examples of some of the operating conditions (tyre overload,

camber angle and road surface) and the importance of different tyre models that have been previously used, such as the Fiala model and the Magic Formula are reviewed.

The chapter then presents the modern modelling techniques used to evaluate the vehicle's performance, emphasising the scaled model that has recently played an important role in investigating the vehicle's performance. Further it presents the development of some vehicle control systems and the progress in the previous years to improve the vehicle's performance and ensure the necessity of control systems. Furthermore, the chapter introduces the significant issues that should be included in the development of control systems, some obstacles which resulted from them and ways to overcome these obstacles to improve the performance. Finally, a summary of the chapter highlights the critical gap in heavy vehicle modelling and control techniques.

2.2 Road accidents main causes

To understand the importance of heavy vehicle handling control and how it affects commercial vehicles' stability. It is necessary to look at heavy vehicle road accidents and understand the motion of the heavy vehicle. Furthermore, it is vital to know the cause of road accidents, reducing or eliminating them. Three main types of road accidents contribute to severe damage when they occur. These types are the following:

- Roll-over
- Jack-knifing
- Trailer swing

2.2.1 Roll-over of heavy vehicle

The roll-over of the heavy vehicle is a severe problem and can be divided into a tripped roll-over and an untripped roll-over. The tripped roll-over is defined as the roll-over that occurs due to the tyre's skidding; the tyre digs into soft soil or strikes an object such as a guardrail with high lateral velocity. The untripped roll-over is known as the roll-over that happens due to avoiding obstacles through manoeuvres[13]. The roll-over index (RI) is a critical factor that indicates the likelihood that the roll-over would occur. The RI relies on inputs from the road, which is influenced by the suspension system motion. The RI is defined as the inner tyre load subtracted from outer tyre load divided by the total weight as given in Equation 2-1 [14]

$$\boldsymbol{RI = \frac{F_{zr} - F_{zl}}{F_{zr} + F_{zl}}} \quad \boldsymbol{Equation}\ 2\text{-}1$$

Where

$F_{zr}\ is\ the\ vertical\ tyre\ right\ (outer)\ load$

$F_{zl}\ is\ the\ vertical\ tyre\ left\ (inner)\ load$

The maximum value of the RI is ±1, which represents the occurrence of roll-over. If F_{zr} and F_{zl} are equal, the RI is equal to zero, indicating that no roll-over occurs. However, if the vehicle encounters lateral acceleration, the roll-over will occur if either force (F_{zr} or F_{zl}) equals zero, which means that one of the sides lifts and the RI is equal ±1. indicating that roll-over occurred.

2.2.2 Jack-knifing of heavy vehicle

Jack-knifing is an incident that occurs in a tractor-trailer when the tractor experiences Yaw instability[15]. If the tractor-trailer moves at high speed of more than 55mph, then it encounters an obstacle. The driver responds with a steep steering angle to avoid this obstacle,

and the jack-knifing phenomena may occur due to an excessive fifth wheel angle [16]. The tractor rear axles are locked up[16]; this results in a large tractor Yaw angle being generated, and if the driver tries to avoid the jack-knifing by giving a steering angle in the wrong direction, the situation gets worse, and the tractor and the trailer hit each other like scissors. the controlled brake system may be used to diminish the occurrence of jack-knifing[17]. The main problem with the controlled brake system is that there are many uncertainties in the system, which will be mentioned later in this chapter.

2.2.3 Trailer swing

Trailer swing can be considered an instability case. The main difference between the jack-knifing and the trailer swing is that the trailer swings if the trailer faces Yaw instability[15], while jack-knifing results from the Yaw instability tractor. Trailer swing is not as severe a problem as jack-knifing as the trailer will return to its typical path while the vehicle is moving onwards and below the critical speed. The main issue in the trailer swing is the fear of hitting vehicles around it. If the vehicle runs in an unusual weather condition (wind and rain) with the vehicle unloaded or partially loaded, this can magnify the problem, especially if the vehicle driver is a non-expert. Furthermore, if the vehicle moves with a velocity higher than the critical speed, the situation will worsen, and it is unlikely to control the trailer's instability [18]. Hence, there is a need to reduce the risk of trailer swing action.

2.2.4 Summary of road accidents

Looking at the leading causes of road accidents and understanding the main parameters contributing to these accidents help to explain how these causes can be reduced. For example, the susceptibility to roll-over can be reduced by developing the suspension systems or finding a control system to minimise the roll-over index[14], which leads to exploring the different

modelling methods and the related control systems developed in this area, so it gives a starting point to enhance these control systems to reduce the susceptibilty to roll-over. Also, developing a brake control system can assist in reducing road accidents caused by jack-knifing.

Moreover, the presence of trailer swing can be moderated by incorporating brake and steering control systems in the vehicle[18], emphasising the importance of developing and integrating different control systems. Furthermore, road accidents show that the driver's competence contributes to the vehicle's behaviour; hence, developing control systems helps eliminate or reduce road accidents. So, reviewing the traditional and modern modelling techniques used in developing these control systems, the different control systems will help understand how to handle dynamics development.

2.3 Conventional handling models

Designing automobiles requires a deep understanding of the vehicle motion representation on the road in different scenarios. The vehicle motion requires testing the physical model in these different scenarios or finding another way to predict vehicle motion. Modelling the vehicle's Equation of motion can replace the testing method, especially in the designing process. Modelling vehicle physical systems accurately will provide the designer with the characteristic of the vehicle. The following section will provide more detail about different conventional handling modelling techniques.

2.3.1 Conventional bicycle model

One of the famous and simplest models is the traditional bicycle model, as shown in Figure 2-1 [19]. This model assumes that there is no effect of the rolling motion and the left and right tyres have the same characteristics. Also, the suspension system effect is negligible

as it acts as a rigid body. In addition to this, the pneumatic tyre is assumed to be linear with no aerodynamic impact. Several researchers employed the two degrees of freedom model to obtain the vehicle's handling performance, such as Wong[20]. Also, other researchers add some modification to the bicycle model; for example, Xia [21] used the bicycle model with non-linear tyres to predict the behaviour of the four wheels steering in a combination of braking and steering with open loop and closed loop condition. Also, he compared the results with the front wheel steering model.

Another example is described by Moldenhauer [22], who developed a new method in examining the lateral stability for recreational vehicles considering Traction forces, longitudinal acceleration and onward resistance (i.e. rolling resistance). In a similar case, Talukdar [19] compared the conventional bicycle model to the flexible bicycle model. It concluded that it is preferable to use the flexible model in handling models, especially in control system design and benefiting from the model's simplicity.

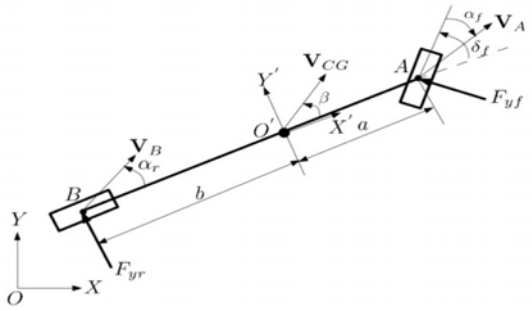

Figure 2-1: Conventional bicycle model[19]

2.3.2 Tandem axle bicycle model

Another variation on the bicycle model analysis is for vehicles with rear tandem axles, as shown in Figure 2-2[23]. If the vehicle is equipped with tandem axles typical in trucks, the

handling performance can be obtained from a simple bicycle model. Williams [24] introduced the handling Equation of heavy vehicles with rear tandem axles. Moreover, he developed a generalised formula for multi-axle vehicles. This formula can compute the handling performance for the tandem vehicles; also, it can be applied for multi-axle vehicles. The existence of a third axle (non-steered) in the vehicle to withstand the loads lead to an increase in tyre wear and a decrease in the directional response, so Williams and Nhila [25] used the same model proposed by Williams in comparing the different methods of steering supplementary axles. They calculate the understeer gradient to investigate the handling performance by assuming an equivalent wheelbase to the truck. Also, Williams and Sherwin [26] proposed a control strategy to enhance the understeer gradient using the same approach for the equivalent wheelbase. The study found that this control strategy is effective in enhancing vehicle performance.

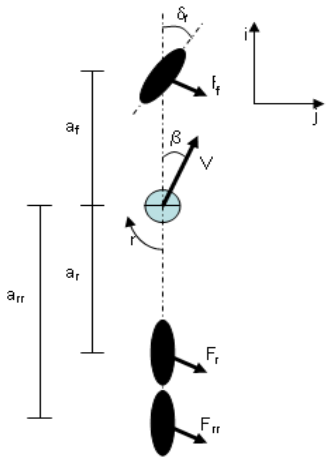

Figure 2-2: tandem axle bicycle model[23]

2.3.3 Tractor-trailer bicycle model

The third bicycle model is for the tractor semi-trailer shown in Figure 2-3[27]; this model is a 3 DOF model that relates the semi-trailer's Yaw motion with the Yaw motion of the tractor by angle βt.

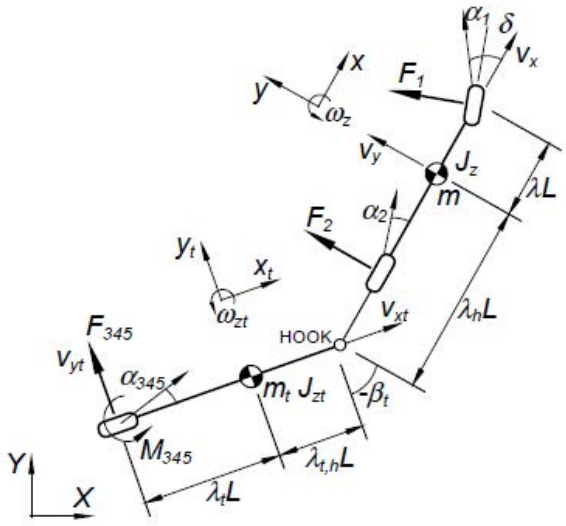

Figure 2-3: Free body diagram vehicles with one articulation[27]

2.3.4 Full vehicle model

The full vehicle model consists of modelling all the motions around the vehicle. The complete vehicle model integrates the tyre forces (which include the tyre model to calculate the longitudinal and lateral forces) and suspension system. The full vehicle model can also consider the driver seat, cabin suspension, and load effect (sloshing motion in liquid tanker truck). When dealing with the full vehicle model, the important thing is to identify the parameters that need to be examined and their performance indicators. For instance, if the whole model is used to study handling, the most crucial output will be the Yaw rate and lateral acceleration. Yuzhuang Zhao et al. [18] used a full vehicle tractor semi-trailer model to investigate the combination of differential braking and AFS control systems. Figure 2-4[18] shows the full vehicle model.

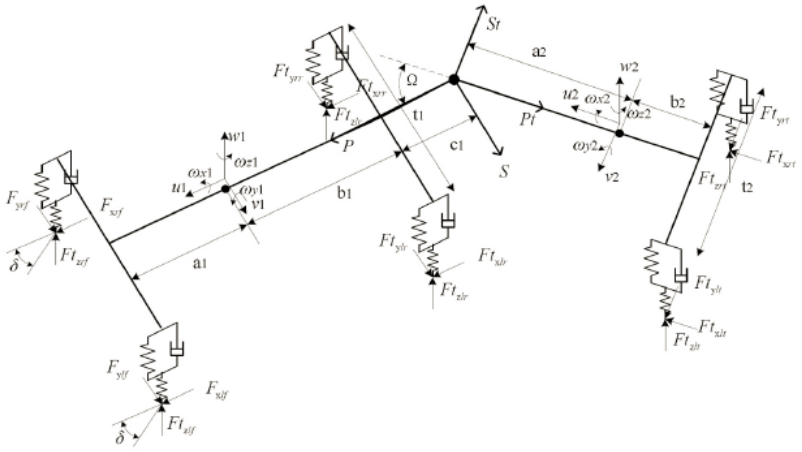

Figure 2-4:Full vehicle model[18]

2.3.5 Summary of handling models

The heavy vehicle consists of many installed systems which interact with each other to complete a whole vehicle. The critical basic systems that can be modelled when studying vehicle handling dynamics are tyres, brake system, steering, and suspension systems. All these systems differ from one vehicle to another vehicle according to the system design in the vehicle. For example, the general freight truck's steering system is a two-wheel steering system, while the steering system for a cement truck is a four-wheel steering system. The model degrees of freedom assumptions and the complexity of the motion equations, whether linear or non-linear, affect the calculated behaviour. However, no model can give a full characteristic of the vehicle as scientists neglect some parameters to simplify it.

Simulation is a popular way used over the past decades to explore the vehicle's behaviour. Simulation of vehicles on computer programs started in the 1970s. It has been used for many types of research; it has also been an effective way of describing the vehicle dynamics' characteristics. Besides, it also helps enhance the vehicle's performance (handling or ride) when redesigning or changing some parameters of the different systems in the vehicle. As mentioned

above, different mathematical modelling techniques can help to understand the characteristics of the vehicle. However, neglecting some design parameters or operating conditions while designing a control system may degrade the performance of the controller. For example, due to the conventional bicycle model's assumptions and neglected parameters and the low number of heavy vehicles with two axles, the conventional bicycle model cannot achieve accurate results for the heavy vehicles' handling behaviour. Thus, it is not recommended to rely on using it. Moreover, the tandem axle bicycle model and the tractor-trailer bicycle model are developments of the conventional bicycle model, and they can be used for heavy vehicles. However, the suspension system's absence in this model, as in the conventional bicycle model, precludes using it.

Furthermore, the full vehicle model can give a better understanding of the characteristics of the whole vehicle as it takes into account all the main sub-systems. These models could be extended to many degrees of freedom and have proved an efficient way of developing control systems. However, modelling the vehicle using differential equations makes it challenging to consider any non-linearity in these systems. These sub-systems (brake, suspension and steering) have different types and geometries, which can also change the vehicle's handling behaviour, as mentioned in [28-30]. Finally, the full model for heavy vehicle includes complicated equations that are not easy to manipulate. These limitations drive the need to find another way of modelling a full vehicle so that the neglected parameters (non-linearity, types and geometry) can be considered. Hence the development of commercial multi-body dynamics software to allow researchers and companies to model the vehicle more precisely.

2.4 Tyre handling model

This section presents the other point of view when modelling the handling of the vehicles. Tyres are the interface of the vehicle with the road. It is the connection between the vehicle and the roadway, and the primary function of the tyre can be summarised into two points

1- To sustain the weight of the vehicle.
2- To develop the forces which control the vehicle motion in the longitudinal (Traction or braking) and lateral (cornering) directions.

In addition to these two main points, the commercial vehicle's tyre should provide some other features such as low rolling resistance to the vehicle motion with excellent Traction, moderate tread wear, and durability.

The tyre is an essential factor when modelling the vehicle dynamics, and the more accurate the tyre model, the more precise the vehicle model is. The pneumatic tyre is a non-linear system due to its construction and design. The pneumatic tyre is a complex system to the vehicle model while considering all the design parameters and operating conditions. Many researchers have worked on tyre modelling to identify tyre parameters and generate available vehicle dynamics analysis models.

When a vehicle moves on the road, the tyre is exposed to different forces and moments. Figure 2-5 [31] shows the tyre axis system

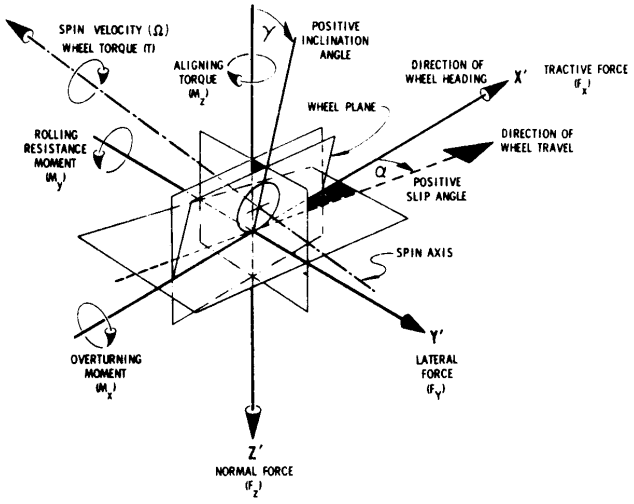

Figure 2-5: SAE Tyre axis systems [31]

These forces and moments are responsible for spinning and steering the tyre and, therefore, the whole vehicle motion. The tyres' construction is a composite of elastomer and various reinforcements, the tyre axis system; the tyre has many design parameters and operating conditions to be considered when modelling the tyre. These design parameters differ according to the tyre model and its assumptions, and as many systems, the tyre has inputs and outputs parameters, and these parameters differ according to the tyre model's complexity. Table 2-1 [32] shows an example of the input/output quantities for a tyre model. These parameters can be calculated by the theoretical or experimental method according to the tyre model. The next sub-sections will mention some examples of the different design parameters and operating conditions for the tyres, then provide some tyre models used in the handling models. Finally, it will provide causes for selecting the used tyre model.

Table 2-1:- Input/output quantities (road surface considered flat) [32]

Input vector		Output vector	
ρ	Radial deflection	F_z	Normal load
κ	Longitudinal slip	F_x	Longitudinal force

Ω	Speed of revolution	M_y	Rolling resist. Moment
α	Lateral slip angle	F_y	Cornering (side) force
φ	Spin, turn slip	M_z	(self) aligning torque
γ	Camber angle	M_x	Overturning couple

2.4.1 Tyre overload

Tyre overload is one of the Different operating conditions of the tyre. Running heavy vehicles with tyre overload will affect the handling performance of the vehicle. Figure 2-6 [33] shows the wheel load effect on the cornering stiffness and the lateral adhesion coefficient. It shows that when the tyre's load was 10 kN, the maximum lateral adhesion coefficient was near one while the cornering stiffness was about 1800 kN/Deg. Increasing the tyre load results in decreasing the maximum lateral adhesion coefficient by 0.4 to be 0.6 at the maximum average load and increasing the cornering stiffness to reach 4500 kN/Deg., Although the cornering stiffness is increased, enhancing the stability, the decrease of the lateral adhesion coefficient leads to a reduction in tyre grip, leading to vehicle instability.

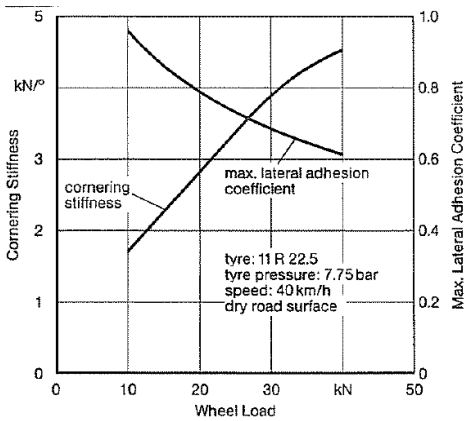

Figure 2-6: Cornering Stiffness and Max. Lateral Adhesion Coefficient as a Function of Wheel Load [33]

2.4.2 Road surface

Another critical factor that influences vehicle handling via the tyre is the road surface. Pazooki A. et al. [34] shows that when road unevenness increases, the roll and Yaw stability decreases. Gohring E. and Von Glasner E. C. [33] indicate that the road surface significantly influences directional behaviour. They showed that the value of the longitudinal deceleration on a wet road surface is less than half of its value on the dry road surface, as shown in Figure 2-7 [33]

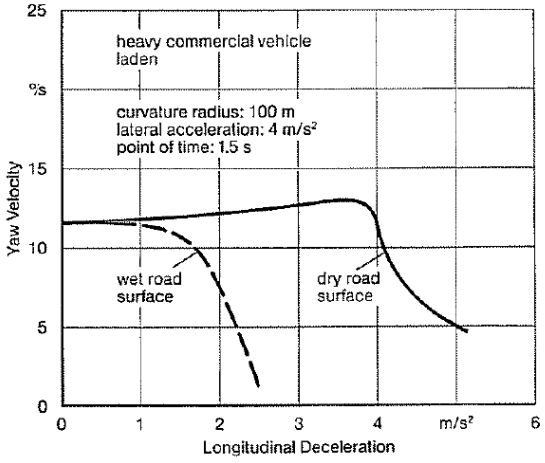

Figure 2-7: Impact of Road Surface with "Braking in a Turn" [33]

2.4.3 Camber angle

The camber angle is one of the significant parameters that affect vehicle handling. Tateishi V. et al. [35] show that a negative camber angle enhances the vehicle's stability and controllability, which indicates that adjusting the wheel camber angle is very important.

2.4.4 Fiala tyre model

As said before, many tyre models are available to describe tyre behaviour. First, tyre models are classified according to road type, so there are on-road tyre models, also off-road tyre models. Because this study is on commercial vehicles which move on-road, it is not essential to consider the off-road tyre models. Also, the tyre models may be used in different situations, some for handling and stability analysis while others may be used for ride comfort analysis, so since this study is oriented mostly to the handling dynamics, the tyre models for handling investigation will be studied., the first one is Fiala's model.

Fiala's model is based on modelling the tyre carcass as springs and the tyre's tread as a beam, as shown in Figure 2-8(a)[36]. Due to the elasticity of the springs and the lateral force exposed to the beam (tread), a shear force between tread rubber and tread base generates and leads to lateral displacement, as shown in Figure 2-8(b)[36].

(a) (b)

Figure 2-8: (a) tyre structure and (b) tyre deflection model [36]

By calculating the lateral displacement with assuming that the contact patch is rectangular and the pressure distribution is regular, the lateral force is determined by the summation of the

integration of the lateral force distribution in the adhering and sliding regions. Fiala's model is simple to build and operate, especially as it is one of MSC ADAMS tyre models, but the problem is that it does not have a wide range of application. Fiala model is available for the pure state slip case with normal load distribution, and the model contains ten parameters that can be calculated from experiment tests, as shown in Table 2-2[37]

Table 2-2: Fiala Tyre Model Input Parameters [37]

parameter	definition
R1	The unloaded tyre radius (units - length)
R2	The tyre carcass radius (units - length)
kz	The tyre radial stiffness (units - force/length)
Cs	The longitudinal tyre stiffness. which is the slope at the origin of the braking force Fx when plotted against slip ratio (units - force)
Cα	Lateral tyre stiffness due to slip angle. which is the cornering stiffness or the slope at the origin of the lateral force F_y when plotted against slip angle a (units - force/radians)
Cɣ	Lateral tyre stiffness due to camber angle. which is the cornering stiffness or the slope at the origin of the lateral force F_y when plotted against camber angle g (units - force/radians)
Cr	the rolling resistant force coefficient, which when multiplied by the vertical force F_z produces the rolling resistance force (units - length)
ξ	The radial damping ratio. The ratio of the tyre damping to critical damping. A value of zero indicates no damping, and a value of one indicates critical damping (dimensionless)

m0	The tyre to road coefficient of 'static' friction. which is the y-intercept on the friction coefficient versus slip graph, effectively the peak coefficient of friction
m1	the tyre to road coefficient of 'sliding' friction occurring at 100% slip with pure sliding

2.4.5 Semi-analytical tyre model

It is based on the mathematical expression of the real physical phenomena related to tyre mechanics. Analytical formulae and numerical procedures are used to compute the longitudinal force Fx, the lateral force Fy, and the self-aligning torque Mz. A belt linked to a rigid wheel centre through radial and lateral non-linear elastic elements is represented by the pneumatic tyre. Parameters express the belt lateral deflection, estimated by a simple FEM sub-model. Also, the gyroscopic effect has been introduced. Figure 2-9 [38] shows a Flow-chart of the computer program for steady-state simulations.

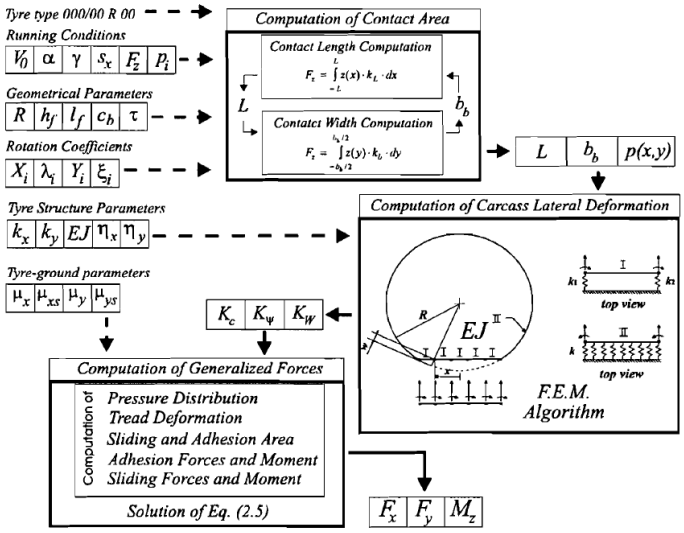

Figure 2-9: a Flow-chart of the computer program for steady-state simulations[38].

This model can be used for tyre design and vehicle dynamics because it obtains the geometrical parameters, tyre structure parameters, and tyre ground parameters by laboratory tests. Also, it is applicable for the steady and transient state, but the problem is that it is not accurate due to the low range of frequency, and it is hard to construct

2.4.6 Semi-empirical tyre model

The semi-empirical modern model built-in 2006 by Svendenius and Gafvert [39] has many advantages. The semi-empirical tyre model is easy to construct; it is based on a standard brush model with only six parameters which are; the camber angle, the relation between cambered combined slip and used pure slip, the pure slips in the longitudinal and lateral directions, the ratio between the adhesive and sliding friction coefficients. It is assumed that the empirical pure slip models are parameterised as camber and slip angles to be calculated and based on the brush model. The tyre model accounts for braking and Traction conditions. Also, the model considers the velocity change and can be integrated with the Magic Formula tyre model. Also, it can be used through various applications and can take into consideration the lateral and longitudinal dynamics. Also, it can be used in combination with a combined slip and camber angle, but the problem is that it cannot be used for short-wavelength road condition.

2.4.7 Magic formula tyre model

This model was started in a co-operation between TU-Delft and Volvo and constructed in many versions (Bakker et al., 1987, 1989, Pacejka et al., 1993) and presented an empirical tyre model as shown in Figure 2-10 [40], which deals with a combined slip with more than fifty parameters to be determined. Magic Formula is different from the Fiala model and semi-imperial tyre model as it is easy to construct and apply with high accuracy and efficiency, and

it can also be used in MSC ADAMS, especially it can model the non-linear behaviour of the tyre. Furthermore, it can be used for both steady and transient state handling models

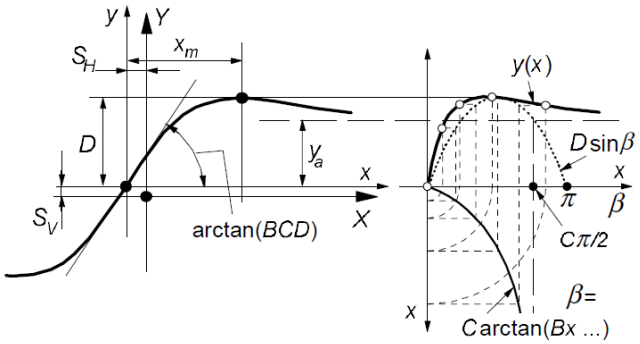

Figure 2-10: Curve produced by the original sine version of the Magic Formula [40]

2.4.8 Summary of the tyre model

After mentioning some design parameters and operating conditions and different tyre models, there are more options to choose from when working with the handling models. However, the Fiala tyre model will be used in this research because of its simplicity and applicability regarding measuring its parameters with the scaled tyre, also because it can work with the chosen software package, MSC ADAMS.

2.5 Modern modelling technique

After presenting the conventional modelling and the tyre models, and start to understand the need for new ways in chassis handling models, also, due to the development of technology that allows scientists to create advanced techniques that can be used in evaluating the performance of the vehicle. This section explains these modern techniques as it allows the vehicle system to be tested safely and inexpensively and predict the performance more accurately than conventional modelling.

2.5.1 Scaled models

Scaled models are one of the old techniques that can be used to determine the required system's behaviour, such as ships and planes, but from around 20 years, scientists start to use scaled models for predicting vehicle performance. For example, S. Lapapong et al. [41] presented a detailed study of scaling a 5-door passenger car (model: Mercury Tracer) to a 1/5 scaled model. Lapapong and his team show the pi-group's derivation for the whole passenger car and how different parameters are measured in the lab to find the pi-groups between the Scaled and Full-size model. Later, the scaled model was used to develop different control systems. Brennan and Alleyne [42] examined the validated roadway using a driver-assisted control algorithm, enhancing the vehicle's transient response by providing a rear steer angle to the car after measuring or predicting the Yaw and lateral vehicle parameters. The study concluded that a validated testbed could also be used in developing vehicle control systems.

Furthermore, Brennan and Alleyne[10] gathered information from the literature about the pi-group. “Pi-group is a dimensionless parameter defined from Buckingham’s theorem which relates the SI unit dimensions between two scaled values”. Brennan and his colleague created a normal distribution from this published data to develop a state feedback robust controller depending on spatial and temporal parameterisation, which have been applied on the same testbed with the scaled model. The merit of Brennan and his colleague's studies is that they show the applicability of predicting a scaled vehicle's handling performance. They propose a control strategy based on linear optimal control to enhance this performance.

Also, Claudio Altafini et al. [43-46] started to use a scaled model, but their team used a scaled tractor semi-trailer. They concentrated on creating and testing a control algorithm to solve the path following the two directions forward and backwards and minimise the off-

tracking for the rearmost wheels. Their studies concluded that if the vehicle is equipped with a control system to handle the problem of backward motion (moving in the reverse direction) and the path following and off-tracking, it can help experienced drivers manage these problems. Later on, T. Kaneko [47] used a scaled articulated bus to develop a front steering control system that could optimise the path following of the articulated bus in turns. Also, L. K. Chen and J. Y. Hsu [9, 11, 48] proposed a dimensionless analysis for a Hino tractor semi-trailer vehicle. They used a scaled 1/14 model to investigate the vehicle's behaviour when applying a brake distribution control to prevent jack-knifing.

Furthermore, Chinmaya B. Patil et al. [49, 50] used the same method to build a testbed for testing an anti-lock braking system in a scaled RC car and test a sliding mode control. Moreover, William E. Travis [51] used the scaled model to test control methodology for preventing the vehicle from roll-over. Also, Randy Whitehead et al. [52] used a scaled car to develop the ESC system for roll-over prevention and to keep the scaled model stable at an appropriate threshold. Furthermore, Liang-Kuang Chen and Sheng-Yung Hsu [53] proposed a roll-over prevention technique using the differential braking of a scaled RC 1/10 model tested on a testbed controlled by a driving simulator, while Lin Cai et al. [54] used the scaled model to develop a genetic Fuzzy controller for steering control. Matthew Polley et al. [55, 56] studied from another perspective as they tried to find a correlation between the tyres used in a scaled model and tyres used in a full-size vehicle. They used the Magic Formula on four different tyre sizes to better understand the non-linear effect of a scaled tyre while using it with a scaled model for investigating its dynamics.

After proving that the scaled model could develop control systems, studies started to focus on developing a control system for a specified type of vehicles and incorporating it into heavy vehicles to prevent roll-over and jack-knifing. For example, Rajeev Verma et al. [57, 58]

started to simulate an HMNWV car with dimensionless analysis. They used a HIL technique on the scaled drivetrain system to capture the vehicles' physical properties and test a crash avoidance system. Their study has shown the advantage of using the similitude for simulating the Full-size vehicle's real response. Later, Chen and Liang[48] introduced a Fuzzy controller, adapted according to the changing load, stabilise the tractor semi-trailer in manoeuvres, and prevent it from jack-knifing. However, they mentioned that the non-linear effect of the fifth wheel and DC motor and steering linkage are not taken into consideration.

Furthermore, a scaled vehicle continues to be used to test different control methodologies such as R. Rajamani et al. [59, 60] for testing a new RI. Muhammad Nasiruddin Mahyuddin et al. [61] used the scaled model for assessing the parameter estimation algorithm. Krzysztof Parczewski and Henryk Wnek [62] used it for validating a truck lateral stability control system.

Finally, after the technology development, the scaled model was used to study advanced driver assistance systems and autonomous vehicles and scaled road traffic modelling and control systems based on autonomous vehicles [63-68]. The scaled model can be fitted with different sensors (inertial measurement system (IMU), a global positioning system (GPS), LIDAR) or cameras, to test the autonomous vehicle algorithms. Also, to investigate their validity and predict vehicles' dynamics parameters such as sideslip angle, which can be fed to the control system to help predict the vehicle performance parameters while manoeuvring.

These studies suggest that the scaled model can perform similarly to the full-scale model and can be used as a tool when studying vehicle dynamics. So, considering that this was the first stage in using the scaled model, it can be found that the main target in this stage was to correlate between the scaled and the full model using the dimensionless analysis. Thus, this

supports the importance of dimensionless analysis in relating the Scaled and Full models' dynamics. However, none of these studies[12, 41] used any mathematical model. Later on, several studies [9-11, 43-48, 53, 57, 58, 63-68] used the scaled models for developing control systems and testing different algorithms.

2.5.2 Hardware in the loop (HIL)

Hardware in the loop is one of the prominent ways of modelling and testing vehicles. The HIL tests the physical system's performance or a sub-system by integrating the physical system in a loop with computer software. The system is typically fixed on a test bench that allows it to work correctly and is operated through the proposed control system to determine the proposed control's suitability with the tested system. Also, the system may be tested in different operating conditions to simulate its behaviour when working in a real environment, such as room temperature or wind force expressing aerodynamics. HIL has been used for different aspects of vehicle dynamics; for example, Edoardo Sabbioni et al. [69] designed a test bench for testing the anti-lock brake system and the ESC system by building the whole brake system in the lab and testing the brake system in different emergency manoeuvres. They also tried to predict different control parameters while testing on different slippery surfaces. The study shows that testing the ABS and ESC on HIL is an effective way to understand and develop control methodologies. Before, Herbert Schuette and Peter Waeltermann [70] used the HIL to test the brake system's controllers. They included an anti-lock braking system, a Traction control system, ESC and integrated control. They presented the test bench for each system and the sensors used. Also, they demonstrated how to brake control systems sensors are connected to the test bench.

Moreover, their main aim is to overcome the stiff behaviour from numerical equations and present a solution to test the lab's developed control systems. Later, Chuanliangzi Liu et al. [71] used the dSPACE HIL simulator to test the electronic steering control system controller. Also, M. Kamel Salaani et al. [72] built a test bench for pneumatic brakes for a heavy vehicle to test electronic safety interventions for the brake system.

2.5.3 Software in the loop (SIL)

Software in the loop is another method. SIL starts before testing with HIL. SIL allows testing developed code in a virtual environment. The term may be expressed as a computer simulation or virtual simulation. SIL is done before the HIL, and the results from the SIL are compared with the HIL. If the results match between HIL with SIL, so the simulation process is robust. For example, Jorge de-J Lozoya-Santos et al. [73] compared the SIL and the HIL for a semi-active suspension system with different control methodologies and the results show that the best controller in the SIL was not the best controller with the HIL.

2.5.4 Co-simulation

The term co-simulation is used when a computer model simulation is done through a combination of two software. The advantage of using co-simulation is integrating the powerful parts from each software to enable various changes and adaptation of the simulation model. The co-simulation has proven that it is a successful method to identify vehicle dynamics' behaviour more precisely than the traditional modelling method. Makarand Datar [74] used co-simulation for a high fidelity model to address the vehicle's non-linear behaviour, powertrain, and tyres and manage the system's uncertainty. John Limroth et al. [75] created a co-simulation between Trucksim and LabVIEW to investigate the ESC algorithm on a tractor semi-trailer model. Sughosh Rao [76] generated a co-simulation between MSC ADAMS/car and MATLAB to

explore the difference between the performance of a Ford Expedition equipped with ESC only or equipped with integrated control (of ESC and electronic suspension). Later, Shengqin Li and Le He [77] used a co-simulation between MSC ADAMS/car and MATLAB to assess ESC depending on the Fuzzy control algorithm. Tobias Eriksson [78] also used it to test the anti-lock braking system on a passenger car (Volvo V40 with diesel engine). Furthermore, co-simulation is also used with tractor semi-trailers to test stability control algorithms, and it can also be used for ride performance[78, 79]. The development of technology can be used for testing autonomous vehicles [80] if integrated with a HIL simulation.

2.5.5 Multi-body dynamics software

Nowadays, various multi-body dynamics software's are available for vehicle dynamics, such as MSC ADAMS, SIMPACK, CARSIM, and dSPACE. Every software gives the capability to model different types of suspension, steering, brakes and more. Also, it can give the ability to design your system from scratch or modify any template inside it. Moreover, some of them can work with passenger cars, trucks, or even bikes, and some have the feature to model any multi-body dynamic system, not just vehicles. Furthermore, they can be connected to other programmes as a co-simulation to integrate other systems that are not modelled inside it, to be in one system with the vehicle, such as the co-simulation between MSC ADAMS/Car and MapleSim, which can model internal combustion engines. The choice of which software to work with depends on the application and the level of precision the model requires.

2.5.6 Summary of modern modelling technique

It can be summarised that the design of a control system and its application on a scaled model can be used to understand how the full vehicle will operate if equipped with this control system. However, scaling the control parameters back to the Full-scale model requires a

dimensionless analysis which was not considered in some studies. Also, the developed control systems that used a mathematical model were based on a linear bicycle model. Moreover, most of the scaled models that have been used have concentrated on a passenger car with few studies on articulated vehicles. Therefore, it can be concluded that using a scaled vehicle provides some advantages over using the Full-scale model in the design and development process of new control systems. However, the deficiency with the existing techniques for using robust mathematical models motivated a new way of developing different control systems. Also, the paucity of studies that have been done using the articulated vehicle highlights the need for investigating its use in research studies, especially with low funded projects. Thus, MSC ADAMS/View was chosen to simulate the scaled model as it facilitates building a model from scratch and testing its handling behaviour.

Furthermore, it has been proved that HIL is an effective way of testing vehicle sub-systems. Also, SIL has shown that the importance of applying the control methodology in a real environment is crucial. Thus, co-simulation is a powerful method to test and validate control systems that are newly designed or developed, mainly when used with multi-body dynamics software.

2.6 Control systems

After mentioning the different techniques used in modelling vehicle dynamics, it is essential to review the control systems' role in enhancing vehicle dynamics. Control system was used in vehicle dynamics more than five decades ago[81]. The main objective of vehicle handling dynamics control systems is to optimise sub-systems' performance, and hence, the whole vehicle. Also, to help in reducing road accidents. In every period, as the technology is developed, new control systems and novel methodologies are produced. These new systems

provide the research community with several algorithms and methods to improve the whole vehicle's performance, either in dynamics or any other aspect. This section provides a review of different control systems developed for enhancing vehicle dynamics.

2.6.1 Brake control systems

The first central sub-system control in the vehicle is the brake control system. The brake control system has been in existence in the automotive for more than 50 years. It has continued to be developed over all these years. It started with the anti-lock brake system until it reached the emergency brakes to reduce the speed or stop the whole vehicle without any intervention from the driver. Figure 2-11[82] shows the development of the brake control system over the years. However, the development of brake system in commercial vehicles and especially the articulated vehicles was different for many reasons; the commercial vehicles depend on pneumatic brakes instead of hydraulic brakes, which lead to a lag in the response time of the brake applied compared to hydraulic brakes.

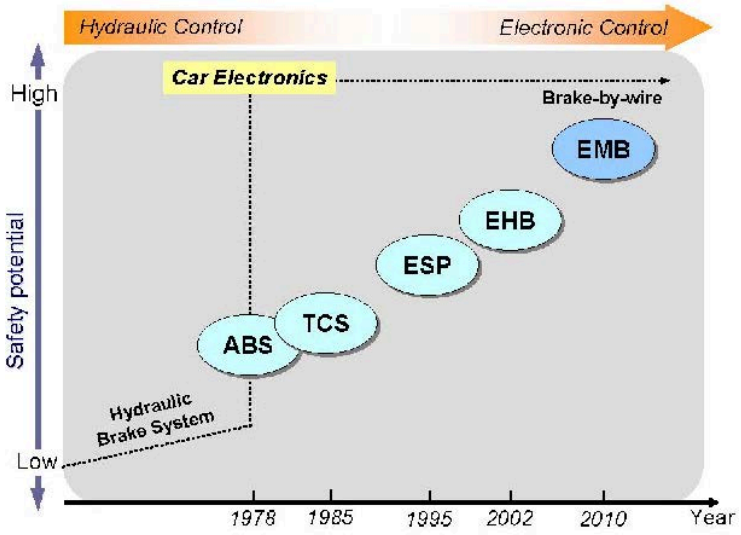

Figure 2-11: Development history of brake control systems[82]

Also, for articulated vehicles, the trailer's brake condition may differ from the tractor, which puts additional loads on the tractor brakes and causes brake lining overheating and wear. These factors and more allow adding more functions to the control systems; for instance, the electronic load sensing overcomes the problems from the passive load sensing, which depends on the static load, not the dynamic load, so the electronic load sensing is added to the anti-lock brake system to avoid the rear axles locking up. Furthermore, developing the whole brake system to be electronically controlled can avoid conventional pneumatic brake systems and add new features such as wear control and anti-slip regulation[17].

The vehicles' handling was enhanced by the anti-lock brake system, as the driver can steer the vehicle and decrease the stopping distance. However, for improving the stability of heavy vehicles in roll-over or jack-knifing, the ABS will not be useful. Thus, finding a way to solve this problem leads to ESC based on the ABS. The ESC started to be equipped in vehicles by the mid of the 1990s [83]. The system can combine two systems; an Anti-lock brake system and a Traction control system. The primary function is to increase or decrease torque on the wheels according to the vehicle's situations. Also, it can apply brake torque on the individual wheel, especially when the vehicle confronts a curve with split μ surfaces. ESC is used latterly in commercial vehicles. In tractor semi-trailers, ESC can prevent Yaw instability (jack-knifing and trailer swing) and the roll-over of the vehicle.

2.6.2 Suspension control systems

The second major sub-system is the suspension system. The suspension system has been developed over the last decades from passive to fully active. The suspension system has a great influence on the handling model. To illustrate more, handling performance can be measured through different parameters. One of the main parameters that measure the handling

performance of the vehicle is the understeer gradient. the understeer gradient Kus for a bicycle model is defined in Equation 2.2. as follows [26]:

$$K_{us} = \frac{F_{zfront}}{C_{\alpha front}} - \frac{F_{zrear}}{C_{\alpha rear}} \quad Equation\ 2-2$$

with front and rear axle loads F_{zfront} and F_{zfront} with front and rear axle cornering stiffness $C_{\alpha front}$ and $C_{\alpha rear}$

The value of the understeer gradient determines the stability of the vehicle; a value equal to 1 represents a neutral steer (ideal situation), a value greater than 1 represents understeer (stable condition) and a value lower than one represents oversteer (unstable condition). From Equation 2-2, the parameters that influence the understeer gradient are the axle loads and the axle cornering stiffnesses. Also, the suspension geometry determines the position of the vehicle roll axis. Due to lateral vehicle motion, a load transfer between the left and right wheel occurs, leading to changing the camber angle and the roll steer, which results in a negative understeer gradient and loss of Yaw stability[84]. Also, the suspension system's elasticity leads to lateral flexibility, which affects the vehicle steer characteristics. Thus, load transfer and tyre characteristics and the effect of lateral and steering compliance, camber steer and roll steer, are involved. Which highlights the importance of the suspension system in handling performance. Furthermore, much work has been done to improve ride, as the suspension system's primary function is to connect between the sprung and unsprung masses, isolate the sprung mass from the road irregularities, and maintain contact between the road and the tyres. Hence, adding control systems to the suspension may help improve the vehicle's ride without affecting the vehicle's handling. So, looking profoundly into the suspension system will help to find out how to enhance the handling behaviour of the vehicle

The active suspension control system was the start point of applying control on the suspension system. The active suspension control system concept applies an actuator force to reduce the excessive force from the ground or the sprung mass's load transfer. The active suspension system has several types and control methodologies. The type of active suspension system depends on the working principles of the actuator used. The actuator can be hydraulic, electromagnetic, pneumatic, or even hybrid from two types. The actuators can be set with the primary suspension in series (low bandwidth, which means control the suspension at low frequencies coming from the tyre) or in parallel (high bandwidth, which means control of the suspension for both low and high frequencies comes from the sprung mass and the tyre).

An example of this is the hydro-pneumatic suspension system developed in the early ’50s by Paul Mages[85]. The system is based on a sphere that is connected to the wheels via a link. This sphere from inside consists of two chambers separated by a diaphragm, one chamber is connected to a hydraulic pump that compresses oil inside it, and the other contains nitrogen gas. The pressure inside the sphere is changing according to the bouncing motion of the wheel. The pressure change allows it to absorb and damp the excessive energy generated by the bouncing motion. This system still exists in some recent Citroen models.

The second one is the semi-active suspension system. Karnopp and Crosby first reported the application of a semi-active suspension system in passenger cars [86]. It depends on changing the suspension’s damping coefficient. The primary purpose of controlling the damping coefficient is to enhance the ride comfort of the passenger. However, the control system's robustness is achieved if the system can enhance the ride comfort without affecting the vehicle's handling behaviour too much. There are different types of dampers, and different configurations with various control methodologies have been used. The magneto-rheological damper (MR damper) is one of the most common types, and the skyhook damper control is also

a popular method for the semi-active suspension system. Ahmadian introduced the first presentation of the semi-active suspension system in commercial vehicles [87]. Lately, a study by Simon et al. [87] uses the MR damper, which resulted in better handling of the trucks. Furthermore, semi-active suspension is also used in-cab and seat suspension.

The third suspension control system is the active anti-roll system. The active anti-roll system transforms the passive anti-roll bar into an active one by integrating a motor that applies a force on the suspension opposite to the suspension's motion, so it can balance the vehicle through turning and decreasing the tendency to roll-over. Citroen first presented an active anti-roll bar in 1995[88], and it can be considered an active suspension system[89]. The active anti-roll bar depends on varying the vehicle suspension's effective stiffness and compromises the vehicle's performance between handling and ride. The active anti-roll can be operated hydraulically or electromechanically. However, it adds weight to the unsprung masses, which limit its presence in heavy vehicles.

Furthermore, it is expensive and requires routine maintenance. Despite these problems, some researchers succeeded in overcoming them by integrating the active anti-roll bar with pneumatic suspension and proved its ability to enhance handling without affecting ride[90]. Thus, using an active anti-roll bar can be useful in commercial vehicles using air suspension.

2.6.3 Steering control systems

The third sub-system is the steering system. The steering system is used for controlling the direction of motion of the whole vehicle according to the driver’s desire. Figure 2-12 [91] shows the vehicle axis system defined by SAE. The entire vehicle is exposed to three forces and three moments. The handling of the vehicle controlled by the lateral force, roll moment and Yaw moment. The lateral force can be generated through internal or external forces (the steering

wheel torque from the driver as internal and the side wind as external), and due to its distance from the centre of gravity, it generates a Yaw moment around the vertical axis and a roll moment around the longitudinal axis. The steering system is then responsible for the tyre's lateral force's activation, so all vehicles' handling behaviour starts from the steering system. Furthermore, the external disturbance also affects the steering system performance. The more precise the steering wheel angle, the more accurate the vehicle handling behaviour, which leads to the development of steering control systems.

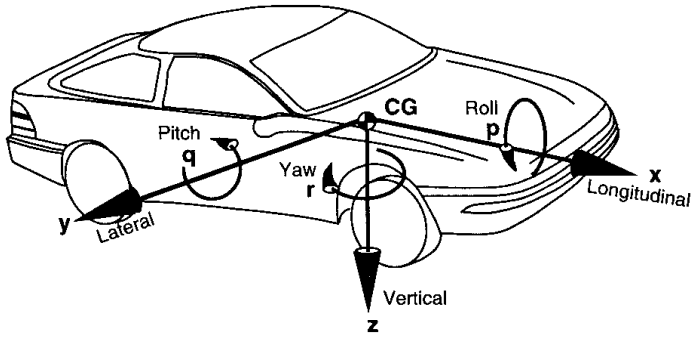

Figure 2-12: SAE Vehicle axis system[91].

The AFS control system was invented by BMW [92]; it depends on the driver’s desire and the vehicle condition. The AFS improves vehicle stability by increasing or decreasing the steering angle depending on lateral acceleration, steering angle, vehicle speed, and Yaw rate. Also, it can optimise the steering ratio, especially when manoeuvring in the curved road at low speed. It also improves stability at high speed. AFS uses a variable steering ratio as the first parameter to optimise steering angle. The steering ratio differs according to the speed, and the motor actuator provides the additional steering angle according to the controller's calculated value. For commercial vehicle, the AFS depends on the type of heavy vehicles. For example,

the general freight truck's steering system is a two-wheel steering system, while the steering system for a cement truck is a four-wheel steering system.

Active trailer steering is the other solution that can reduce the tyre wear and control the trailer rear axles' path following. Active trailer steering can control the steering of the rearmost axle or all the trailer axles. The main advantage is that the control can optimise the steering angles instead of the self-steering axles that was integrated before[93]. The value of the steering angles differs according to the vehicle condition.

A study by Kim [93] mentioned that for articulated vehicles, the AFS might not be the only way to achieve tractor-trailer stability as other design parameters should be considered, such as path tracking and tyre wear. Furthermore, the study mentioned that the AFS could achieve better performance than the passive one, but the optimum solution will be if the articulated vehicles are equipped with active steering for both the tractor and trailer.

2.6.4 Chassis control systems

The fourth sub-system in the vehicle handling control is a chassis control system. Chassis control systems can be defined as the control systems that depend on sensors integrated with the main body to measure one of the chassis' movements (i.e. displacement, velocity, and acceleration in three directions). Each chassis control system assesses the vehicle's situation, and according to its algorithm, it uses the main sub-systems (brakes, steering, suspension) to implement an action to stabilise the vehicle or reduce the vibration of the sprung mass.

Yaw control is one of the chassis control systems responsible for preserving the vehicle's handling dynamics. The Yaw control system can use the brake system or the steering system to achieve its goal depending on the control methodology. However, most control methodologies

use the electronic stability system. The problem for heavy vehicles is that their braking force is much higher than the passenger car because of the loads, limiting the use of hydraulic brakes. So, improving Yaw stability for heavy vehicles is still a wide area for research, and solutions are showing up. For instance, Seunghwan Chung and Hyeongcheol Lee [94] propose a new concept that uses pneumatic brakes to apply the ESC on a bus for enhancing the Yaw stability. Xiujian Yang et al. [95] created a novel control methodology using Fuzzy logic control to reduce the jack-knifing and roll-over of a tractor-trailer trailer swing. Yuzhuang Zhao et al. [18] used AFS to achieve Yaw stability. Thus, investigating heavy vehicles' performance in terms of Yaw stability using the steering or brakes is an exciting research area.

The roll control system is another chassis control system that helps in controlling the roll-over of the vehicle. The roll control system, as mentioned above, evaluates the likelihood of rolling overusing the RI. The main goal for any roll control system is to keep the RI near zero, especially in turns or manoeuvres with much higher speed. The roll control system uses the brakes, suspension, and sometimes steering systems to retain its stability. Using these sub-systems depends on the control strategy and the readiness of these sub-systems. For example, roll control can use the suspension system to stabilise the vehicle if the vehicle has air springs in the suspension system or an active roll bar.

It is found that different aspects are applied to address the roll-over of the heavy vehicle and find a way to detect roll-over's tendency. For instance, Hsun-Hsuan Huang et al. [13] presented a multiple RI and compared it with a single one. The multiple indexes' proposed concept is based on the lateral load transfer ratio, which computes the wheel lifting for each axle separately. Also, they applied the linear-quadratic control method for the optimisation of the performance index. Then they compared the performance with the single RI. The study concluded that the single RI is much better than the multiple ones because the multiple RI uses

many actuators to control the roll-over of the vehicle. Controlling many actuators simultaneously causes signal interference affects the performance of the vehicle.

On the contrary, using a single RI does not cause the same problem. Also, Xiaoping Shi and Juan Bao [96] developed a three degree of freedom non-linear model with which they can predict the presence of roll-over by calculating the lateral load transfer ratio, and the results show that it is much closer to the real physical model. Moreover, Maciej Czechowicz and George Mavros [97] developed a 165 degrees of freedom model taking into consideration the kinematics and compliance of the suspension and non-linear tyre model to understand and test the different scenarios for the vehicle roll-over and concluded that the tyre and suspension have an evident influence on the vehicle roll-over which should be taken into consideration while developing a control system for roll-over. Furthermore, roll control can affect the Yaw control system, motivating to find a way for coordination between the two different control systems. This coordination creates new roll-over indices or, in other words, different ways to control the roll of heavy vehicles.

The third one is the lateral control system which is like the Yaw control system, but the difference is the controller's objective. The lateral control tries to keep the vehicle moving on the ideal path without shifting through manoeuvres. The lateral control can use the steering and/or the braking systems to maintain the vehicle on its way. For example, Chieh Chen and Masayoshi Tomizuka [98] used both the steering and the brakes to decrease the trailer's tracing fault. Later, Arash Hosseinian Ahangarnjead [99] used the Fuzzy logic controller to control the vehicle's lateral behaviour by integrating three sub-systems; the active rear steering control, the hydraulically interconnected suspension control and the torque vectoring control system. The proposed system from Arash boosts the functionalities for each sub-system individually and

can enhance the inclusive vehicle performance by diminishing the objective conflicts of the sub-systems.

2.6.5 Integrated control systems

Integrated control systems started around 20 years ago. The main target was to combine two different control systems to achieve better performance than each one individually. The challenge in any integrated control system is the coordination between the controller for each sub-system and the final objective, as sometimes the working of one control system can negatively affect the other. For instance, Bing Zhu et al. [100] combined the Yaw control with the front steering using 14 degrees of freedom model with the PI controller method, and the results show that the proposed control enhanced the performance of the vehicle. Carlos A. Vivas-Lopez et al. [101] introduced three control layers to coordinate between the suspension, steering and brakes. They used Fuzzy logic, and the control enhanced the brake stopping distance and Yaw stability. Furthermore, Yan-Yang et al. [102] integrated two systems and found that the integration reduces the interaction between the two controllers when working solely. Thus, combining the control systems can give better performance than the individual control system.

2.6.6 Control systems methodology

From another point of view, the control algorithm that has been used to achieve the goal has changed over the past years. Also, the control algorithm can deal with linear and non-linear systems. Therefore, a simple control system or a robust control system can be used. For instance, most of the ABS, in the beginning, depended on a bang-bang control system that relies on an on-off control. Still, after a while, the neural control has been applied to the ABS, which has proved to give better stopping distance and more steering controllability than the bang-bang

control system[103]. Although there are several control algorithms and methodologies, the concentration on finding the best and optimum control system for brakes can differ because of the brake system composition, modelling technique, assumptions made and the uncertainties in each system. Therefore, designing and optimising control systems is a broad area of research.

Consequently, ESC also has different control methodologies, and the performance can be different according to this methodology. For instance, Van Putten et al. [104] designed ESC using the linear-quadratic controller. Also, John Limroth et al. [75] state that the most common control method used with the ESC is the linear-quadratic controller. They stated that if the system's feedback signal is just one, a single PD controller can be used. Also, they mentioned that it had been proved that the sliding mode controller is effective and can be used. Later Sheng-qin Li and Le He [77] used the Fuzzy controller to co-simulate ADAMS and MATLAB to develop ESC. The method they used showed that the Fuzzy controller is an active way of enhancing the vehicle's stability.

Likewise, the most common control methodology used with the AFS is a linear-quadratic controller [105]; also, the PID controller was used for simplicity [106]. Later, mixed $H_2/H\infty$ proves its effectiveness in providing better results [107]; however, the mixed $H_2/H\infty$ deals with the system in a state-space form which is not suitable for the non-linear system. Xuejun Ding et al. [108] compared the linear-quadratic controller and Fuzzy controller and found that both enhance the system's stability, with the linear-quadratic controller having an advantage over the Fuzzy controller. However, the Fuzzy controller is less computationally intensive. The linear-quadratic regulator was the most common control methodology used with active trailer steering[109].

Fuzzy logic was introduced in 1965 by Professor Lotfi Zadeh. It is a multi-valued logic system that allows mean values to be specified between standard Boolean logic like yes/no, white/black, true/false. The Fuzzy logic controller has grown as an alternative or complementary to the traditional control schemes in different engineering fields. Fuzzy logic has been used in vehicle system control for many years and has had significant impact when used. Fuzzy logic is suitable for the control of non-linear systems, particularly with parametric uncertainties. Also, it provides a simple way to tune the rules used between the input and output signals. Besides, it can be used with another control strategy for the optimisation process. For instance, Mehdi Ahmadian [110] used Fuzzy logic control for a semi-active suspension system that shows its effectiveness to enhance a truck's roll motion. Also, Xuejun Ding et al. [108] compared the Fuzzy controller with the linear-quadratic controller and found it could enhance the vehicle's performance.

2.6.7 Summary of control systems

From the perspective view of control, there were different ways of improving the vehicle's control systems. One of them was developing the control algorithm itself. The other was to redesign sub-systems or add new parts or materials, such as changing the brake pads material or suspension geometry or adding secondary sub-systems control. One more method was to incorporate more input/output parameters into the control algorithm and seek to predict the system's uncertainties more precisely. All these methods are to enhance the performance of the control system. Other ways of improving the control systems were expanding the actuators and their response time, introducing new accurate and reliable sensors, integrating data from other systems and merging different types of sub-systems. All the above control systems that have been mentioned have shown that the control systems can help reduce road accidents and improve the vehicle's handling performance. However, each sub-system (brake, suspension and

steering) has some disadvantage that requires considering other factors to provide the desired performance.

For Brake system, Although ESC can enhance Yaw and roll stability, it will affect the vehicle velocity and may not satisfy the driver’s desire [111]. So, integrating the brake system with another sub-system can reduce this problem.

For suspension system an active suspension system's effectiveness in handling enables it to deal with roll and pitch and provides stability for the vehicle even at high speeds. The system's main problems are the high cost of the actuators and the system's high energy consumption, limiting its application in commercial vehicles. However, the active suspension system can be used in commercial vehicles in the driver's seat to provide ride comfort, primarily for driving long distances. The semi-active suspension system solves the problem of using much energy and the high cost of actuators that was the problem with the active suspension. Also, it can be applied in commercial vehicles, but the effectiveness with roll and pitch is limited. Thus, although the semi-active suspension system cannot enhance the heavy vehicle handling performance like the active suspension, it can be integrated with another sub-system (i.e. brake or steering) to give much better results[112].

For steering system, if the tractor AFS is integrated with another chassis control system, better performance for the whole articulated vehicle could be achieved than tractor AFS.

Besides, the integrated control can eliminate or reduce the problem from the interference between different control systems. The integrated control system will also help apply the advanced driver assistance systems (ADAS) or Autonomous control as the integration between different systems paves the way for future technologies.

Finally, Fuzzy logic was used with different control systems, and although it is not better than the linear-quadratic controller, it is computationally less intensive.

2.7 significant Issues for control systems design

The robust control systems depend on the precise monitoring of vehicle states. However, some control systems neglect some of these parameters, such as chassis flexibility, kinematics and compliance for the suspension. One of the main advantages of simulating a scaled model on a multi-body dynamics programme is that it allows the tune of these parameters on the simulation programme and runs thousands of tests to enhance the control system before testing it physically. The following section illustrates some of these parameters and the importance of each one, and their effectiveness.

2.7.1 Design parameters

Several studies were conducted to prove that optimising design parameters can enhance the whole vehicle handling behaviour. Changxin Wang et al. [113] used a virtual model on MSC ADAMS/Car to tune the suspension parameters. They used the genetic algorithm to change the suspension stiffness and to optimise the ride behaviour. Balaji Lomada et al. [114] investigated the steering linkage optimisation for longer front overhang vehicles. Moreover, Yunbo Hou et al. [115] tested four different vehicles configurations on a roundabout and measured the roll-over predisposition for each one and found that a single-unit truck has the highest roll-over ability.

Building a new model may need some modifications to the different design parameters for the various sub-systems to optimise these parameters to enhance handling dynamics, which can be done in three steps. The first step is choosing the parameters that will be studied, Xiujian

Yang et al.[116] optimise the most critical design parameters. They state that they chose eight parameters that will affect the vehicle's behaviour by measuring four performance parameters; they write that these design parameters had been determined according to their research experience.

1. Tractor wheelbase
2. The height of tractor C.G.
3. Tractor rear suspension stiffness
4. The longitudinal distance between trailer axle and hitch point
5. The longitudinal distance between trailer C.G. and hitch point
6. Trailer suspension stiffness
7. The longitudinal distance between hitch point and tractor rearmost axle
8. The longitudinal distance between tractor C.G. and front axle

The second step is to set the parameters' levels and determine a statistical method for testing them. As an example, Xiujian Yang and his team chose the Taguchi method. The last step is to check each combination with the proposed control strategy to optimise the parameters according to the required criteria. Thus, modelling a scaled model on a multi-body dynamics software allows changing these parameters quickly and conducting different tests through the design of experiments included in the software.

2.7.2 Operating conditions

The operating conditions are of primary importance in testing the stability of the heavy vehicles handling performance. The change in working conditions can cause severe accidents. The robustness of control systems can be measured by how this control method copes with operating conditions changes. Therefore, developing a control system requires manipulating

different operating conditions to prove its applicability. Moreover, some studies focus on how the proposed control can adapt to changes in operating conditions. For example, Narayanan Kidambi et al. [117] created an algorithm for predicting the vehicle mass and the road inclination, while Qiushi Wang et al. [109] tested the linear-quadratic technique with the active trailer steering with different loading conditions.

2.7.3 Chassis flexibility

Chassis flexibility is also an important parameter that should be considered while designing or tuning vehicle control systems. Many studies have proven the effect of chassis flexibility on vehicle behaviour. Ibrahim et al. [117] used a truck's finite element model to explore the effect of chassis flexibility on ride performance. The study shows that the chassis flexibility affected the cab pitch acceleration, the driver vertical acceleration, the acceleration of a point on the chassis below the c.g. and the acceleration of a spot on the frame below the cab, also the root mean square for them rose by 125, 18, 52, 64 % respectively. Also, Justin Sill et al. [118] studied the difference between the rigid and flexible chassis in a roll control system and concluded that chassis flexibility should be considered.

2.7.4 Kinematics and compliance

Kinematics and compliance play an essential role in analysing the suspension system. As mentioned above, the suspension system affects heavy vehicles' handling behaviour, especially in rolling motion. The conventional vehicle mathematical model does not account for the suspension's kinematics and compliance, reinforcing the multi-body dynamics model's usage. Moreover, the kinematics and compliance effect will help in addressing and tuning the control system. For instance, Byung-Lyul Choi et al. [28] studied the effectiveness of the bushing stiffness of the suspension system on handling and tried to optimise it for better

performance. Youngwon Hahn [29] used the finite element method with the multi-body dynamics method to integrate ABAQUS and ADAMS to optimise the suspension system's kinematics and compliance. Furthermore, Yahya Oz et al. [30] used K and C to optimise the steering and suspension system's hardpoints. Also, Changxin Wang et al. [113] used the kinematics and compliance concept to tune the chassis of a heavy vehicle by checking the rear and front suspensions' kinematics.

2.7.5 Driving cycles

Modelling the vehicle and testing its performance in simulation programmes requires changing the input signal for the different sub-systems, for example, changing the steering input from a ramp steer to a sinusoidal input, changing the speeds, or even the trajectory of the vehicle. Changing these signals and comparing the vehicle's behaviour for different scenarios to test the developed control systems in different running situations is known as the running driving cycles. Driving cycles is a way to understand the vehicle's behaviour and develop and tuning it through testing. For example, MATLAB has built-in driving cycles in Simulink that can be used to change the vehicle's speed or load while testing. Thus, co-simulating multi-body dynamics with MATLAB allows using this feature in testing the proposed control system. Also, the robustness of a control system means that it fits more than a standard driving cycle. Meanwhile, the driving cycle is not considered in this study.

2.7.6 Uncertainties

The uncertainty in a control system is any parameter that sensors cannot measure and is changing through the different operating conditions, also need to be predicted to feed it to the control system so that the control system can take the correct decision[119, 120]. The uncertainty is the most critical factor when designing a control system, especially for heavy

vehicles. The primary basis for identifying a heavy vehicle control system's robustness is to know how the uncertainties are considered and how well this control system predicts the uncertainties to match the real values[121]. The heavy vehicles uncertainties are much higher than the normal passenger cars, especially the tractor semi-trailer, as the tractor can pull different trailer configurations and various masses. Furthermore, in most cases, trailers are not equipped with sensors to integrate it with the tractor control system, which increases the number of unknown parameters in the control system[122]. So, finding a way to predict these values accurately and feed them to the control system can enhance the whole vehicle's behaviour. Modelling the uncertainties is a vast area of study, and each control method can vary with the uncertainty’s models, which increases the importance of adaptive control in some cases. Co-simulation can deal with this by integrating different software packages to create an algorithm to predict the system's uncertainties.

2.8 Summary

Articulated heavy vehicles are complicated multi-body dynamic systems that need to operate safely and avoid road accidents from roll-over and jack-knifing. Control system can be applied to individual sub-systems (brake, steering, suspension) or merged to achieve better performance and avoid road accidents. When a control system is developed for a heavy vehicle, it needs to be tested safely and inexpensively. The scaled model provides a safe and inexpensive way to test a vehicle. Many researchers have used it as a first step to validate a newly developed control system. However, most of them have been applied to passenger cars, while few studies have been applied to heavy vehicles, particularly articulated vehicles. Even the studies that used the articulated vehicle stuck with only one trailer configuration, not considering the effect of

different trailers in developing the control systems as in the reality since tractors can be towing different trailer configurations.

Furthermore, the mathematical model used for control development was limited to bicycle model and non-articulated models. Meanwhile, the multi-body dynamics system has been used and has proved a feasible solution in predicting heavy vehicle dynamics. Therefore, the scaled model simulation in a multi-body dynamics system needs to be investigated.

To achieve safe operation, control systems should be applied, as they can help the driver manipulate the vehicle's handling behaviour on the road. Finding a new way to test different control methodologies on different articulated vehicles needs to be investigated. Thus, co-simulation will be used to facilitate the testing of new control systems. Meanwhile, ESC will be tested and compared with the integration control between ESC and AFS. Also, Fuzzy logic control methodologies will be used for both control scheme.

The robust control systems depend on the precise monitoring of vehicle states. Traditional modelling techniques ignore significant parameters, such as operating conditions. Therefore, investigating the scaled model's simulation in a multi-body dynamics system will help consider these significant parameters. Moreover, it can help improve the control methodologies' performance by co-simulating it with other software and efficiently studying different aspects and tuning control systems safely and inexpensively before transferring it to a full-scale model to test it in the final stage. Meanwhile, the kinematics and compliance and the different operating conditions (Laden and unladen) will be investigated. Although chassis flexibility and the control uncertainties can affect the control behaviour, they will not be addressed in this study for time limitation. However, they are proposed in future work.

Chapter 3: MSC ADAMS model

3.1 Introduction

To accomplish the aim and objectives of this study and fill the gap of using simple vehicle models (bicycle, non-articulated) in developing control systems found in the literature, the need for a safe and inexpensive way to test these control systems and control methodologies is a challenge. Particularly, the traditional models neglect essential factors such as non-linearity, velocity change, different trailers configurations, mass change and distribution, chassis flexibility, kinematics and compliance of the suspension system. These parameters can affect the whole vehicle behaviour, highlighting the importance of finding new techniques and methodologies to develop control systems to consider any essential factor. A scaled RC model is used to investigate the fidelity of simulating tractor semi-trailer using multi-body dynamics software. This chapter illustrates the process of measuring scaled model parameters that have been used later to feed the software, steps to simulate on MSC ADAMS/View, problems encountered through simulation and physical model testing using a simple data acquisition system. At the end of the chapter, the results from both models are presented and discussed. ***Figure 3-1*** shows an overview of the simulation process.

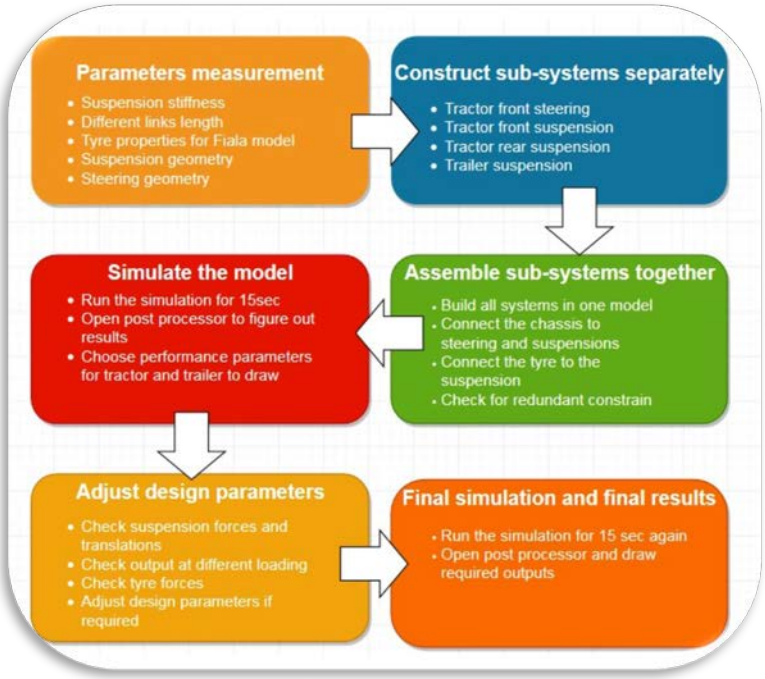

Figure 3-1: Simulation process

3.2 Methodology

Modelling a full vehicle for a tractor semi-trailer on MSC ADAMS is divided into modelling each sub-system separately, then merging all these sub-systems to build the full model. At the beginning of building the simulation model on a multi-body dynamics software, MSC ADAMS/Car was first chosen as it is a package specialised in vehicle dynamics. Each sub-system was built using the building template for ADAMS Car, and then the whole model was assembled in the standard model. However, the model all the time gave an error, and nothing worked. After several investigations and searching for the error cause, after consulting the software provider (MSC software), it was discovered that ADAMS Car could not be used to build a scaled model. The leading cause of this is that the scaled model dimensions and hardpoints are measured in millimetres. So, any small differences in setting the measurements at the beginning can cause the system to lock or fail to operate through the simulation. Also,

the system was built without any engine or driveline system, which was a problem for some simulations which could not run without it.

Furthermore, the ADAMS Car simulation cannot be monitored step by step, which does not give the ability to observe what is happening to each sub-system through simulation. It is hard to find how each sub-system behaves through simulation, mostly built from scratch. The other option was choosing MSC ADAMS/View to monitor what is happening through simulation. Also, it is more straightforward in modifying the model and simulating it. The challenge is to create the vehicle's dynamic tests as there is no driving simulator like ADAMS/Car. Although MSC ADAMS/View is used to model the whole of the vehicle, each sub-system should be modelled first in a different file to be sure that everything is working, because if all the sub-systems are modelled in the beginning in one model, without testing them individually, and the model gives errors, it is tough to know where the error comes. So, testing each sub-system first will help adjust the hardpoints and parameters and validate it before integrating it with the other sub-systems.

The study's main objective is to check the scaled model's ability to be built on a simulation model and study its handling characteristics. So, building the electric motor and the driveline in the scaled physical model is neglected, and the driving torque of the vehicle is applied directly to the wheel hub of the tractor rear axle. The main parameters that need to be measured are the dimensions of each part, weight and hardpoints for each tractor-trailer sub-system. However, some parameters need to be tested to determine their properties which are fed into the simulation model. These parameters are the Fiala model's tyre parameters, leaf spring stiffness, damper damping coefficient. After collecting all the data and analysing each sub-system, the simulation model can be built. Then all the tested sub-systems can be assembled into one model to run the simulation.

The simulation model's validation was done through a simple data acquisition system integrated with the physical model. The tractor and the trailer's main motions were gathered to be compared with the results from the simulation model.

3.3 Scaled model description

3.3.1 General description

The model consists of two main parts; the tractor, a scaled model of the Scania R620 with a dual rear axle and the trailer with three axles. The tractor is divided into eight sub-systems; chassis system, front steer-suspension, tandem rear suspension, front & rear leaf springs, front & rear tyres and auxiliary parts, while the trailer consists of four sub-systems; the chassis system, three axles rear suspension, leaf springs, and tyres system. When modelling these sub-systems, some measurements should be made to be fed to the software to build each sub-system. Also, some design parameters such as the roll centre and the weight distribution should be measured for the whole model to set the appropriate data. Table 3-1 and Table 3-2 present the different parameters of the tractor and trailer.

Table 3-1:Tractor specifications

Total chassis Length	520 mm
Width	187 mm
Height	293 mm
Weight (without electric option)	3.7 kg
Wheelbase	237 + 103 mm
Tread (front)	156 mm

Tread (Rear, Double)		138 mm
Chassis		Aluminium & polycarbonate resin ladder frame
Caster angle (front/rear)		0º
Camber angle (front/rear)		0º
Toe angle (front/rear)		0º
Dampers		Aluminium dummy dampers
Transmission gear ratio	1st gear	32.49:1
	2nd gear	17.76:1
	3rd gear	10.66:1
Differential		3- bevel differential
Motor type		RS 540
Tyre width		22 mm
Tyre Diameter		83 mm
Servos		2
Battery		7.2 volt

Table 3-2: Trailer Specifications

Total chassis Length	917mm
Width	188mm
Height	300mm
Unloaded weight	30 N

Loaded weight	100 N
wheelbase	630mm
Tread	150mm
Chassis	Aluminium & polycarbonate resin ladder frame
Caster angle (front/rear)	0^o
Camber angle (front/rear)	0^o
Toe angle (front/rear)	0^o
Dampers	Aluminium dummy dampers
Tyre width	22 mm
Tyre Diameter	83 mm

3.3.2 Measuring Leaf spring parameter

As mentioned before, some components' characteristics need to be measured in a laboratory, while other parameters are taken from literature. The scaled model is equipped with leaf springs for all its axles; the tractor has four leaf springs while the trailer has six-leaf springs. Each of the leaf springs consists of three non-equal layers. MSC ADAMS/Car has a built-in function to draw each leaf's profile separately and describe the connection, axle configuration, and material properties and then it builds the leaf spring system. However, since the system is built on MSC ADAMS/View, which does not have this built-in function, the stiffness for each spring is measured by a compression test on a tension-compression test rig as shown in Figure 3-2 and Figure 3-3. Then the stiffness determined from the curve is fed to MSC ADAMS/View. Figure

3-4 presents the force-displacement curve. Moreover, from the curve, the spring stiffness coefficient is 33.2 N/mm.

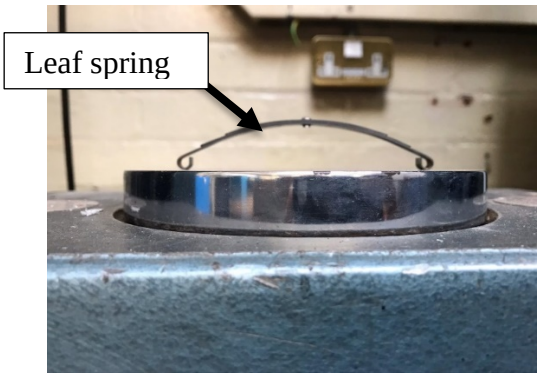

Figure 3-2: Leaf spring on the compression test rig

Figure 3-3: Instron machine test rig

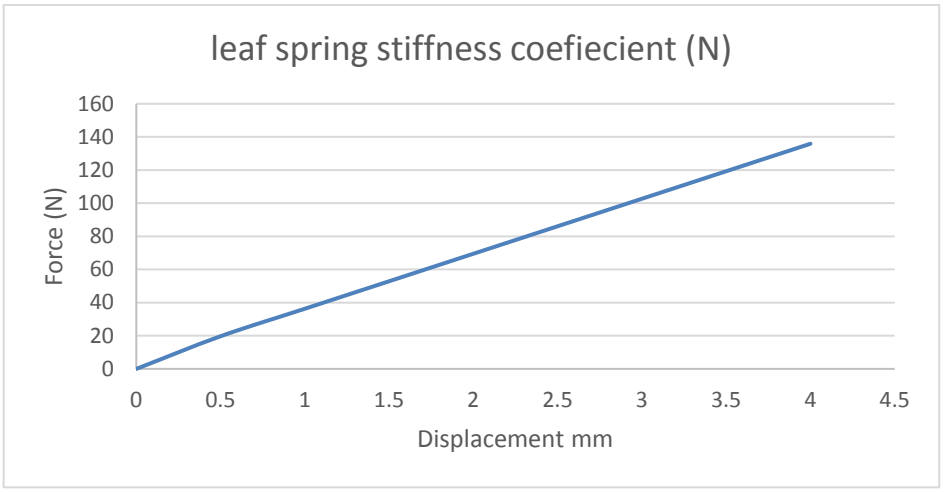

Figure 3-4: Force-displacement leaf spring curve

3.3.3 Damper

The damper is responsible for damping the vertical motion of the vehicle. The scaled model is equipped with twelve typical dampers, six for the tractor and six for the trailer. The damping coefficient is not measured experimentally, as it is very tiny, and no test rig was available to measure it. So, the value of the damping coefficient has been calculated based on the damping ratio. For the vehicle suspension, the damping ratio is assumed to be 0.2, and by using the formula, the damping ratio with the damping coefficient from [123] is stated in Equation 3.1. Then finally, by measuring the mass of different wheels to calculate the average load per wheel (0.750 kg). The damping coefficient is calculated to be approximately 2 N.s/m. Figure 3-5 shows the damper equipped in the vehicle.

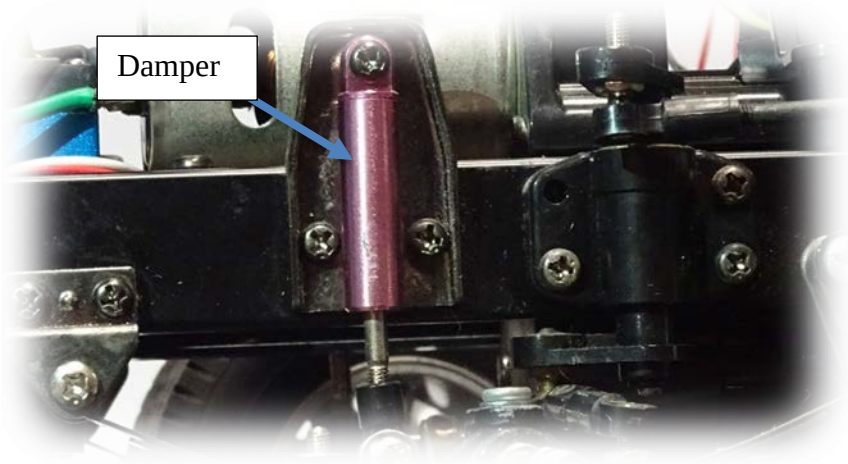

Figure 3-5: Damper

$$C = 2\lambda\sqrt{km} \quad Equation\ 3-1$$

Where:

C : $is\ the\ daming\ coefficient\ measured\ in\ N.\frac{s}{m}$

λ: is the damping ratio

k : is the spring stiffness N/m

m: is the mass kg

3.3.4 Tyre

The tyre parameters are one of the foremost vital parameters that need to be adequately measured. The tyre is the connection between the vehicle and the road, and the handling characteristics can vary very much if the tyre is simulated incorrectly. The default tyre model that is used in MSC ADAMS/View is the Fiala model. The tyre property file (Appendix A) in MSC ADAMS needs eleven parameters to fill it; four parameters for the tyre dimensions(radius, width, aspect ratio and shape), three parameters describing the relation between the tyre and

road surface, including the maximum and minimum road adhesion and the tyre rolling resistance, the rest of the parameters are the vertical tyre stiffness and damping, tyre lateral and longitudinal slip stiffnesses. Measuring the tyre parameters gives an initial understanding of the values used and inserted in the tyre property file; the tyre is tested alone in MSC ADAMS/CAR (Standard mode) to ensure the correct values. The values have been tuned by running different simulations, and by trial and error method, the parameters are adjusted according to the longitudinal force versus the slip curve. Some parameters were not measured because they need a special test rig, so the values are taken from the literature [55]. Figure 3-6 shows the measurement of the tyre diameter as an input to the Fiala model. Figure 3-7 presents the tyre on the Instron machine for measuring the material properties. The Instron machine is used to measure the vertical stiffness of the tyre. Figure 3-8 presents the designed test rig to measure the tyre's lateral stiffness using a force gauge. The tyre rim is fixed to a box, a handwheel with thread is fitted from the box's underside, and the force gauge is replaced in passage to allow the force gauge movement in one direction. The handwheel is rotated to move the force gauge; when the tyre is deflected, the force's value and the tyre's deflection are recorded. After collecting the tyre force and deflection from the test, the lateral tyre stiffness is calculated.

Figure 3-6: Measuring outer tyre diameter

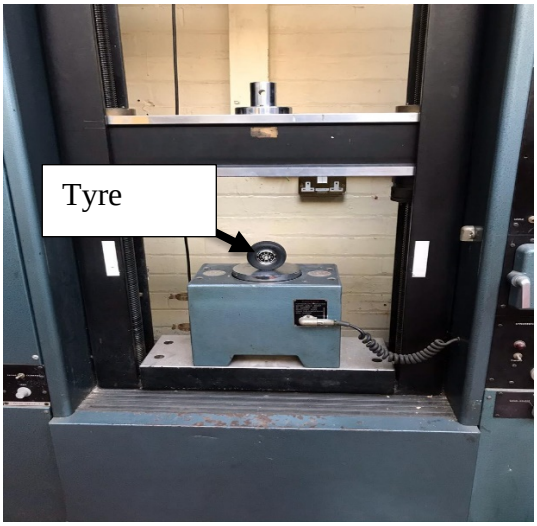

Figure 3-7: Testing tyre on the Instron machine test rig

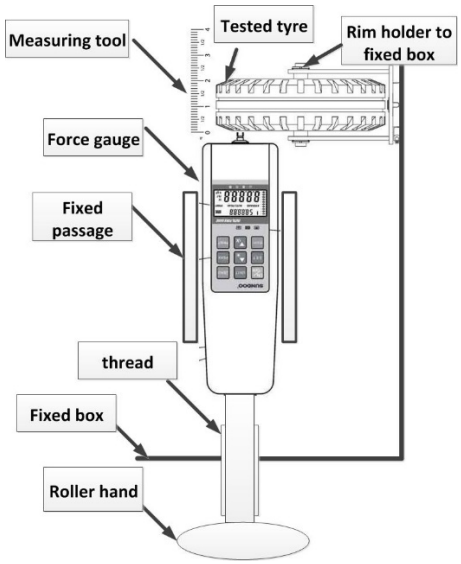

Figure 3-8: Force Gauge

3.3.5 Measuring different lengths

The rest of the scaled model needs some measurements to identify the dimensions and masses for each part. An example of measuring these dimensions is shown. Figure 3-9 demonstrates an example of the way for collecting different dimensions from the trailer. Figure 3-10 depicts another method used for collecting small measurements from the tractor.

Figure 3-9: Measuring different dimensions for trailer parts

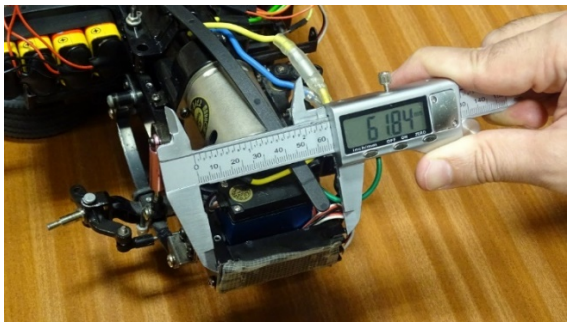

Figure 3-10: Measuring different dimensions for tractor parts

3.3.6 Measuring mass and moment of inertia

The masses of the whole tractor and trailer have been measured. Every single part was measured to be fed to the model; the way it is added to the simulation model is by changing the part's density to adjust every single part's mass. The simulation model calculates the different mass moments of inertia for each part according to its mass and geometry. After the whole model is constructed, the simulation software validates the model joints and degrees of freedom. Also, a table was constructed in excel to calculates the tractor yaw moment of inertia Iz. The trailer moment of inertia was not calculated as there is no need for it in the reference model later. The calculation was based on the parallel axis theorem by knowing the mass moment of inertia for

each part, its centre of gravity in the x,y,z-directions, and the main centre of gravity of the tractor. Table 3-3 shows the values of mass and mass moment of inertia.

Table 3-3: Mass and mass moment of inertia values

part	value
The total mass of the tractor	2.000478116 kg
The total mass of the trailer	13.557 kg
Moment of inertia for tractor	371524.3*10e-06 $kg.m^2$

3.4 Tractor simulation model

As mentioned above, the simulation model is built on MSC ADAMS/View. The system is 168 degrees of freedom and includes eighty-two parts. The tractor is the first component of the model and is responsible for towing the trailer and directing it. The tractor simulation model consists of five sub-systems, as the front and rear leaf springs are integrated with the front and rear suspensions and the steering integrated with front suspension. Some simplifications assumed to facilitate each sub-system's simulation and will be mentioned in each section and the reason for this assumption. Each link of the tractor has been measured, and each link's mass has also been considered. The hardpoints on each link have been specified relative to the lower-left front point of the vehicle chassis.

3.4.1 Tractor chassis

The tractor chassis consists of two C channel vertical beams 20mm*5mm*1mm connected with five side beams, three are I channel, and the others are C channel. Also, there are different links and parts connected to the chassis to facilitate assembling the rest of the vehicle. The chassis is

simulated in MSC ADAMS/View as one rigid box with dimensions 500*60*20 mm with eight holes 40mm*20mm depth inside it to reduce the total chassis weight. Also, there are small links attached to the chassis for suspension attachment. Moreover, aluminium's material was chosen to enable the modelled chassis' weight to equate to the original chassis's measured weight. The tractor chassis is the first part of being built-in the whole model, and the tractor axis system is chosen such that the positive x-axis means that the vehicle is moving in the forward direction, the positive y-axis means the vehicle is going left, and the positive z-axis is in the upper direction. Figure 3-11 shows the tractor chassis representation in MSC ADAMS/View.

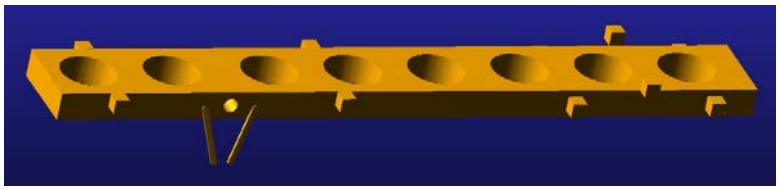

Figure 3-11: Simulation model tractor chassis

3.4.2 Tractor front steer-suspension

The front steer-suspension consists of sixteen parts; a front axle has been divided into three parts, the left and right parts connected to two uprights, while the middle part connects the left and right parts. Besides, two dampers have been placed. Furthermore, two leaf springs are connected, one leaf between the left side of the front axle with the tractor chassis and the other one between the right side of the front axle and the tractor chassis. The leaf springs are based on SAE standard (i.e. three links for each leaf connected with bushing) [37]. A tie rod is connected between the left and right uprights to complete the Ackerman steering geometry. Three links are connected with the tractor chassis from one end and to the steering geometry from the other end; namely, Pitman's arm, steer link arm and steer arm, and they are responsible for generating the steering angle that the simulation model will move with it. Two parts from

the left and the right named spindle are the connection between the front steer-suspension and the front tyres. Figure 3-12 shows the tractor front suspension's physical model, and Figure 3-13 presents how the tractor front suspension is analysed; then Figure 3-14 shows how the tractor front suspension is represented in the simulation model.

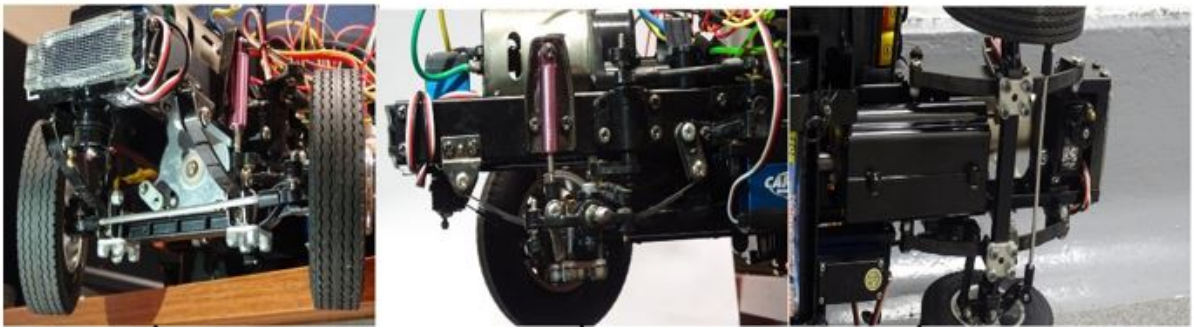

Figure 3-12:Physical model tractor front suspension

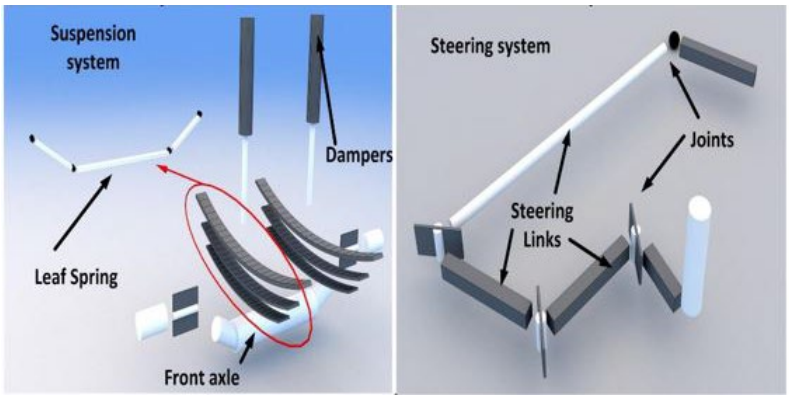

Figure 3-13: Physical systems analysis for tractor front suspension (hardpoints and joints)

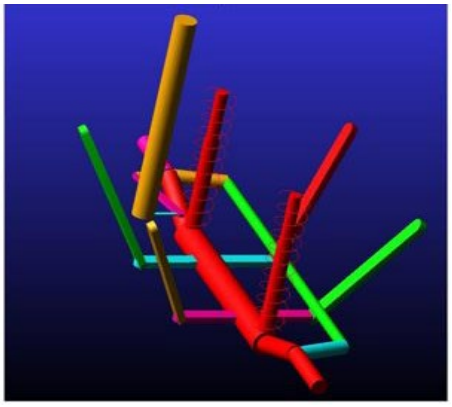

Figure 3-14: A simulation model for tractor front suspension

3.4.3 Tractor rear suspension

The tractor rear suspension consists of twenty-one parts; a tandem suspension system, which has two axles. Also, they are the driven axles, so each one has a differential that connects the axle to the driveline system. The axles are connected to the chassis through small links and a fixed plate. Moreover, the two axles are connected through a leaf spring. Also, the left and right leaf springs are connected through a link going through the tractor chassis. The leaf springs are based on SAE standard (i.e. three links for each leaf connected with bushing). The dampers are connected between the tractor chassis and a fixed link to the axles.

Furthermore, four hubs are connected to the axles from the left and right axles so that the dual tyres can be connected to them. Figure 3-15 illustrates the torque calculated according to the DC motor characteristic curve, the gearbox speed ratio, differential ratio and different simulation trials to achieve a specific velocity curve (refer to the velocity curve).

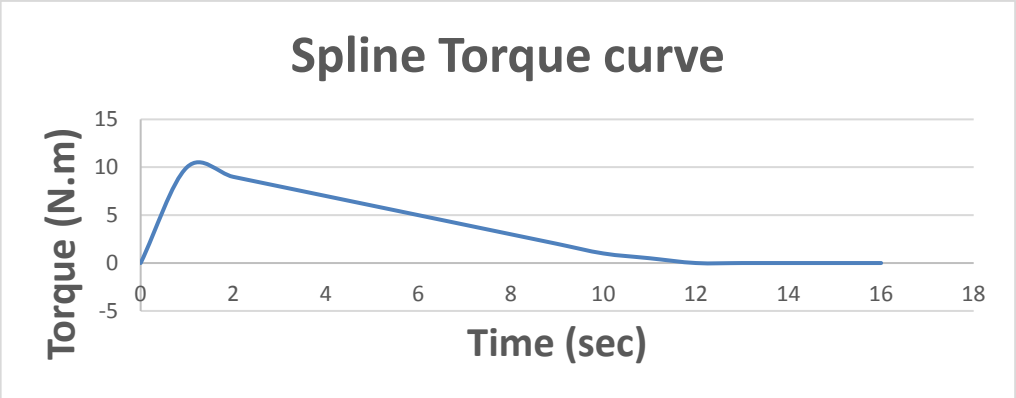

Figure 3-15:spline torque curve

Figure 3-16 shows the tractor rear suspension's physical model, and Figure 3-17 presents how the tractor rear suspension is analysed. Then, Figure 3-18 shows how the tractor rear suspension is represented in the simulation model.

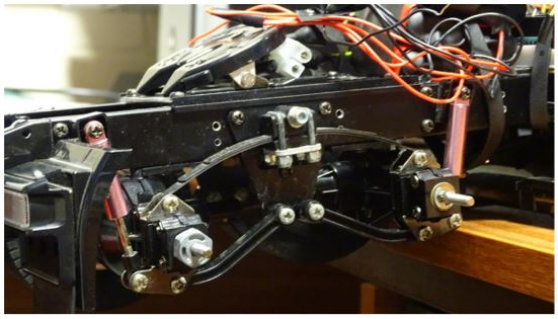

Figure 3-16: Physical model rear suspension

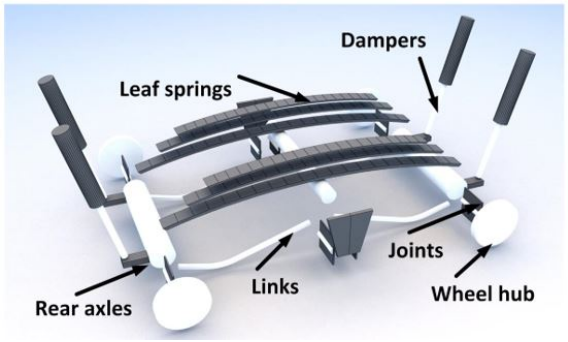

Figure 3-17: Physical system analysis (hardpoints, parts and joints)

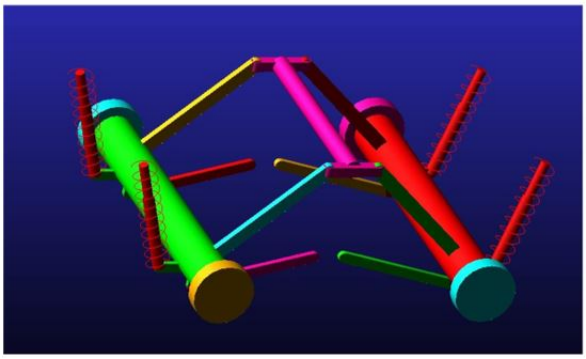

Figure 3-18: A simulation model

3.4.4 Tractor tyre

The tractor has ten tyres, two tyres at the front axle and eight tyres at the tandem rear axles. For the tandem rear axle, the inside and outside tyres are connected with fixed joints. The main torque that moves the whole tractor is set up on the hub of the inside wheel. MSC ADAMS has a template for several tyre models as the work will concentrate on handling. Fiala model was chosen as mentioned before because of its simplicity as a handling model. Also, characterising the Fiala model requires fewer parameters to identify to build the model. The tyre's orientation is (0,90,0), and the road attached to the tyre is a flat 3D smooth road. Figure 3-19 shows the tyre simulation.

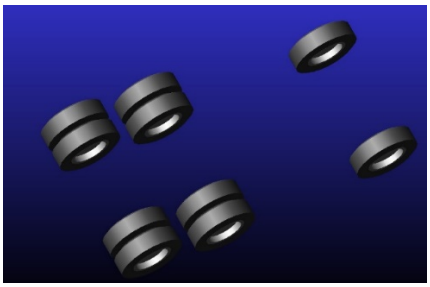

Figure 3-19: Simulation model tractor tyres

(c)

3.4.5 Tractor fifth wheel

The fifth wheel is a single-cylinder part that is connected between the tractor chassis and the trailer chassis. The fifth wheel is connected to the tractor chassis with two bushings; the bushings are located with an offset from the fifth wheel centre, one to the left and one to the right, as shown in Figure 3-20. Also, it is connected to the trailer with one bushing in the centre. The translational stiffness and damping values and the rotational stiffness and damping for the bushing are selected by trial and error.

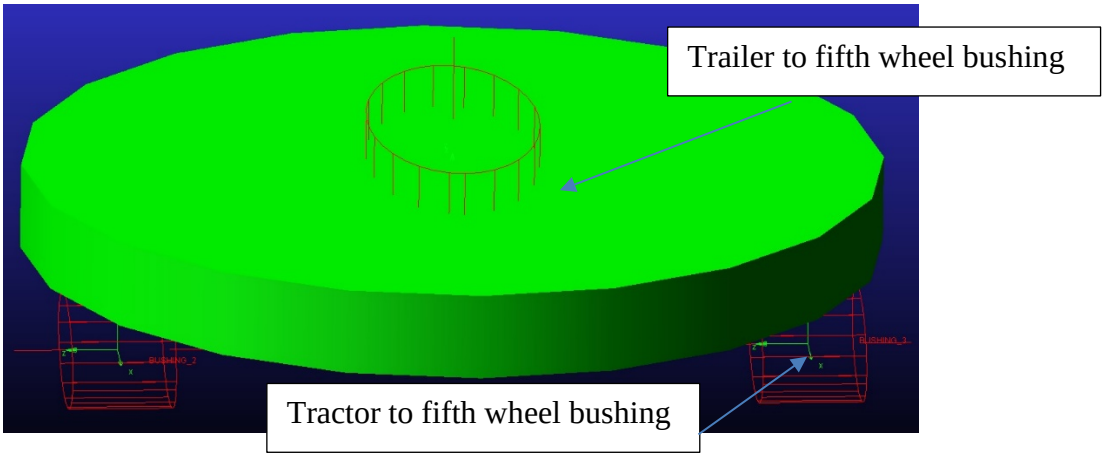

Figure 3-20:fifth wheel for the tractor semi-trailer

3.5 Trailer Simulation model

The trailer is the second component of the model and consists of four sub-systems. The trailer tyre is the same as the tractor tyre, and the trailer axles have a single wheel on each side. The trailer is subjected to some modifications in the sub-systems' simulation to build the trailer like the tractor. The trailer is 1/14. They were scaled from a 40-ft extended trailer holding a container. Each link of the trailer has been measured, and each link's mass has also been considered. The hardpoints on each link have been specified relative to the lower-left front point of the vehicle chassis.

3.5.1 Trailer chassis

The chassis system for the trailer is a two L channel non-uniform beams connected with five side beams, three of which are I channel, and the rest are C channel. Some tiny parts are connected to the chassis to allow the suspension to be attached to the trailer chassis. The chassis is simulated in MSC ADAMS/View as two rigid boxes in one part, the first of which is connected to the tractor chassis with the dimensions 1000*60*20mm, the second rigid box with the dimensions 900*60*20mm. The two markers for both boxes have the same x-axis, y-axis value, and z-axis. The chassis has nine holes 40*20mm Depth to adjust the chassis's weight; some small links are also present. Moreover, aluminium's material was chosen to enable the modelled chassis' weight to equate to the original chassis's measured weight. Figure 3-21 presents the trailer chassis in the simulation model.

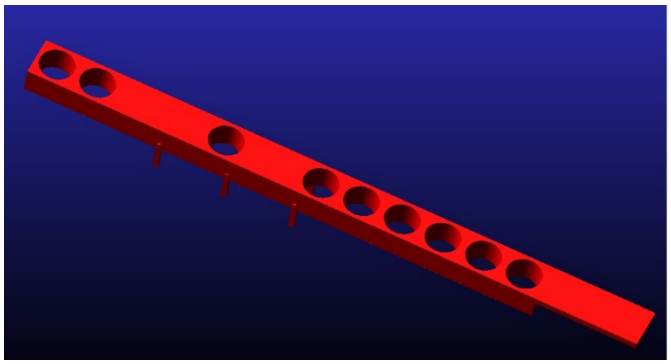

Figure 3-21: Simulation model trailer chassis

3.5.2 Trailer suspension

The trailer suspension is a three axles dependent suspension with a single tyre on either side of each axle. The tractor suspension consists of thirty-nine parts. The axles are connected to the chassis through small links and a fixed plate. Moreover, the three axles are connected through coupled leaf springs. The leaf springs are represented similarly to the ones in the tractor. The

dampers are connected between the tractor chassis and a fixed link to the axles. Furthermore, six hubs are connected to the axles from the left and right axles so the single tyre can be connected to it. Figure 3-22 shows the trailer suspension's physical model, and Figure 3-23 present how the trailer suspension is analysed, and Figure 3-24 shows how the trailer suspension is represented in the simulation model.

Figure 3-22: Physical model trailer suspension

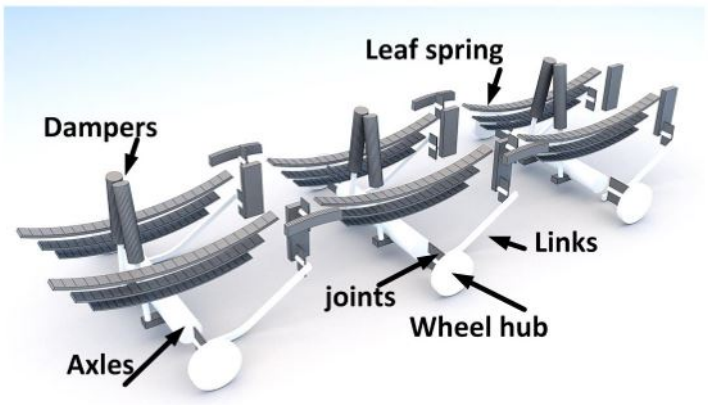

Figure 3-23: Physical systems analysis (hardpoints, parts and joints)

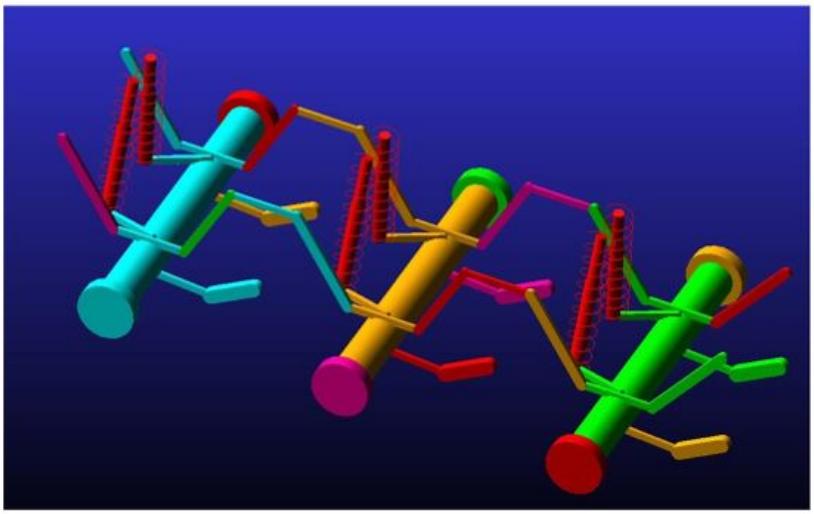

Figure 3-24: A simulation model

3.5.3 Trailer load

The trailer load is represented by a box that is attached to the trailer chassis by fixed joints. The box dimension is 900mm in length, 180mm in width and 190mm in height. So, the weight is distributed equally along with the trailer chassis and symmetrically about the longitudinal axis. The box's material density is adjusted to represent the 100 Newton that should be loaded into the trailer. The 100 N load is obtained by scaling according to the full-scale trailer's maximum load. The load is scaled by dividing the maximum load of 27440 kg by $(14)^3$; the cubic scaling size [58]. Figure 3-25 presents the trailer load.

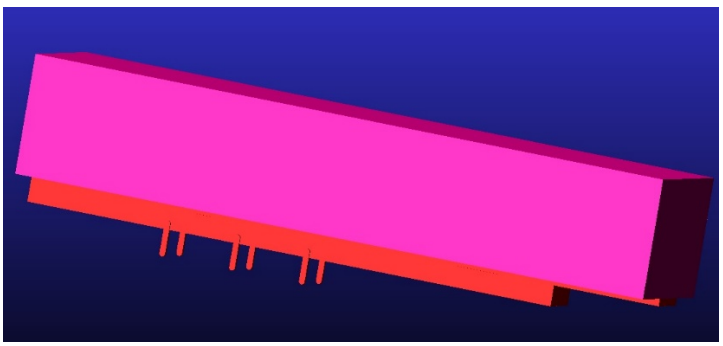

Figure 3-25: Simulation model trailer load

3.6 Physical tests on a Scaled model

A vehicle road test is one of the most critical methods in determining vehicle characteristics. The road test aims to identify the vehicle's real performance, whether it is a prototype or a new feature has been added. The road test is carried out according to standards; each standard specifies the essential variables that should be measured and the critical values for these variables. The vehicle is equipped with different sensors to measure the output variables according to the test standard; then, all the data is collected for analysis. In developing any control system, the vehicle is tested twice (one without the controller and one with the controller) to compare the control's effectiveness. The physical RC Scaled model is used to validate the simulation model. The RC Scaled model is modified to perform standard tests autonomously. The reason for programming a controller to drive the vehicle autonomously is because the radio controller was not giving a precise steering angle and not providing precise motor speed control.

Moreover, the controller allows integrating ultrasonic sensors for measuring the distance to avoid obstacles and accelerometers, gyroscope and magnetometer for calculating heading. The next section illustrates the set up for the tractor and trailer in detail.

3.6.1 Tractor initial set up

The tractor is responsible for towing the trailer, so most of the driving and controlling parts are integrated. The tractor was designed to be controlled through a radio control signal. The radio control signal depends on a transmitter and a receiver. The radio control controls the DC motor, which provides the motion to the tractor and two servo motors; the first motor for the steering mechanism and the second motor for the gearbox selection. The two servo motors are connected to the transmitter, and the DC motor is connected to a speed controller, and this speed controller

is connected to the transmitter. So, the radio control is responsible for moving the vehicle forward and backwards, steering the vehicle and shifting the gearbox's gears.

3.6.2 Tractor modified set up

The physical test's control is so essential that the vehicle performs the standard test as accurately as possible, so the tractor was modified to replace the radio control and the speed controller with a programmed microcontroller board. This microcontroller is equipped with sensors integrated into the tractor, so by the feedback from the sensors, the microcontroller performs the required tests via a developed programme installed in it. The following section will describe the controller, sensors, actuators, and power source used to perform the tests before illustrating more. Figure 3-26 shows the physical model control circuit. Figure 3-27 presents the controller used for controlling the vehicle motion. Figure 3-28 demonstrates how the microcontroller depicts the vehicle motion.

3.6.3 Tractor controller

The controller is the central part of any control system. The controllers used for the tests are Arduino Mega 2560 and Arduino Uno. The Arduino Mega 2560 and Uno microcontrollers are based on ATmega2560 and AT mega 328, respectively. They differ in the number of input/output ports and their types. Both are used together in the tractor as the Arduino Mega controls the tractor motion, and the Arduino Uno is used for recording the six motion results and the heading. The Arduino Mega can do both together, but the maximum sampling rate will be 3 Hz, so the Arduino Uno is added to the system to record the data on an SD card, while the Arduino Mega is controlling the motion only. Integrating two Arduino microcontrollers allows raising the sampling rate to 10 Hz.

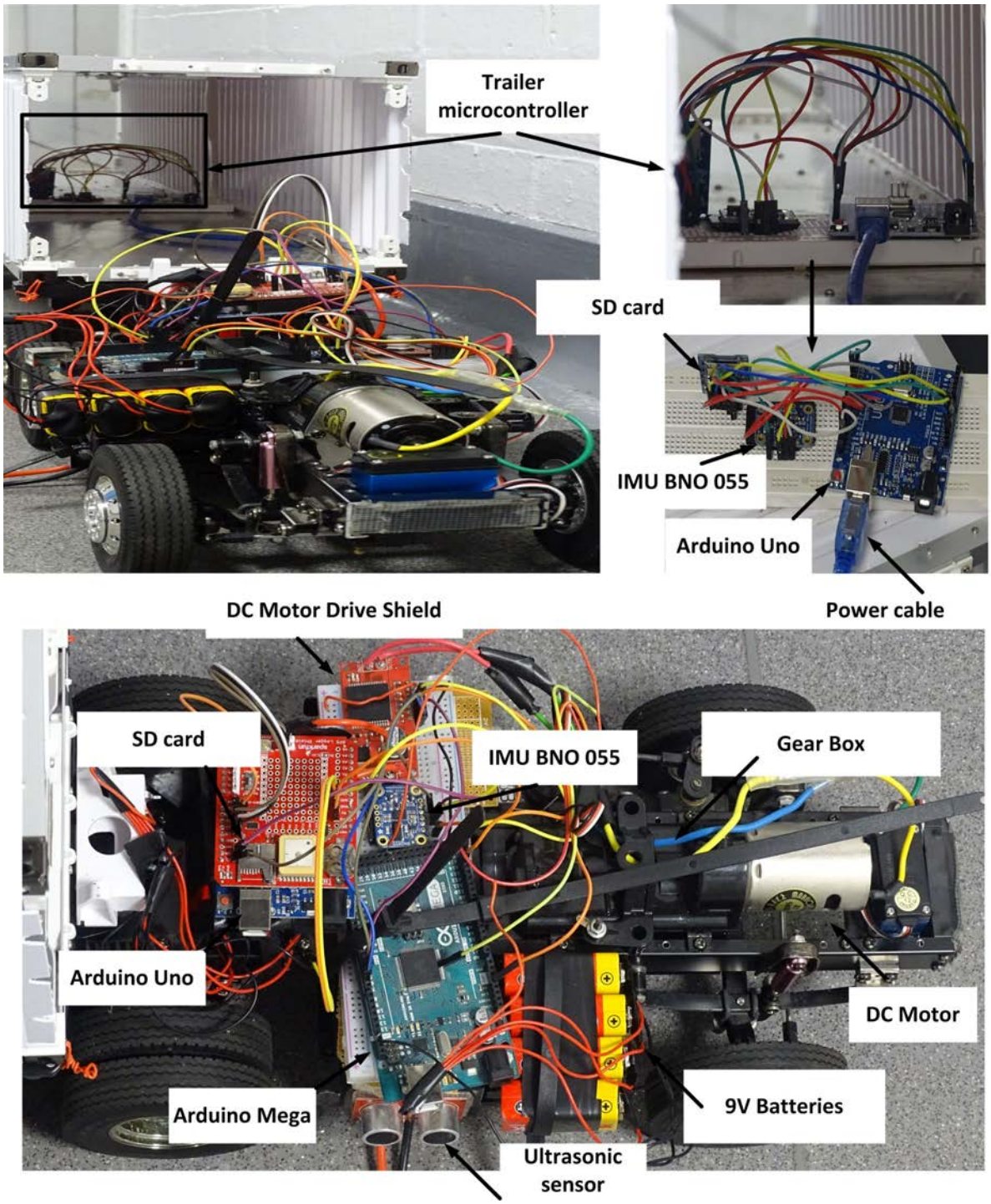

Figure 3-26: Physical model control circuit

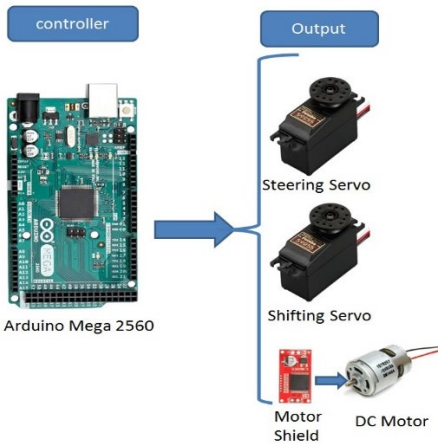

Figure 3-27: Motion controller

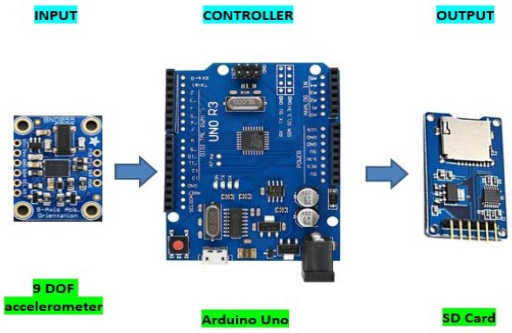

Figure 3-28: Motion gathering controller

3.6.4 Ultrasonic sensor

The ultrasonic sensor is used to avoid tractor-trailer crash with any obstacle while performing the tests. The ultrasonic sensors that are used are HC-SR04. This kind of sensor uses sonar to determine the distance. This sensor's range is between 2cm to 400 cm, and it gives readings at a frequency of 40Hz. The ultrasonic sensor is fitted on the tractor chassis on three different sides (front, left and right). The ultrasonic sensor is connected to the Arduino Mega 2560 through the digital pins (one pin for transmitting the signal and the other for receiving it). The ultrasonic sensor is ideal for the model running at low speeds; however, if the vehicle were to

move at a higher speed, say more than 12 km/hr, the ultrasonic sensor will not be efficient as the inertia of the vehicle will require much longer stopping distance, and the vehicle will collide with the obstacle unless there is a brake system in the RC model.

3.6.5 Inertial measurement unit

The inertial measurement unit (IMU) is used to capture the tractor's longitudinal, lateral and vertical accelerations and the pitch, roll, and Yaw rate of the tractor. The BNO 055 is a System in Package (SiP), a three-axis 16-bit gyroscope with a ±2000 degrees per second, combining a three-axis 14-bit accelerometer, a three-axis geomagnetic sensor and a 32-bit cortex M0+ microcontroller running Bosch Sensortec sensor fusion software, in a single package. The chipsets are combined into one single 28-pin LGA 3.8mm x 5.2mm x 1.1 mm frame. The BNO 055 is fitted out with digital bidirectional I2C and UART interfaces[123]. An SD card shield is connected to the Arduino Mega to record the results. The SD card uses the SPI ports for Arduino Mega.

3.6.6 Dc motor and motor shield

The DC motor is responsible for moving the tractor, as mentioned before. The DC motor is RS-540SH-5045 with a maximum speed of 17500 rpm at no load and 15080 rpm at maximum efficiency. The DC motor can produce 50.1 watts with a maximum torque of 31.8 mN.m and a current of 5.93 amperes. The Arduino cannot deliver high current to the DC motor, so a motor shield must bridge the microcontroller and the DC motor. The motor shield used is the single monster motor shield that can deliver up to 30 amperes.

3.6.7 Servo motor

The tractor is equipped with two servo motors, one for the steering and the other for shifting the gears. The servo motor works with 5V and ground from the Arduino pins and a digital pin signal. The servo motor can rotate 180 degrees. However, the steering servo ranges from 20 to 140 degrees and the shifting servo from 0 to 180 degrees. It is preferred in the future to use a high torque servo motor so it can provide a more precise steering angle. Also, inserting hard links for the steering will avoid any tolerances (backlash) in the steering system and provide a precise steering angle.

3.6.8 Power source

The power source that the tractor is equipped with consists of two sources; the first one is a lithium battery for the DC motor and the second one is eight 9V batteries for the controller. The lithium battery is provided with the vehicle, the maximum voltage produced is 8.4V, and the maximum capacity is 4800 Ah. The 9V battery is a zinc-carbon cell with 50mAH. To deliver the controller and the sensors' power, eight 9V batteries are connected in parallel to deliver the required current to the whole circuit. Furthermore, a power bank has been used to deliver power for the controller of the trailer.

3.6.9 Trailer

The trailer is more straightforward than the tractor. The trailer has the same IMU sensor to record the different motions. An SD card shield is connected to the Arduino Uno to record the results. The SD card uses the SPI ports for Arduino Uno, and the programme is designed to collect data using the same sampling rate as for the tractor. The power source is taken from the

tractor via two wires connected to the Arduino Uno, and the whole kit is placed at the centre of gravity of the trailer.

3.6.10 Wiring diagram

The wiring diagram shows how each sensor or actuator is connected to the controller. Figure 3-29 shows the DC motor controller, while Figure 3-30 presents the IMU connection.

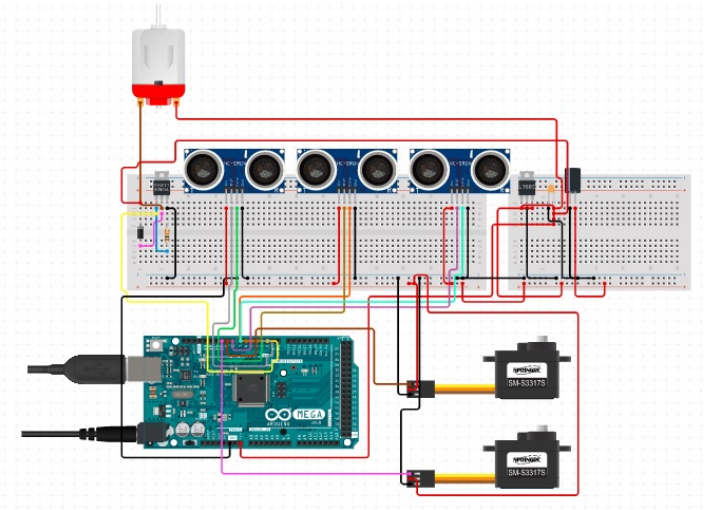

Figure 3-29: DC motor controller

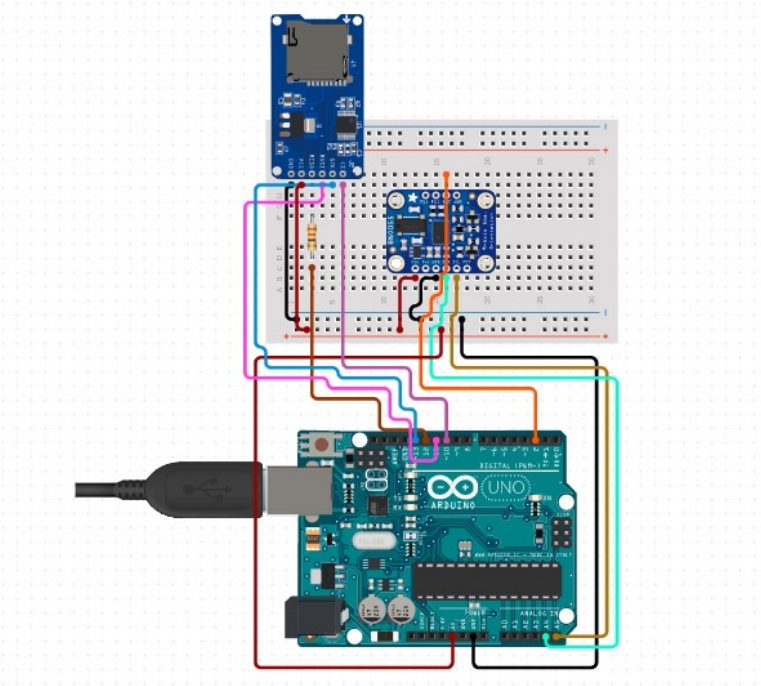

Figure 3-30: Inertial measurement unit circuit

3.6.11 Program IDE

The IDE is the interface software used to write, modify, compile and upload the Arduino program on the microcontroller board. The IDE uses the C++ language to write the Sketch of the controller. At the beginning of Sketch, the microcontroller software defines the different hardware parts and then runs a loop to control the hardware. As there are three microcontrollers in the circuit, there are three programmes; two of them are similar, and the other is for controlling the tractor's motion. The IDE programmes that are used are in (Appendix B)

3.7 Important notes about Simulation and Physical modelling

The scaled model has small tiny parts, and connecting them needs two essential things; the first is to ensure the correct orientation of the part while assembling, the second thing is to tighten the parts because the vehicle's motion will cause disassembly of any loose part. Furthermore, for measuring the accelerations and the angular velocity from the sensor, a PCB is preferred to

be integrated after testing all the parts together on a breadboard; also, any loose connection in the wires will cause missing reading or improper control. Moreover, the system's orientation and direction of each axis's positive and negative aspects should be unified with the simulation model and the SAE axes standard.

3.8 Standard tests

3.8.1 Introduction

Testing the performance of a vehicle requires many tests before it can be launched. These tests firstly ensure that the vehicle will achieve the minimum safety requirements. Also, they can be used as regulations for designing new vehicles.

Furthermore, these tests can be used to compare different vehicles' performance and determine which is better. These regulations are set up through authorised organisations. The International Standards Organisation (ISO) is one of these organisations that have set up standards for different situations to measure the vehicle's performance and specify if the vehicle is safe enough or not. As the physical model is a scaled model, for simplicity, two standard tests were chosen to test the vehicle's performance and compare the output with the simulation model. After reviewing the commercial vehicle standards (BS ISO 14791:2000, BS ISO 14793:2003, BS ISO 18375:2016), two tests were chosen to be performed to investigate the simulation model's validation of the physical model.

3.8.2 Straight-line test scenario

In this test, the physical tractor-trailer is tested inside an indoor tennis court, so the distance was not too long, limiting the whole test to be not more than 16 seconds due to the court length. The vehicle starts from rest and keeps accelerating in a straight line, and no steering angle is

provided in this test; The DC motor is operated to the full load in the beginning so it can give a high torque on the wheels, as it is multiplied by the gearbox ratio and the differential ratio. After moving, the torque starts to be reduced on the wheels, and when it reaches 6 seconds, the torque starts to diminish, and the vehicle starts to decelerate until it stops, which takes another 10 seconds. To validate the simulation model with the physical model, the simulation model is applied with a torque using the spline curve shown in Figure ***3-15***, which is calculated from the DC motor characteristic curve with the driveline data, and the test time is adjusted to be 16 seconds to match the one from the physical test. The speed for both the physical and simulation models when moving in a straight line is up to 3 m/sec.

3.8.3 Results from the straight-line test

Two main outputs were considered, longitudinal acceleration and longitudinal velocity, as shown from Figure 3-31, which displays the longitudinal velocity. The physical and simulation models follow the same trend of the velocity through the whole test from the two curves.

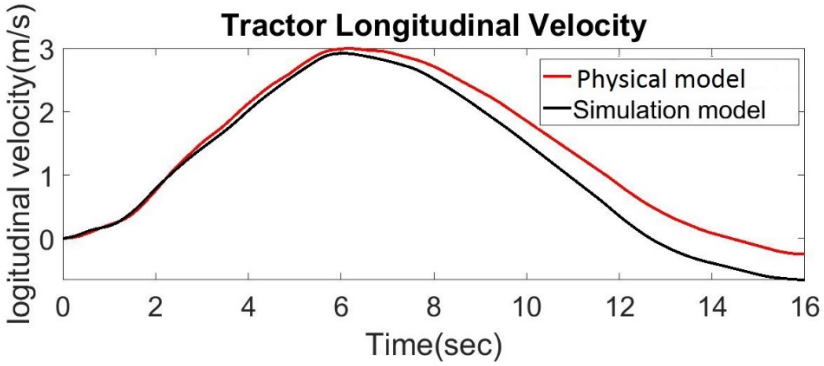

Figure 3-31: Tractor-Trailer longitudinal Velocity

Figure *3-32* shows a comparison between the tractor longitudinal acceleration for the simulation and physical test. The longitudinal acceleration measured in the physical test is slightly higher than the simulation model predicts. It is observed that the simulation model accelerated until it reached the required speed, but the velocity was not maintained at a constant value, unlike the physical test, which maintained a constant velocity for a short time before decelerating. The velocity curve illustrates why the simulation model's tractor acceleration profile was lower than for the physical test. However, both curves follow the same trend, reflecting the connection between the velocity and the acceleration curves.

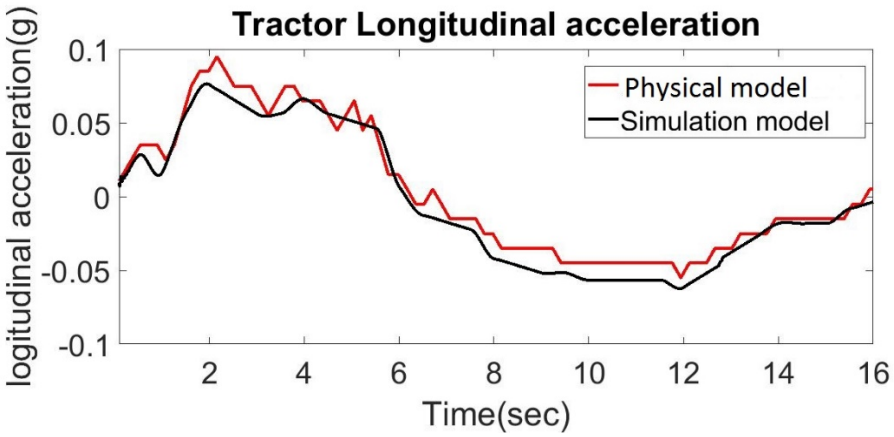

Figure 3-32: Tractor longitudinal acceleration

Figure *3-33* presents the longitudinal acceleration for the trailer in which simulation and physical test nearly match each other. The acceleration in the physical model is lower slightly than the tractor. Some of the acceleration effects diminish in the connection between the tractor and the trailer.

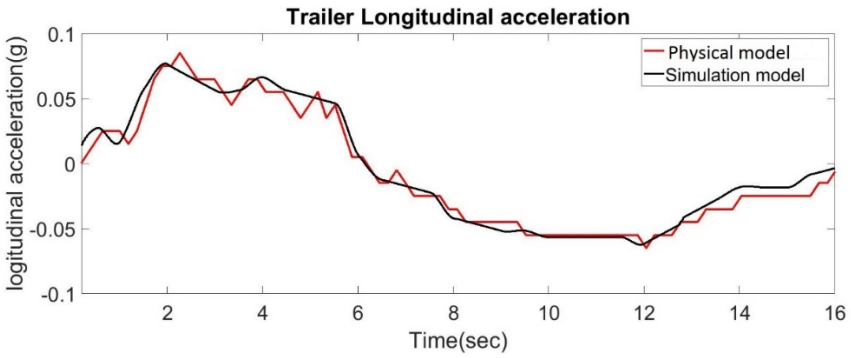

Figure 3-33: Trailer longitudinal acceleration

3.8.4 Lane-change test scenario

When the tractor-trailer is tackling a lane-change manoeuvre, it can present the performance in handling situations to test and develop control systems after the validation process. Figure 3-34 presents the path followed by both the physical model and the simulation model to achieve the lane-change scenario. First, the vehicle is moving in a straight line and starts to accelerate until it reaches a required speed, and then at the sixth second, it starts to give a steering angle which makes the vehicle deviate from its original path. After this, the steering angle of the vehicle is reversed, so the vehicle returns to a straight position that returns the whole vehicle to move in a straight line again with the new lane parallel to the first one. The path shown in ***Figure 3-34*** describes the lateral distance between the two lanes measured in mm., which is suitable for the width, length and articulation of the tractor semi-trailer.

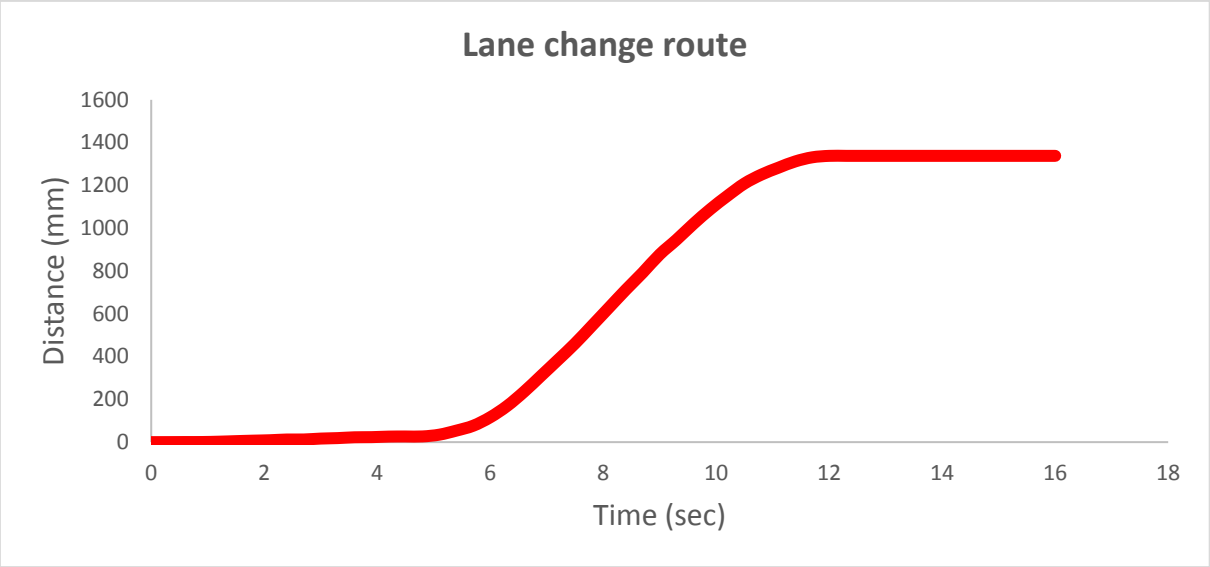

Figure 3-34: Lane-change route

3.8.5 Results from the lane-change test

There are two primary responses collected; lateral acceleration and Yaw rate. Those parameters are used to identify the handling behaviour for both the physical test and the simulation model. The test starts with the vehicle accelerating from rest until the test speed is achieved, then it executes a lane-change manoeuvre until the tractor-trailer completes the manoeuvre. Figure 3-35 and Figure 3-36 display the lateral acceleration for both the tractor and the trailer, and from the figures shown, the simulation model curve is smoother than that of the physical model. However, there is a good match between simulation and physical test results, and both follow the same trend.

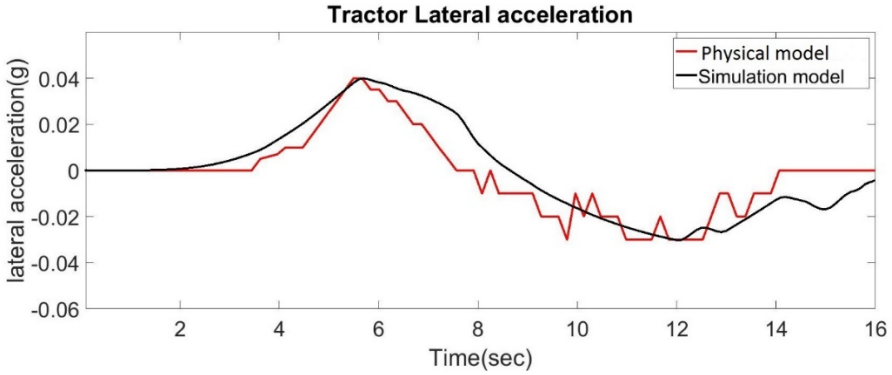

Figure 3-35: Tractor lateral accelerations

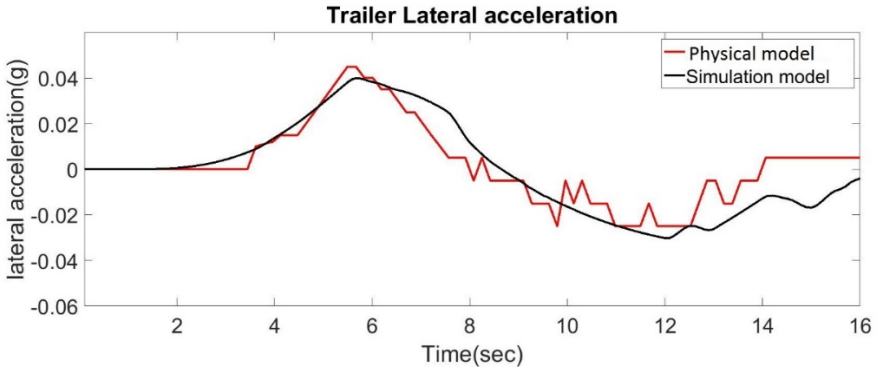

Figure 3-36: Trailer lateral acceleration

Figure *3-37* and Figure *3-38* display the yaw rate for both of physical test and simulation model. The yaw rate is almost the same, but there is a substantial delay in the build-up of the yaw rate in the physical test, which may be due to friction in the fifth wheel.

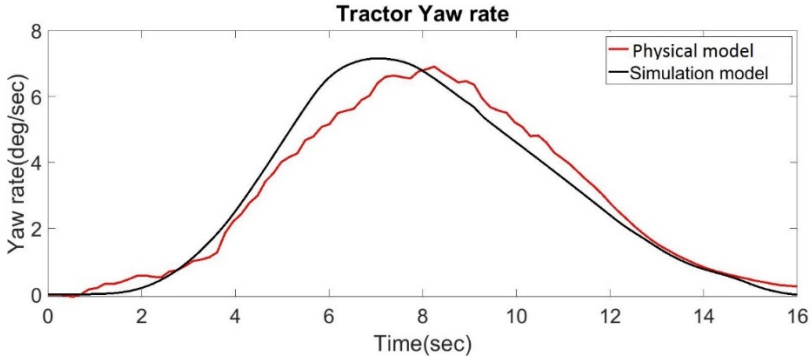

Figure 3-37: Tractor Yaw rate

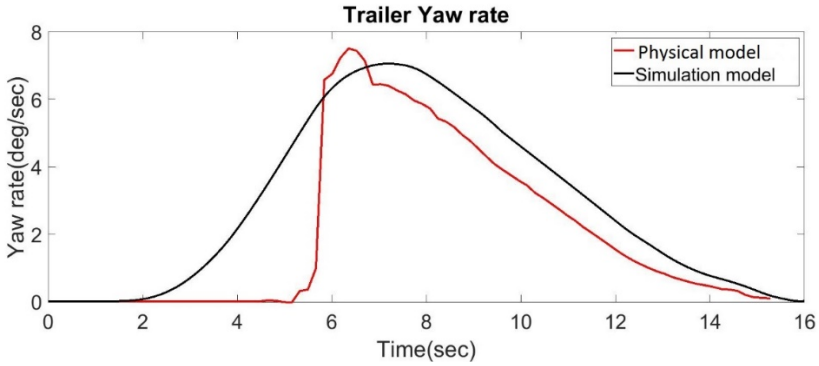

Figure 3-38: Trailer Yaw rate

3.8.6 Discussion of results

Two tests were conducted to validate the simulation model, the first one is the straight line acceleration test, and the second one is the lane-change test. The figures show a comparison between the results of the simulation model and the physical tests. The simulation model can produce a massive amount of data from each part of the model as the simulation model can show the different displacements, velocities, accelerations, forces, and torques. However, four necessary responses are chosen to be compared to physical tests. The sensors that are integrated with the test vehicle produce the accelerations in three directions (X, Y, and Z) and the rates of rotation (roll, pitch, and Yaw), but because the ride is not considered in this study, the

acceleration in the Z direction is not taken into consideration, and also the roll and pitch rates are ignored.

The straight line acceleration and the lane-change results for both simulation and physical test have been shown to follow the same trend; however, the simulation model curves were always smoother than the physical model. At the first look, it may seem like a noise in the system caused by the electrical connections and electronic circuit, but the reality is the sampling rate. It is straightforward to change the sampling rate for the simulation model from the toolbox of the simulation package either by step size or by the number of points in the simulation. However, it is different in the physical test because the controller script takes time for recording data on the SD card, so recording of results was restricted to a sampling rate of 10Hz. Recording the data on an SD card rather than recording it on the microcontroller memory then transferring it was because the microcontroller memory is too small (64 bytes). Although the sampling rate is relatively low, it can still give a good representation of the vehicle motion.

The velocity peaked at 3m/sec; this speed seems to be high if compared with the equivalent speed of the full vehicle model (42 m/sec as related to scale) after converting it by the dimensionless analysis. The normal range for a tractor semi-trailer conducted before was 2 m/s, as mentioned in[9, 11, 48]. However, the main aim was to validate the simulation model, and the speed in the simulation model could be adjusted through the simulation, so after the validation process, the speed could be adjusted easily in the software. This speed was generated from a powerful DC motor and dedicated gearbox and differential supplied with the scaled model; this could be adjusted in future work.

Furthermore, the longitudinal acceleration results, Yaw rate and lateral acceleration were in the same range as mentioned in[64, 124, 125], which prove that the measured value is

reasonable and the parts in the simulation model are appropriately connected. The trailer's curves from the simulation model fit with the physical model more than the tractor results except for the yaw rate due to friction in the fifth wheel.

Chapter 4: ESC control

4.1 Introduction

After verifying the simulation model and using it in developing the control, the second important part of the study is developing the stability control of the scaled multi-body dynamics simulation model. This chapter introduces the development of ESC using Fuzzy logic. The chapter introduces the reference model used in the control system to regulate the simulation model's output according to the reference values from the reference model. Then it explains how the co-simulation between the control and the simulation model is effective. A simple control system can be built internally within MSC ADAMS. However, in the case of a more complicated control system, an MSC ADAMS model can be co-simulated with EASY5 or MATLAB to create and test control systems on its model. Thus MATLAB/Simulink is used to co-simulate with MSC ADAMS/View to test the ESC system using Fuzzy logic control. Also, the Fuzzy controller algorithm for the fuzzification, defuzzification and membership functions were explained. The stability control tests results are then presented, and their effectiveness on the different performance parameters is discussed. Finally, the control algorithm is tested under different operating conditions (loaded and unloaded condition), and the results are presented with a discussion on it.

4.2 Reference model

Building control systems require a reference value to compare with the actual value, compute the error, and adjust the actual model performance. This reference value can be estimated from a reference model. The reference model can be linear or non-linear according to the control

methodology; also, the number of degrees of freedom depends on the controlled parameters. In other words, the reference model provides the reference value for the controlled parameter. Three degrees of freedom reference model have been used to control the scaled model's performance with Fuzzy logic control. The reference model output is the tractor Yaw rate and the articulation angle of the tractor-trailer. The reference model is shown in Figure 4-1 [95]. The equations that describe the reference model are stated below [equations 4.1 to 4.8].

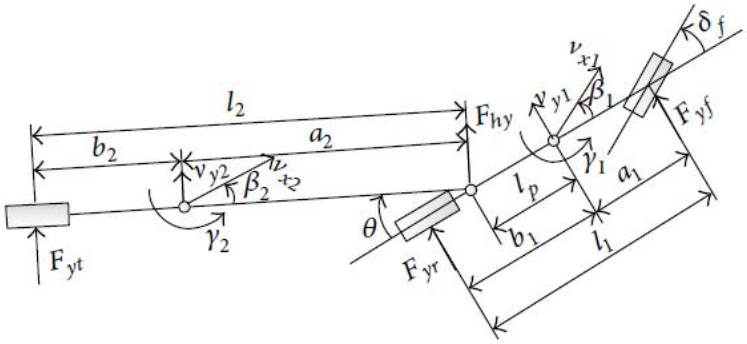

Figure 4-1: three degrees of freedom reference model ***[95]***

$$\gamma_{1t}^{*} = \frac{v_x/l_1}{1 + K_s v_x^2}\delta_f \quad Equation\ 4.1$$

$$K_s = \frac{b_1 l_2 m_1 + (b_1 - l_p) b_2 m_2}{l_1^2 l_2 C_{y1}}$$

$$- \frac{a_1 l_2 m_1 + (a_1 + l_p) b_2 m_2}{l_1^2 l_2 C_{y2}} \quad Equation\ 4.2$$

$$|\gamma_{1t}^{*}| \leq \frac{\mu g}{v_x} \quad Equation\ 4.3$$

$$\gamma_1^* = \begin{cases} \gamma^*_{1t, |\gamma^*_{1t}| < \frac{\mu g}{v_x}} \\ \frac{\mu g}{v_x}, |\gamma^*_{1t}| \geq \frac{\mu g}{v_x} \end{cases} \quad Equation\ 4.4$$

$$\theta^* = \frac{p_1 + (p_2 + p_3)v_x^2}{1 + K_s v_x^2}\delta_f \quad Equation\ 4.5$$

$$p_1 = -\frac{l_p - b_1 + l_2}{l_1} \quad Equation\ 4.6$$

$$p_2 = \frac{a_2 m_2}{l_1 l_2 C_{y3}} \quad Equation\ 4.7$$

$$p_3 = -\frac{a_1 l_2 m_1 + (a_1 + l_p) b_2 m_2}{l_1^2 l_2 C_{y2}} \quad Equation\ 4.8$$

Where

K_s: *is the yaw stability factor*

θ^*: *is the articulation angle* (rad)

γ_1^*: *is the reference yaw rate* $(\frac{rad}{\sec})$

γ_{1t}^*: *is the tractor yaw rate* $(\frac{rad}{\sec})$

v_x: *is the tractor longitudinal speed* $(\frac{m}{\sec})$

l_1: *is the tractor wheelbase* (m)

l_2: $is\ the\ logituidnal\ distance\ from\ the\ fifth\ wheel\ position\ and\ the\ trailer\ rear\ axle\ (m)$

δ_f: $is\ the\ tractor\ front\ tyre\ steering\ angle\ (rad)$

l_p: $is\ the\ longitudinal\ distance\ from\ tractor\ C.G.to\ the\ fifth\ wheel\ position\ (m)$

m_1: $is\ the\ tractor\ mass$ (kg)

m_2: $is\ the\ trailer\ mass\ (kg)$

a_1: $is\ the\ longitudinal\ distance\ from\ tractor\ front\ axle\ an\ the\ tractor\ C.G.\ (m)$

a_2: $is\ the\ longitudinal\ distance\ from\ the\ fifth\ wheel\ position\ and\ the\ trailer\ C.G.\ (m)$

b_1: $is\ the\ longitudinal\ distance\ from\ tractor\ C.G\ and\ the\ tractor\ rear\ axle\ (m)$

b_2: $is\ the\ longitudinal\ distance\ from\ trailer\ C.G.and\ the\ trailer\ rear\ axle\ (m)$

$C_{\gamma 1}$: $is\ the\ cornering\ stiffness\ for\ the\ tractor\ front\ tyre\ (\frac{N}{rad})$

$C_{\gamma 2}$: $is\ the\ cornering\ stiffness\ for\ the\ tractor\ rear\ tyre\ (\frac{N}{rad})$

$C_{\gamma 3}$: $is\ the\ cornering\ stiffness\ for\ the\ trailer\ rear\ tyre\ (\frac{N}{rad})$

g: $is\ the\ gravity\ acceleration\ (\frac{m}{sec^2})$

μ: $is\ the\ road\ adhesion\ coeffient$

p_1, p_2, p_3: $are\ constants\ for\ symplifying\ the\ articulation\ angle\ equations$

The reason for choosing the reference model as three degrees of freedom from a published source is that it is already verified. The reference model is built on MATLAB/Simulink, and

there are two main inputs to the reference model; the first one is the steering input, and the other one is the scaled model speed. The trailer reference Yaw rate is estimated by differentiating the articulation angle and adding it to the reference tractor Yaw rate, which is the first output from the reference model.

4.3 ADAMS/MATLAB model co-simulation

MSC ADAMS View is co-simulated with MATLAB/Simulink to achieve the control system. After building the multi-body dynamics model on ADAMS, a group of system elements are created to send and receive the input and output control signals. The number of output elements is seventy-three, expressing the lateral, longitudinal, vertical tyre forces for tractor-trailer wheels, also the longitudinal slip of tyres and wheel angular velocity, as well as the tractor velocity and Yaw rate, pitch rate, roll rate for the tractor and trailer, besides the actual steering angle and the trajectory of the vehicle. For the tractor rear axles, it is assumed that the dual wheels are one wheel, so the inside and outside tyre forces are added together. There are thirteen input elements to the simulation model, including the steering angle and the tyres' brake torque.

Building the system elements for the output signals can be defined in two different ways, the first one by defining a user function, the second one by a user-written subroutine. When creating a system element using a user-defined function, the expression function builder can be used. The expression function builder has built-in functions, and these functions can be used to create the required user function that needs to be added through the system elements. The user-defined function is used for measuring the tractor and trailer characteristic, so, for example, the Yaw rate can be measured by building a function that measures the angular velocity around the z-axis of the tractor centre of gravity (tractor.cm). This expression function builder has many built-in functions that can be used to build a user-defined function. However, defining tyre

forces in the system elements used with this control system requires using the second method, a user-written subroutine. The user-written subroutine uses a code to call the tyre, as it is a defined function in ADAMS, this code identifies that the element is requiring to measure a parameter in the tyre, but an ID should be added in the system element to identify this specific parameter.

One of the most important things that need careful consideration is to unify the outputs of the outputs to be compared correctly with the reference model output. After exporting the M file from MSC ADAMS/View and running it in MATLAB, A command called “Adams_sub” should be written in the MATLAB command window to open the Simulink model that contains the simulation model block so that it can be copied to the control model. Then, insert the ADAMS model into the control model and connect the different signals while considering the unit conversions. Finally, run the model and tune the values of the controller, as will be discussed later. Figure 4-2 presents a diagram for the co-simulation between MSC ADAMS and the Fuzzy controller. Appendix C shows the steps followed with figures to build the elements, export these elements, identify them in MATLAB, and connect it to the control model blocks.

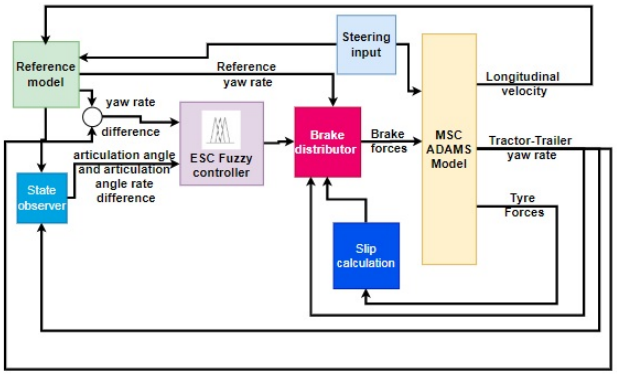

Figure 4-2: a diagram illustrating the ESC system using co-simulation

4.4 Fuzzy control system

4.4.1 Introduction

As mentioned in the literature, Fuzzy logic control is an adaptive control system. The controller is built on the Fuzzy toolbox in MATLAB and used in Simulink. The Fuzzy logic controller is based on three inputs. The input signals are the error resulting from the ADAMS simulation model and the reference model. These signals are the tractor Yaw rate error, articulation angle error and articulation angle rate error. The Fuzzy logic system is divided into two Fuzzy controllers to simplify the Fuzzy rules. The Fuzzy controllers' output is the correcting torque that is applied on the tractor and trailer wheels. The first Fuzzy controller input is the tractor Yaw rate error, and its output is the correcting torque applied on the tractor wheels; this torque can be positive or negative on the tractor rear axles as the system simulates the ESC; however, the torque on the tractor front axles is just a braking torque. The second Fuzzy controller inputs are the articulation angle error, the articulation angle rate error, and the output is a brake torque on the trailer's wheels. When applying the corrective torque to the wheels, the controller calculates the tyre slip rate. In-wheel locking due to high braking force, the brake logic distributor changes the braking force amount to unlock the tyre. A unit delay should be added into the Simulink model before the (ADAMS block) inputs signal (braking torque). This delay between the ADAMS input and output signal avoids errors from the Simulink model while running. The three steps for the control method (fuzzification, membership function and defuzzification) will be illustrated in the next sections.

4.4.2 Fuzzification

Fuzzification is the first step for the Fuzzy control system, in which the input signal (the error resulting from the reference and actual model) is converted to a linguistic variable. A few Fuzzy sets for each input to the control system: the more sets used, the more precise the output values obtained. The Fuzzy sets can have different shapes; they can be triangular, trapezoidal or bell curve. Also, each Fuzzy set has a range, which can be set according to the control system. Furthermore, the whole set should be specified with a range of values for the input parameter. Moreover, for this control, the scaled range is from [-1,1].

The Fuzzy logic control inputs are based on five sets for each input. The shape for these sets is the Gaussian membership function based on Xiujian Yang et al. [95]. It is divided into five primary knowledge-based rules as follow

- Positive Big (PB)
- Positive Small (PS)
- Zero (ZE)
- Negative Small (NS)
- Negative Big (NB)

Figure 4-3[95] shows the Fuzzy set for the tractor Yaw rate error, while Figure 4-4[95] presents the Fuzzy set for the articulation angle error and Figure 4-5[95] shows the Fuzzy set for the articulation angle rate error.

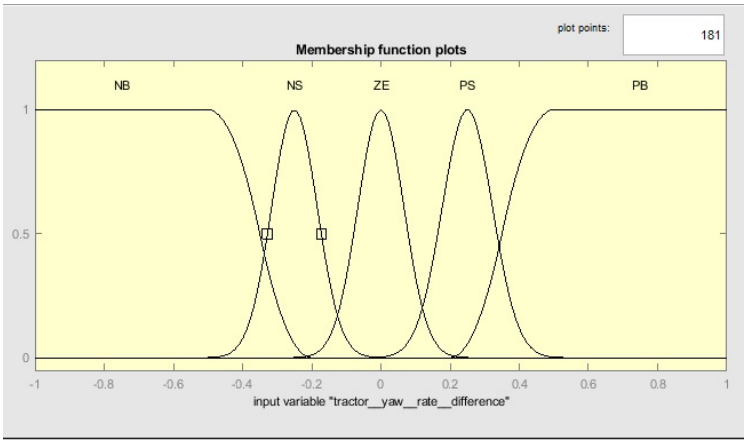

Figure 4-3: tractor Yaw rate error Fuzzy set***[95]***

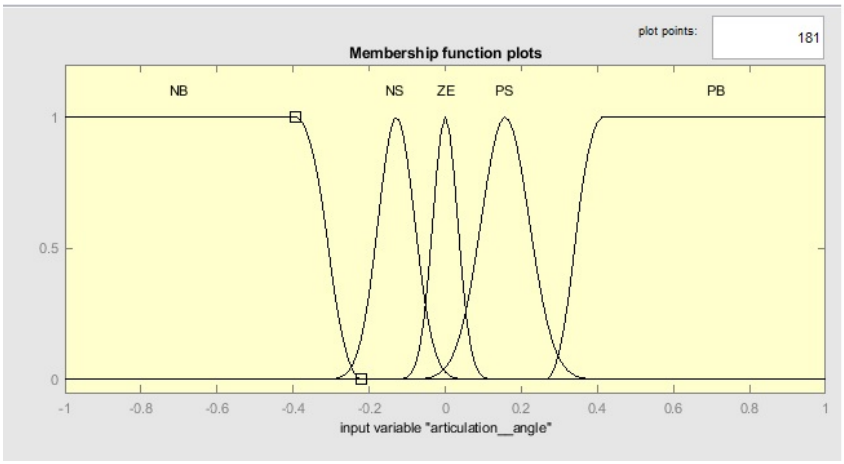

Figure 4-4: articulation angle error Fuzzy set***[95]***

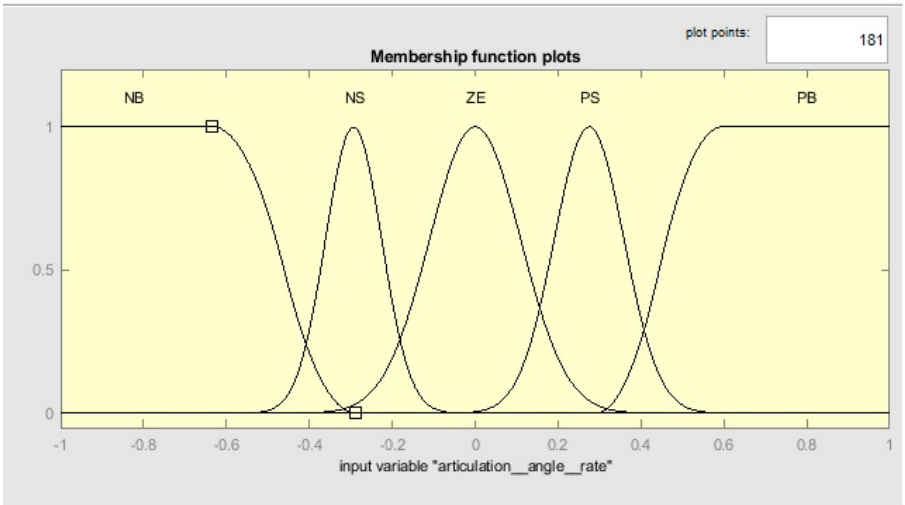

Figure 4-5: articulation angle rate error Fuzzy set***[95]***

4.4.3 Membership function

The membership function is the second step in the Fuzzy controller, and it relates the input and output signals by rules which come from experience. The number of rules depends on the number of inputs and outputs to the Fuzzy controller. Due to having three inputs and two outputs, the number of rules is going to be enormous. So the Fuzzy controller is divided into two controllers, (Yaw rate error input with tractor corrective torque) and (articulation angle error and the articulation error inputs with trailer corrective torque), to reduce the number of inputs and outputs per control and to reduce the number of rules which facilitate tuning these rules.

The first control has five rules which are summarised in ***Table 4-1***[95]. These rules are the relation between the Yaw rate error and the corrective Yaw moment for the tractor. Also, the rules can be presented as a 2D line graph since there are only two parameters, which is presented in Figure 4-6[95]. The Fuzzy Logic method that is used is Mamdani's method. The number of

rules for the second controller is twenty-two rules which are presented in ***Table 4-2***. The rules are the relation between the articulation angle, articulation angle rate and the corrective Yaw moment. The rules can be shown as 3D surface shape since they are three parameters as shown in Figure 4-7.

Table 4-1: tractor Yaw rate error with corrective Yaw moment rules***[95]***

Rule number	Yaw rate error	Corrective Yaw moment
1	NB	PB
2	NS	PS
3	ZE	ZE
4	PS	NS
5	PB	NB

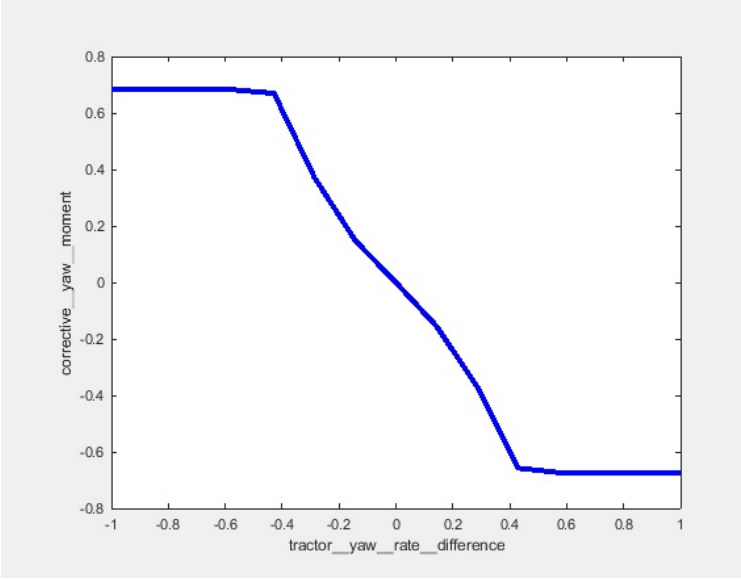

Figure 4-6:membership function as a line graph for tractor Yaw rate difference vs correcting moment***[95]***

Table 4-2: membership rules for articulation angle and articulation angle rate with the corrective moment

Rule number	Articulation angle	Articulation angle rate	Corrective moment
1	NS	PB	ZE
2	ZE	PB	NS
3	PS	NB	PB
4	PS	NS	PS
5	PS	ZE	ZE
6	ZE	NB	PB
7	ZE	PS	PS
8	NB	PS	ZE
9	NB	ZE	PS
10	NS	ZE	ZE
11	PB	ZE	NB
12	PS	ZE	NS
13	ZE	NB	PS
14	ZE	ZE	ZE
15	NS	NS	ZE
16	NS	ZE	ZE
17	NS	PB	ZE
18	NS	PS	ZE
19	NB	ZE	ZE
20	NB	PB	ZE
21	ZE	NS	ZE

22	NB	NS	ZE

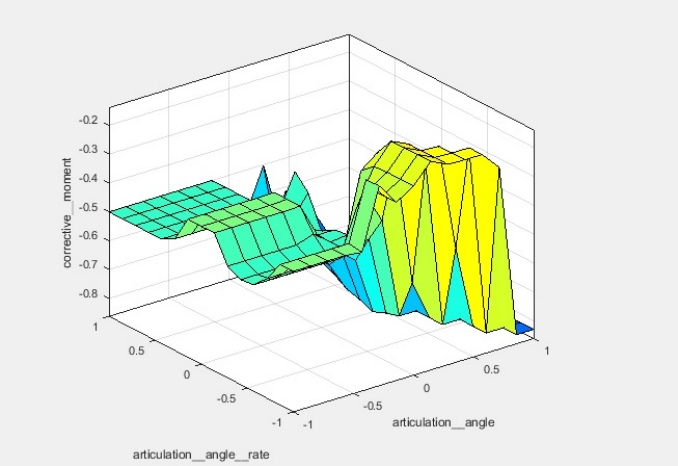

Figure 4-7: membership surface shape for articulation angle and articulation angle rate vs trailer corrective brake torque

4.4.4 Defuzzification

The defuzzification is the last step in the Fuzzy controller, which converts the linguistic expression to a real value used in the control loop to correct the error. The Fuzzy logic control outputs are based on five sets for each input. The shape for these sets is triangle membership function based on Xiujian Yang et al. [95]. It is divided into five primary knowledge-based rules [PB, PS, ZE, NS, NB], representing positive big, positive small, zero, negative big and negative small. Moreover, the output from the Fuzzy controller is defined according to the range for the Fuzzy sets.

Moreover, for this controller, the scaled range for the tractor's corrective moment is [-1,1] and for the trailer [0, -1] with taking into consideration to reject the positive value for the front wheels of the tractor. Figure 4-8[95] and Figure 4-9[95] demonstrates the membership function for the corrective moment for both the tractor and the trailer.

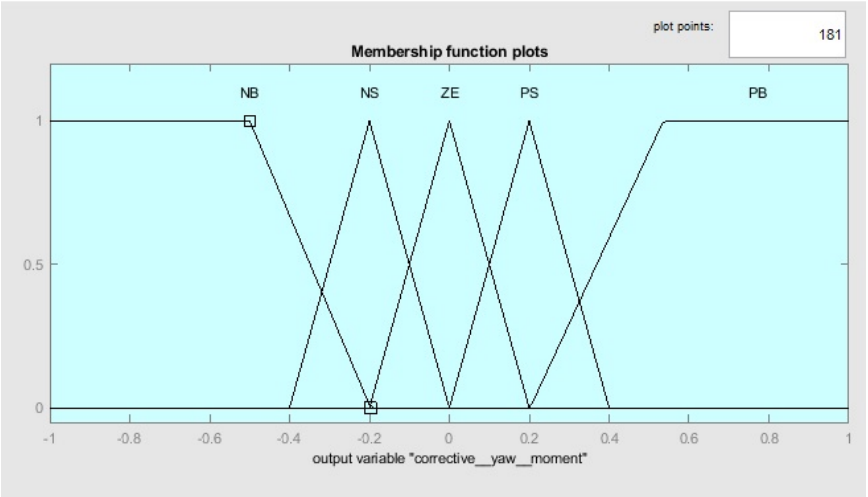

Figure 4-8: Fuzzy set for tractor corrective Yaw moment***[95]***

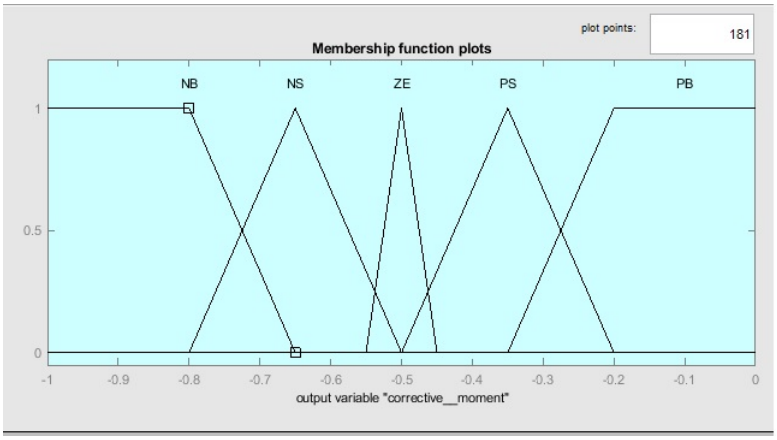

Figure 4-9: Fuzzy set for corrective trailer moment***[95]***

4.4.5 Brake factor

The last part for this controller is a factor that is multiplied by the output from the controller. These factors are then multiplied by the corrective moment for each axle separately. So for the tractor front axle, the factor is multiplied to the tyre diameter divided by the front axle track width, and for the rear axles, it is multiplied by the tyre diameter divided by the rear track width, while for the tractor, it is multiplied by the tyre diameter divided by the trailer axle track width.

Equations 4.9 to 4.11 express these relations.

$$\Delta T_{bf} = \frac{2\Delta M_f R_w}{T_{wf}} \quad Equation\ 4.9$$

$$\Delta T_{br} = \frac{2\Delta M_r R_w}{T_{wr}} \quad Equation\ 4.10$$

$$\Delta T_{bst} = \frac{2\Delta M_{st} R_w}{T_{wst}} \quad Equation\ 4.11$$

Where

$\Delta T_{bf}: is\ the\ braking\ torque\ for\ tractor\ front\ axle$

$\Delta T_{br}: is\ the\ braking\ torque\ for\ tractor\ rear\ axles$

$\Delta T_{bst}: is\ the\ braking\ torque\ for\ the\ trailer\ axles$

$\Delta M_f: is\ the\ difference\ of\ the\ corrective\ braking\ force\ for\ tractor\ front\ axle$

$\Delta M_r: is\ the\ difference\ of\ the\ corrective\ braking\ force\ for\ tractor\ rear\ axles$

$\Delta M_{st}: is\ the\ difference\ of\ the\ corrective\ braking\ force\ for\ trailer\ axles$

$T_{wf}: is\ the\ tractor\ front\ axle\ wheel\ track$

$T_{wr}: is\ the\ tractor\ rear\ axles\ wheel\ track$

$T_{wst}: is\ the\ traciler\ axles\ wheel\ track$

$R_w: is\ the\ wheel\ tyre\ raduis$

The tractor front axle factor is 2.5, and for the rear axle, 0.1, while the factor for the trailer was 0.05. these factors are obtained through the trial and error method.

4.5 Brake logic distribution

The brake logic distribution means the decision of which tyre needs a brake torque in which situation. The brake distribution is divided into two main parts—the first part for the tractor and the other one for the trailer. Table 4-3 shows the tyre notation for the tractor-trailer, and Table 4-4 presents the logic for the tractor brake torque distribution. Table 4-5 shows the logic for the trailer brake torque distribution. The brake distribution depends on the theoretical and actual Yaw rate for the tractor and the trailer. The brake distribution is built on Simulink using the IF function. In other words, the amount of the brake or Traction force is specified by the controller, but which tyre will apply this force is determined by the brake logic.

Table 4-3:tractor-trailer tyre notation

tyre notation	brake
1	The front left
2	The front right
3	The tractor rear left first and second
4	The tractor rear right first and second
5	The trailer left first, second and third axles
6	The trailer right first, second and third axles

Table 4-4: tractor brake distribution logic

Reference Yaw rate	Actual Yaw rate	comparison	Target brake wheel
$\psi_{ref1} > 0$	$\psi_1 > 0$	$\psi_{ref1} < \psi_1$	1
$\psi_{ref1} > 0$	$\psi_1 > 0$	$\psi_{ref1} > \psi_1$	3

$\psi_{ref1} > 0$	$\psi_1 > 0$	$\psi_{ref1} = \psi_1$	-----
$\psi_{ref1} < 0$	$\psi_1 < 0$	$\psi_{ref1} < \psi_1$	4
$\psi_{ref1} < 0$	$\psi_1 < 0$	$\psi_{ref1} > \psi_1$	2
$\psi_{ref1} < 0$	$\psi_1 < 0$	$\psi_{ref1} = \psi_1$	-----
$\psi_{ref1} > 0$	$\psi_1 < 0$	$\psi_{ref1} > \psi_1$	2
$\psi_{ref1} < 0$	$\psi_1 > 0$	$\psi_{ref1} < \psi_1$	1
$\psi_{ref1} = 0$	$\psi_1 < 0$	$\psi_{ref1} > \psi_1$	2
$\psi_{ref1} = 0$	$\psi_1 > 0$	$\psi_{ref1} < \psi_1$	1
$\psi_{ref1} > 0$	$\psi_1 = 0$	$\psi_{ref1} > \psi_1$	3
$\psi_{ref1} < 0$	$\psi_1 = 0$	$\psi_{ref1} < \psi_1$	4
$\psi_{ref1} = 0$	$\psi_1 = 0$	$\psi_{ref1} = \psi_1$	-----

Table 4-5: trailer brake distribution logic

Reference Yaw rate	Actual Yaw rate	comparison	Target brake wheel
$\psi_{ref2} > 0$	$\psi_2 > 0$	$\psi_{ref2} < \psi_2$	6
$\psi_{ref2} > 0$	$\psi_2 > 0$	$\psi_{ref2} > \psi_2$	5
$\psi_{ref2} > 0$	$\psi_2 > 0$	$\psi_{ref2} = \psi_2$	-----
$\psi_{ref2} < 0$	$\psi_2 < 0$	$\psi_{ref2} < \psi_2$	6
$\psi_{ref2} < 0$	$\psi_2 < 0$	$\psi_{ref2} > \psi_2$	5
$\psi_{ref2} < 0$	$\psi_2 < 0$	$\psi_{ref2} = \psi_2$	-----
$\psi_{ref2} > 0$	$\psi_2 < 0$	$\psi_{ref2} > \psi_2$	5
$\psi_{ref2} < 0$	$\psi_2 > 0$	$\psi_{ref2} < \psi_2$	6

$\psi_{ref2} = 0$	$\psi_2 < 0$	$\psi_{ref2} > \psi_2$	5
$\psi_{ref2} = 0$	$\psi_2 > 0$	$\psi_{ref2} < \psi_2$	6
$\psi_{ref2} > 0$	$\psi_2 = 0$	$\psi_{ref2} > \psi_2$	5
$\psi_{ref2} < 0$	$\psi_2 = 0$	$\psi_{ref2} < \psi_2$	6
$\psi_{ref2} = 0$	$\psi_2 = 0$	$\psi_{ref2} = \psi_2$	-----

4.6 Results

4.6.1 Introduction

The model runs for 6 seconds with a ramp steering input. The main output results are the tractor-trailer Yaw rate, articulation angle and lateral acceleration, and the brake torque applied to each wheel.

4.6.2 Input signal

The input signal to the system is the steering signal based on a ramp function, as shown in Figure 4-10. The steering signal starts after 3 seconds from moving, allowing the simulation model to reach an appropriate speed to start the manoeuvre. The tyre steering input angle is three degrees; Then the vehicle remains at this steering angle for one second and then goes down again from three to zero degrees. The simulation model speed is input for the reference model; it reaches 3 m/s before manoeuvre, varies between 2-3 m/s for the rest of the simulation, and is presented in Figure 4-11. The vehicle's response depends on the input signal, so if the input signal is changed (e.g. step input or sine wave), The output response will change.

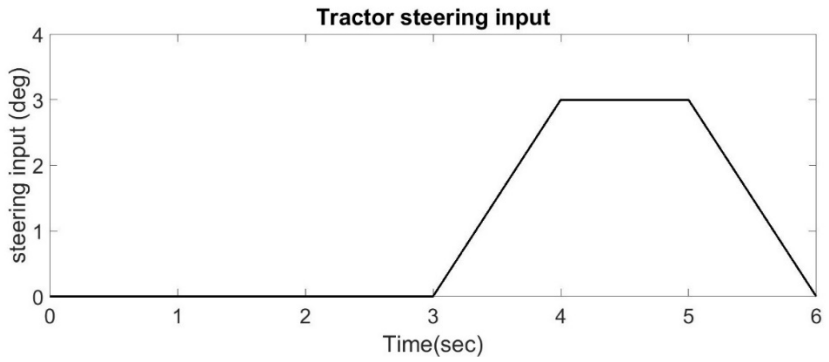

Figure 4-10: steering Input signal to the Simulation Model

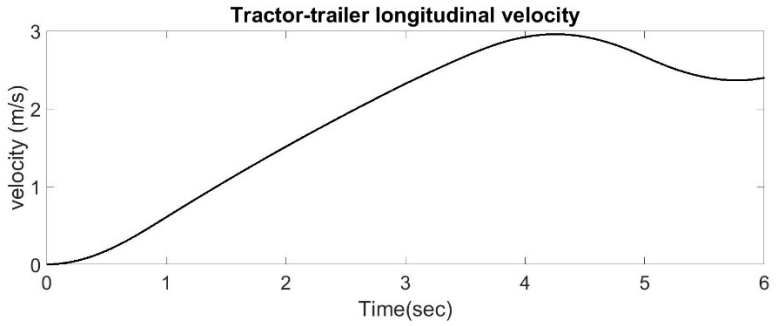

Figure 4-11: simulation model longitudinal velocity

4.6.3 ESC output results

Figure 4-12 presents the tractor Yaw rate for the controlled model, uncontrolled model and the reference model. The curve shows that all of the Yaw rate values from the three compared models were the same until the third second when the steer manoeuvre was initiated. Then, from the third second to the fourth second, there was little difference between the controlled model and the other models. After the fourth second, when the steering angle reverted to zero and was then subsequently reversed, the controlled model continues to follow the same trend as the reference model. However, from the fourth second, the uncontrolled model starts to show

a significant difference from the reference model until it reaches its peak at 40deg/sec in the fifth second, then it decreases to around 4 deg/sec by the end of the simulation. The controlled and reference models have a smooth peak in their curves and return to zero by the end of the simulation.

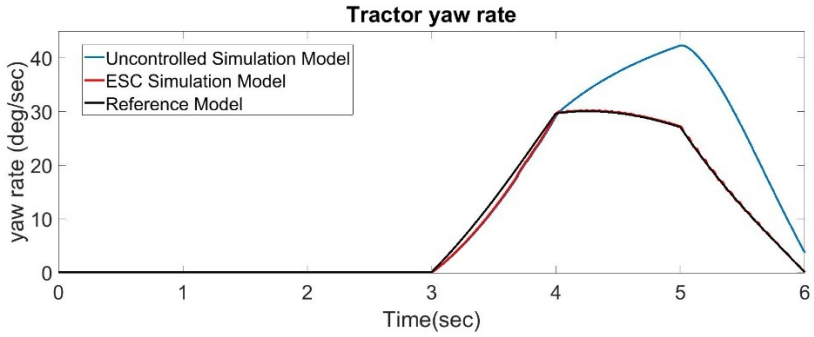

Figure 4-12: tractor Yaw rate

Figure ***4-13*** presents the trailer Yaw rate for both the controlled and the uncontrolled model; in the trailer curves figures, the reference model is absent because the reference model used in control is three degrees of freedom as described at the beginning of the chapter. The two curves follow the same trend of the tractor Yaw rate for both values with slightly higher values for the Yaw rate of the uncontrolled simulation model. Both Yaw rate figures for the tractor and the trailer demonstrate the effectiveness of the control in reducing the yaw rate by around 25% at the manoeuvre.

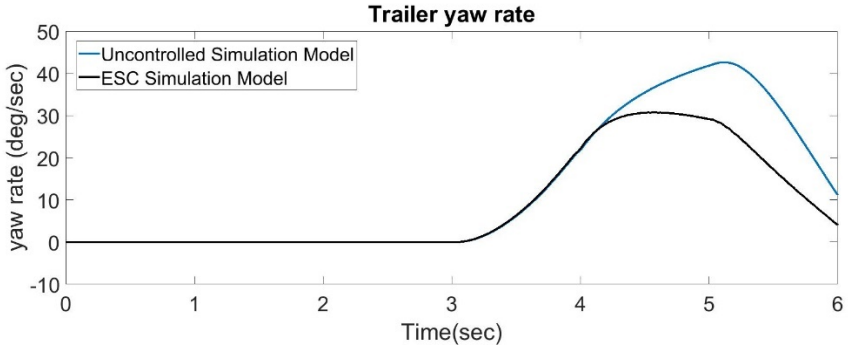

Figure 4-13: trailer Yaw rate

The comparison of the articulation angle between the three scenarios is clearly shown in Figure 4-14. From the figure, the articulation angle remains the same in the first three seconds. The vehicle is moving in a straight line, so there is no articulation angle. After the third second, there is a difference between the reference model and the other models till the fourth second. The other two models start to differ, and the controlled model starts to follow a trend below the reference model. The uncontrolled model starts to go above the reference model until it reaches a peak value at the fifth second. Then, all the articulation angle tends to decrease. However, ESC achieved the lowest value. The tractor and the trailer's articulation angle is less than the normal by 1 deg as the brake torque for the tractor front left is active at the manoeuvre.

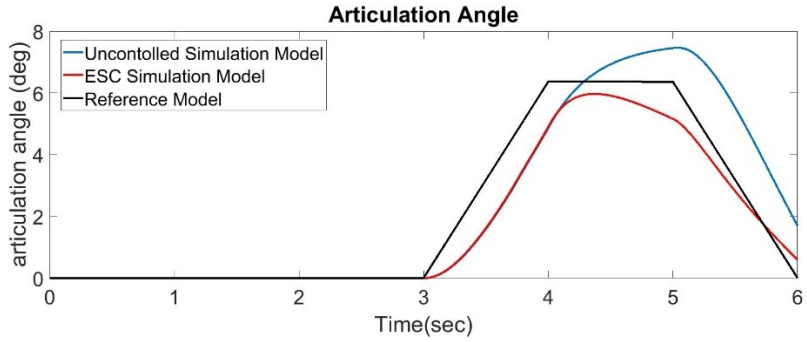

Figure 4-14:tractor-trailer articulation angle

Moreover, the ESC enhanced the tractor and trailer lateral acceleration performance, as shown in Figure 4-15 and Figure 4-16. The two curves show that the difference between the

uncontrolled and controlled models starts to be clear after the fourth second, which is the time for the steering angle to return to the straight position. This value of the lateral acceleration reaches its peak value at the fifth second; then, it decreases as the vehicle returns to the new path. Lateral acceleration curves for the controlled model of both the tractor and the trailer are less than the uncontrolled model by around 20% at the manoeuvre, which is reasonable with the Yaw rate improvement at the same interval.

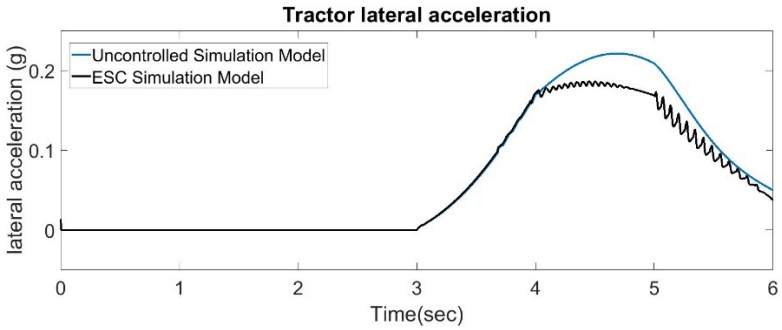

Figure 4-15: tractor lateral acceleration

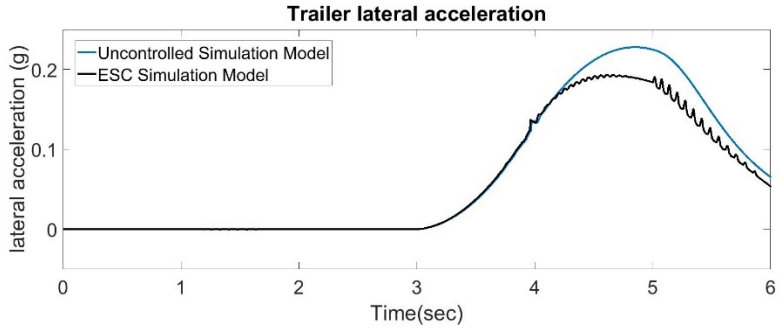

Figure 4-16:trailer lateral acceleration

Furthermore, the trajectory of the vehicle is presented in Figure 4-17. The difference between the two trajectories starts to be clear after the fifth second, there is a diversion from the two path and the controlled one tends to take narrower path than the uncontrolled one.

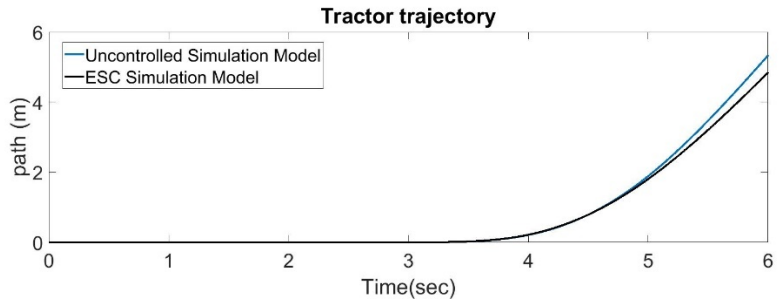

Figure 4-17: tractor trajectory

Figure 4-18 to Figure 4-29 show the amount of brake torque applied through the whole simulation to stabilise the vehicle according to the control methodology. The brake torque is different on each wheel, as described in the control section. Also, the tractor rear axle can have traction or brake torque. So, each one shows different brake torque according to the situation, and the control specifies the amount of the brake or traction torque required. For example, in Figure 4-18, there is no need for the brake torque on the front left brake for the tractor until the fourth second; then, as the vehicles start to have a steering angle, there is a brake signal that appears at this time. The brake starts with a spike at around 6 N.m then it starts to fluctuate and stops this fluctuation before the fifth second and then returns to fluctuate again with higher values at the fifth second until it almost reaches zero again at the end of the simulation. The controller determines the value and the way of the brake torque according to the state of the vehicle.

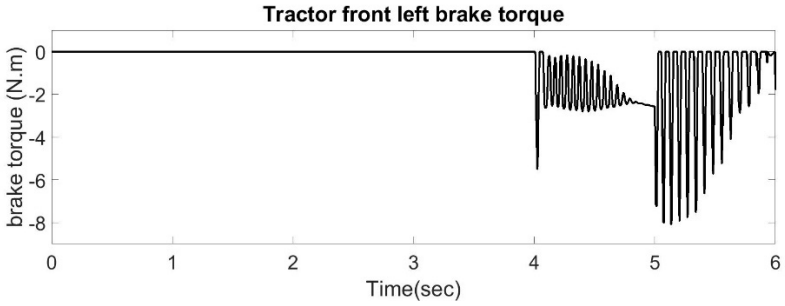

Figure 4-18: tractor left front wheel brake torque

Figure ***4-19*** shows the brake torque for the tractor right front wheel, and from the figure, it is clear that the amount of brake is almost 0.005 N.m for the whole period except for the first three seconds, which has a maximum value of 0.012 N.m then it decreases until it reaches the stable value at the third second. This shows the robustness of the controller as it considers even the small values.

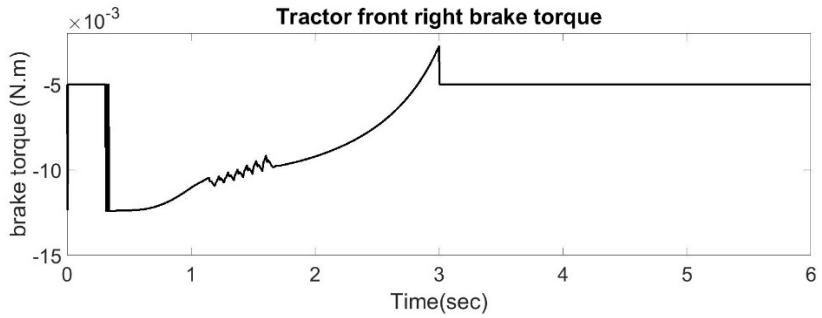

Figure 4-19: tractor front right wheel brake torque

Figure ***4-20*** and Figure ***4-21*** show the traction torque on the first and second tractor rear axle. This is the same traction value coming from the spline curve, acting on the simulation model. However, a small value is added to the original curve from the third to the fourth second.

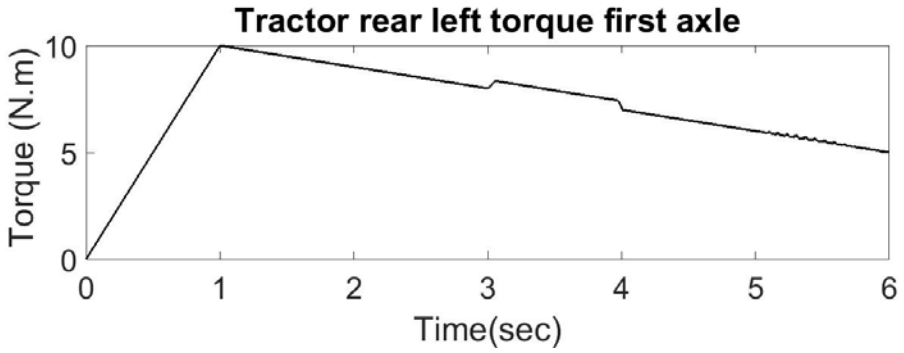

Figure 4-20: tractor rear left wheel first axle torque

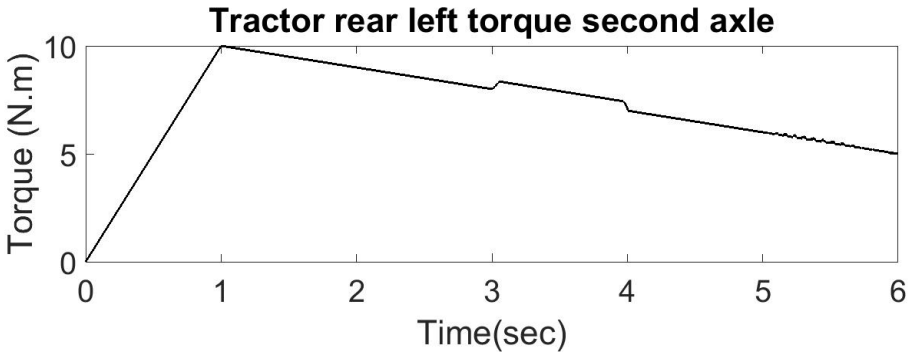

Figure 4-21: tractor rear left wheel second axle torque

The same happens in Figure ***4-22*** and Figure ***4-23*** as this is the tractor rear right wheel. However, these two figures are different from the rear left wheel as there is no added value from the third to the fourth second.

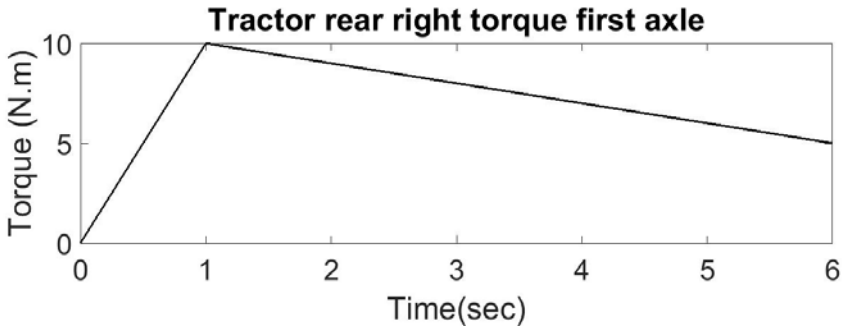

Figure 4-22: tractor rear right wheel first axle torque

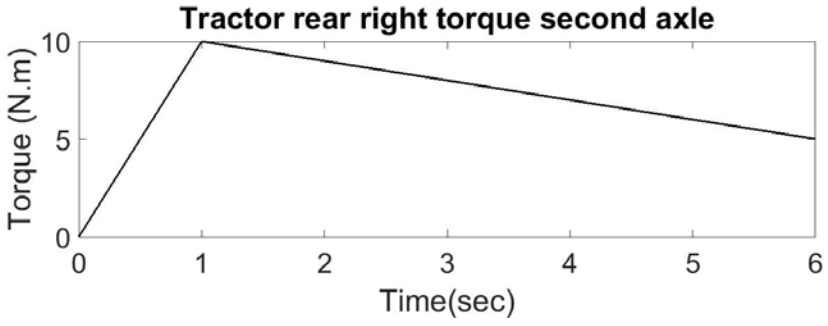

Figure 4-23: tractor rear right wheel second axle torque

Figure 4-24, Figure 4-25 and Figure 4-26 show the same brake torque for the trailer left wheels for the three axles, as all of them take the same signal. For achieving stability in the tractor-trailer through the whole simulation, the control starts to develop a brake torque to the trailer left side. The brake torque starts after the first second.; this brake fluctuates between zero and 0.15 N.m for half a second then remains constant at 0.15 N.m till the third second, then from then it decreases and increases randomly for a second and a half until it reaches zero from the fourth and half a second till the end of the simulation.

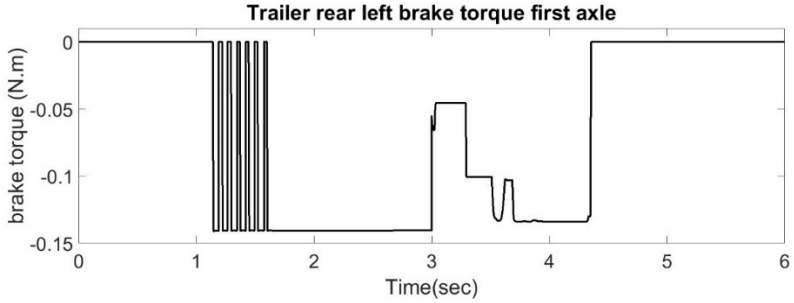

Figure 4-24: trailer left wheel first axle brake torque

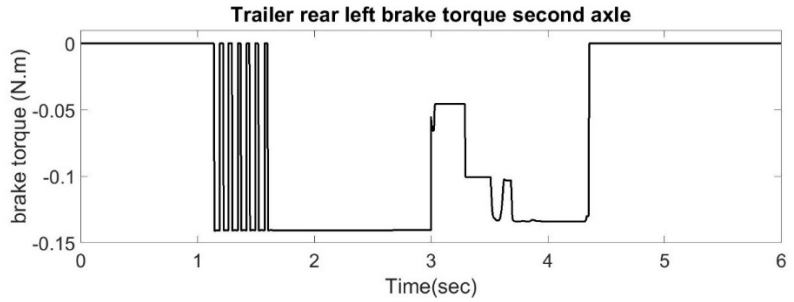

Figure 4-25: trailer left wheel second axle brake torque

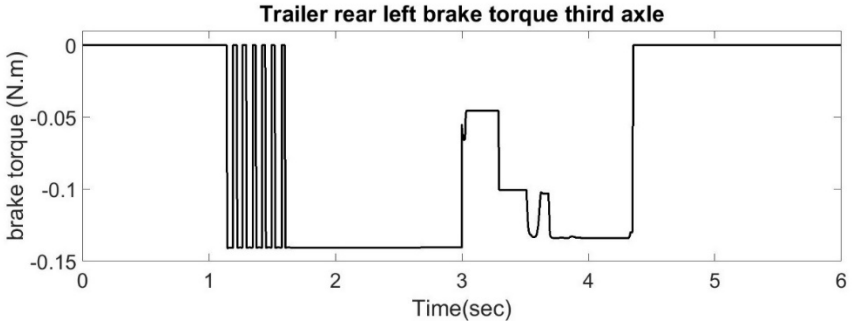

Figure 4-26: trailer left wheel third axle brake torque

In Figure 4-27, Figure 4-28 and Figure 4-29, the brake torque is also the same for the trailer right three axles; it starts to fluctuate after 1.2 seconds and returns to zero from 1.5 seconds till 4.4 seconds, then it starts to develop a brake torque from this moment till the end of the simulation.

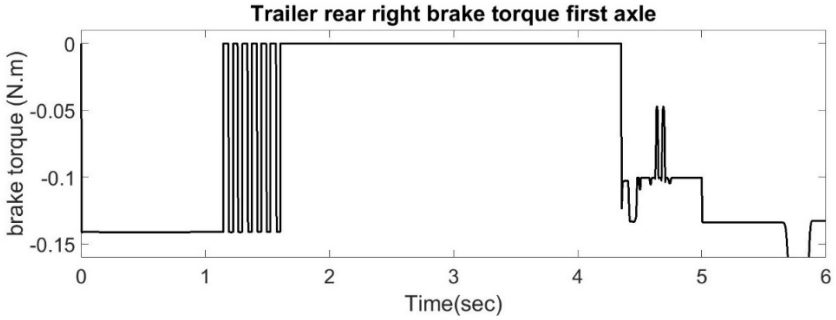

Figure 4-27: trailer right wheel first axle brake torque

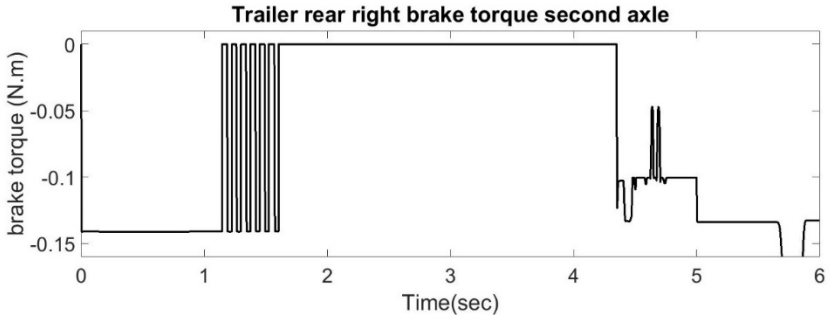

Figure 4-28: trailer right wheel second axle brake torque

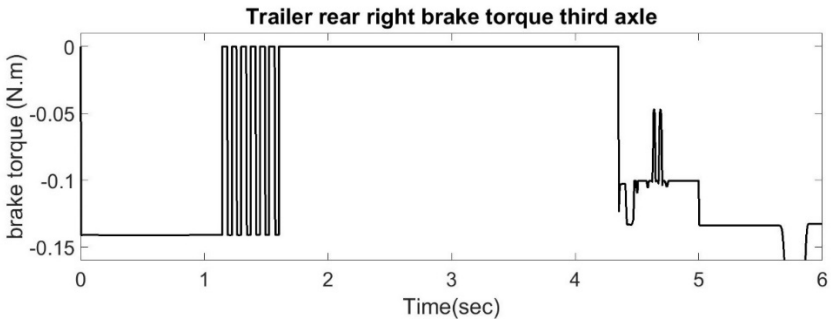

Figure 4-29: trailer right wheel third axle brake torque

4.6.4 Discussion of results

The vehicle results have revealed the ESC control system's effectiveness in improving the vehicle's stability using the tyres' force, whether it is a brake force on the whole vehicle or Traction forces on the rear tyres. These forces can make the vehicle stable and put it on the right path. This is obvious in the tractor and trailer Yaw rate. In the figures, we can find that by using the ESC control system with the tractor Yaw rate, the results are more similar to the reference model, but it was quite different to the uncontrolled model, which proves the effectiveness of the ESC control system. Besides, there is a decrease in the articulation angle.

Moreover, the ESC regulates the tractor and trailer lateral acceleration, and the vehicle starts to follow the desired path; however, the trajectory is not completed as the simulation is just 6 seconds because more than 6 seconds the tractor will fall from the road (the chosen road in MSC ADAMS/View is not too wide) that it is moving on. The brake torques shown in the first three seconds for the different tyres because of the difference between the Yaw rate for both the controlled and the reference model (the tractor Yaw rate difference for the first three seconds appeared in the figures are very slight, but it is not shown because of the figures drawing scale range). Also, there is no braking torque applied to the tractor rear right first and second axles. Left and right axles have a positive traction torque applied which corroborate the concept of

combining the Traction force with the brake force in stabilising the vehicle rather than using the brake force solely.

The fuzzy controller responded to the variation of vehicle state very quickly and varied the amount of the braking torque according to the assessed situation. The fuzzy controller depends on two main factors in determining these amounts; the first one is the membership function, and the second one is the number of rules. If the membership function was more than five, then the rules will increase as well, which may need an optimization method to set the different rules and optimize the performance of the vehicle.

4.6.5 Effect of unloaded condition

The advantage of building the scaled model on a multi-body dynamic system can be demonstrated by changing one of the operating conditions to see the effectiveness of the control system and to allow for tuning the control system in the future. One of the essential operating conditions that can differ in the commercial vehicle's handling performance is the load condition, so changing the load and seeing how the controller will perform is another aspect of this study. The vehicle is simulated in the unloaded condition. The difference between the loading and unloading conditions is that the trailer's load (12.5 kg) was removed from the trailer chassis. The unloaded condition's effect is tested to show the simulation programme's ability to adapt to the design parameters and operating conditions. Some results were selected to compare the effect of removing the load condition. First, the speed is shown in Figure 4-30, which compares the longitudinal speed for the two cases' model. The simulation model run at the same speed, which is up to 3 m/s. The two simulation model show the same speed from the beginning to the end of the simulation.

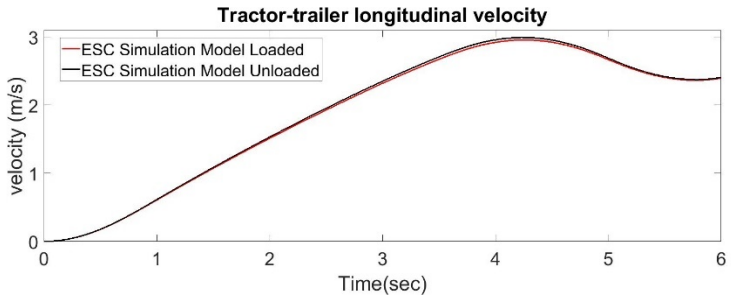

Figure 4-30: tractor-trailer longitudinal velocity loaded vs unloaded

Figure 4-31 compares the tractor Yaw rate for the simulation model, loaded and unloaded. The two curves have the same trend for all the simulation model, and both of them achieve a maximum Yaw rate of 30 deg/sec.

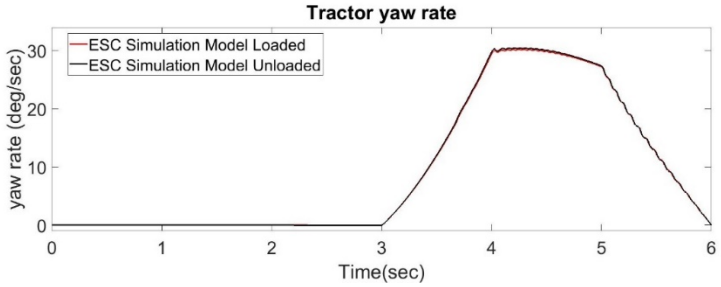

Figure 4-31: tractor Yaw rate loaded vs unloaded

Figure 4-32 presents the trailer Yaw rate's performance for both the loaded and the unloaded; however, these two curves are smoother than the tractor one with the same peak value 30 deg/sec.

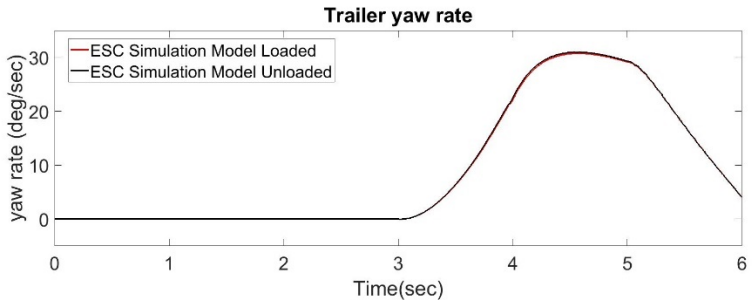

Figure 4-32: trailer Yaw rate loaded vs unloaded

Figure 4-33 shows the articulation angle for both cases. The articulation angle is the same as the red line is not appearing in the figure. The maximum articulation angle reaches 6 degrees at 4.4 seconds and starts to decrease from this point until it reaches almost 0.5 degrees by the end of the simulation.

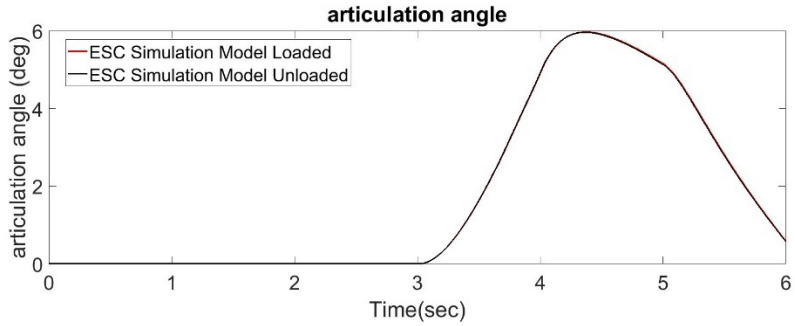

Figure 4-33: tractor-trailer articulation angle loaded vs unloaded

Moreover, Figure 4-34 and Figure 4-35 demonstrate the lateral accelerations for both vehicles. The loaded and unloaded simulation models follow the same trend with a slight difference from the fourth second until the end of the simulation; The lateral acceleration of unloaded simulation model is higher than for the loaded one.

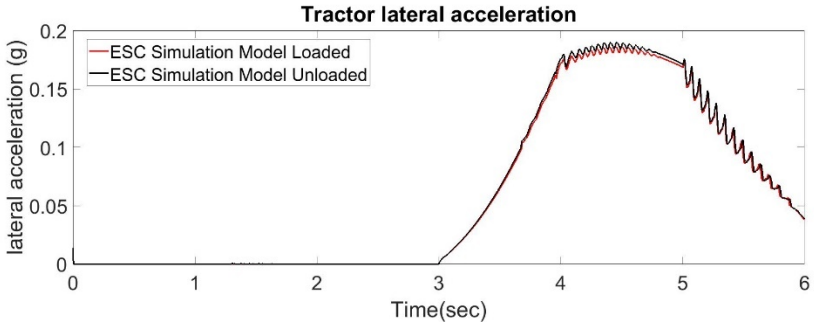

Figure 4-34: tractor lateral acceleration loaded vs unloaded

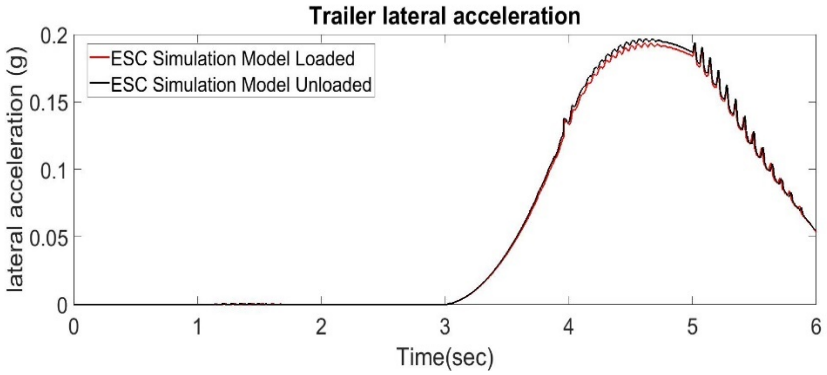

Figure 4-35: trailer lateral acceleration loaded vs unloaded

Figure 4-36 to Figure 4-39 present samples of the brake torque for some tyres. For example, Figure ***4-36*** shows the brake torque of the tractor front wheel. The two simulation models follow the same trend; however, the loaded one requires more brake force, explaining why it is higher than the loaded one even with the small break values.

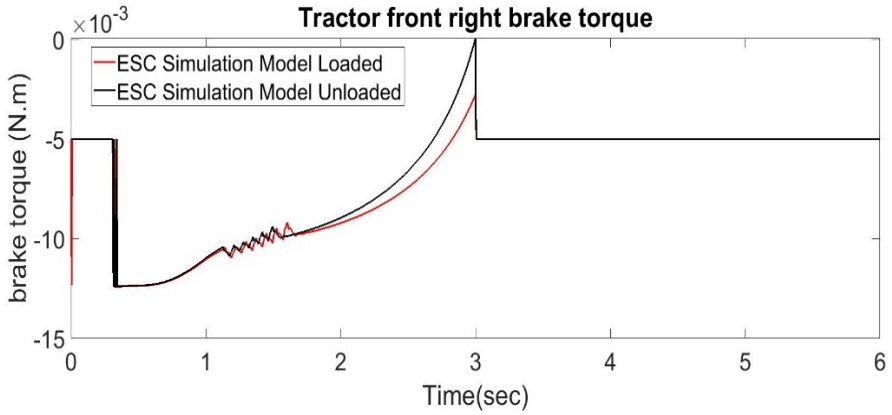

Figure 4-36: tractor front right wheel brake torque loaded vs unloaded

Figure ***4-37*** presents the traction torque applied on the tractor rear axle left side, and from the figures, there is no difference between the loaded and the unloaded model as both of them are fed with the same torque spline explained before. No braking torque is applied through the whole simulation on this wheel side.

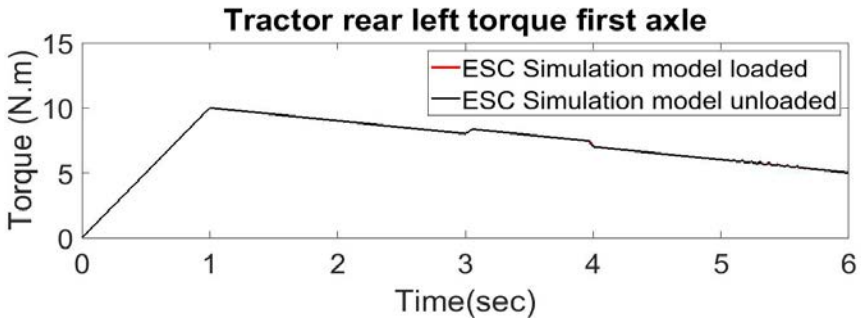

Figure 4-37: tractor left rear wheels first axle torque

Figure ***4-38*** shows an example of one of the three axles of the trailer left side as all of them are the same. The figure shows that the same fluctuation happens to the brake in the unloaded model, like the loaded model and the brake torque for both follow the same trend.

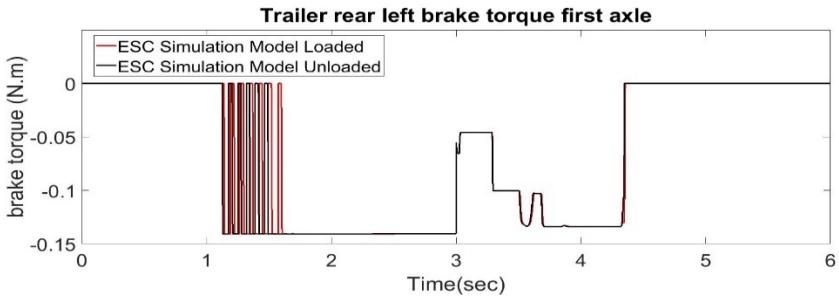

Figure 4-38: trailer left wheel first axle brake torque

Figure ***4-39*** also shows an example of one of the three axles of the trailer right side. The figure shows that the same fluctuation happens to the brake in the unloaded model, like the loaded model and the brake torque for both follow the same trend.

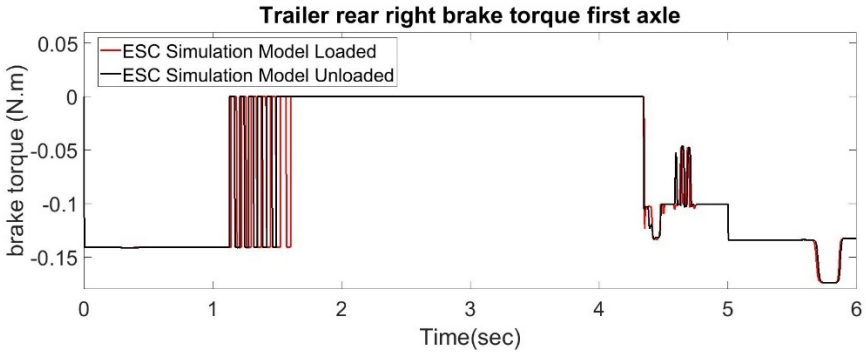

Figure 4-39: trailer right wheel first axle brake torque

4.6.6 Discussion of results for the unloaded condition

The simulation model was tested for two different conditions, loaded and unloaded, but there is no significant difference between control achieved in the two conditions because the controller can adapt to the changes in the vehicle parameters. The number of degrees of freedom for the simulation model did not change. From the response curves, it is obvious that even with the small masses for a scaled model, the loaded vehicle is as stable as the unloaded vehicle as the lateral acceleration is below the standard safe limits.

The figures above show a slight difference in the signal shape between the loaded and unloaded ones, which is expected as the maximum brake force amount depends on the weight on each wheel, which is different due to mass change. Also, the load was distributed on the trailer equally, which relate the same amount on each wheel after removing it, while this could be changed with the undistributed load.

Testing the vehicle in two different loading conditions ensure the effectiveness of the controller through the different operating conditions. However, many other different operating conditions and design parameters could be tested, but this was not done due to time availability.

After finishing the testing and development of the controller on the simulation softwares, the controller should be uploaded on the microcontroller to be able to test it physically. The physical scaled model was not equipped with a brake system to apply the proposed brake force for each tyre. However, this could be achieved by integrating DC motors at each wheel to achieve this target.

Chapter 5: Integrated chassis control

5.1 Introduction

As illustrated in the previous chapter, the simulation model can be controlled through ESC. The ESC system has proved to have many advantages, as described in the literature. However, the integration between the brake control system and the steering system should retain and enhance the vehicle handling performance. In this chapter, the integration between the steering and brakes on the scaled model is investigated. The Fuzzy controller algorithm (fuzzification, defuzzification and the membership function) of the AFS will be illustrated with the integration method, and the results will be presented and discussed. Figure 5-1 shows an illustration diagram of the integrated control.

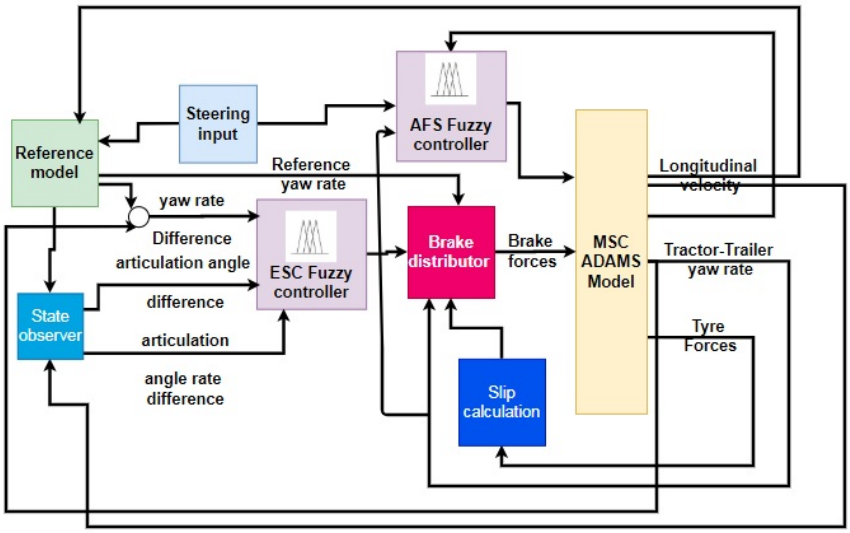

Figure 5-1: an illustrative diagram of the integrated control

5.2 AFS Fuzzy control system

5.2.1 Introduction

Before illustrating the integration process, the AFS model will be demonstrated, then the integration criteria will be mentioned. The AFS is built based on using the Fuzzy logic system. The AFS control requires a multi-body dynamic system modification to transform the passive steering system into an active steering system. This modification lies in adding an actuator to carry out the control system's corrective signal, which leads to the enhancement of the system performance. A motion can be assigned to the scaled model's passive steering system to give the vehicle a steering angle through the Pitman's arm. An actuator is added through another motion to the system to re-correct the excessive steering angle, but the model’s degrees of freedom will be changed, affecting the whole performance, as illustrated in the integrated control section. The next sections will introduce the reference model and the control methodology.

5.2.2 Reference model

As mentioned in the previous chapter, the control system requires a reference model to compare its response with the actual response and calculate the error. The reference model output parameters for the AFS is represented by Yaw rate and sideslip rate. The desired sideslip is assumed to be zero to simplify the equations of motion [124]. Considering this assumption, the sideslip rate error will result in the simulation model sideslip rate value. Consequently, the previous reference model is nearly the same as the reference model of the ESC in chapter 4 but with a slight difference; as the AFS reference model considers for sideslip rate, but it ignores articulation angle, while the ESC reference model considers an articulation angle but ignore the

side slip rate. Therefore, the ESC reference model can be used without considering the articulation angle. Later, all the values will be accounted for it. The integration control reference model, which combines the two control systems (stated above), provides the opportunity to use both angles, whether the sideslip or the articulation, without ignoring one of them.

5.2.3 Fuzzification

The Fuzzy logic control has two inputs, the sideslip and the Yaw rate error, each input based on five sets. The shape for these sets is triangle membership function based on Sun et al. [124]. These sets are divided into five primary knowledge-based rules;

- PB Positive Big,
- PS Positive Small,
- ZE zero,
- NS Negative small
- NB Negative big

Figure 5-2[124] shows the sideslip rate error's Fuzzy set, and Figure 5-3[124] shows the Fuzzy sets of the Yaw rate error.

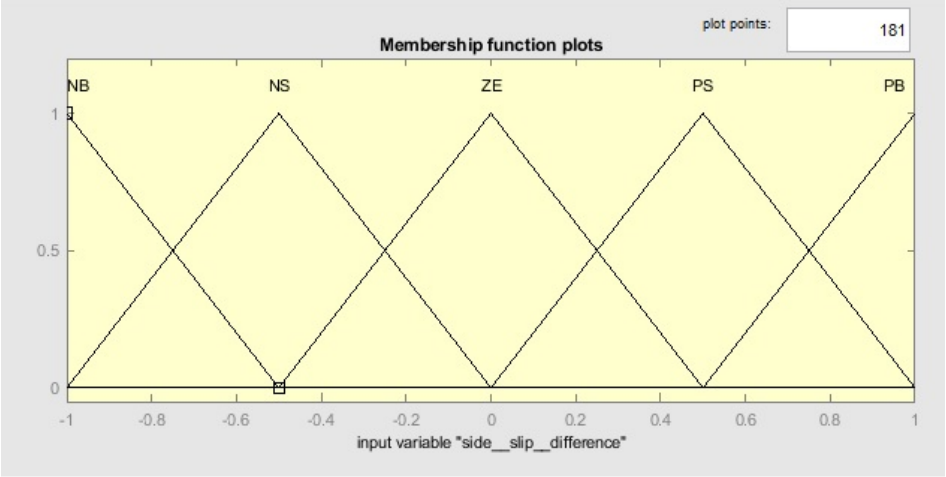

Figure 5-2: the Fuzzy set of side slip error***[124]***

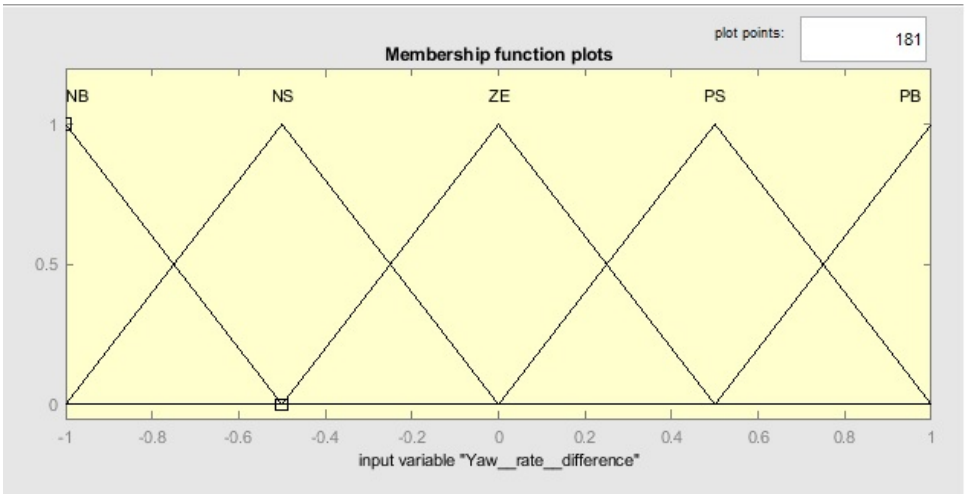

Figure 5-3: the Fuzzy set of the Yaw rate error***[124]***

5.2.4 Membership function

The AFS membership function has two inputs and one output, so twenty-five rules resulted from these inputs and output. The rules can be shown as 3D surface shape since they are three parameters, as shown in Figure 5-4[124], and the rules are presented in

Table 5-1[124]. The rules are the relation between the Yaw rate difference, side slip difference and steer angle. The membership function is based on Mamdani's method.

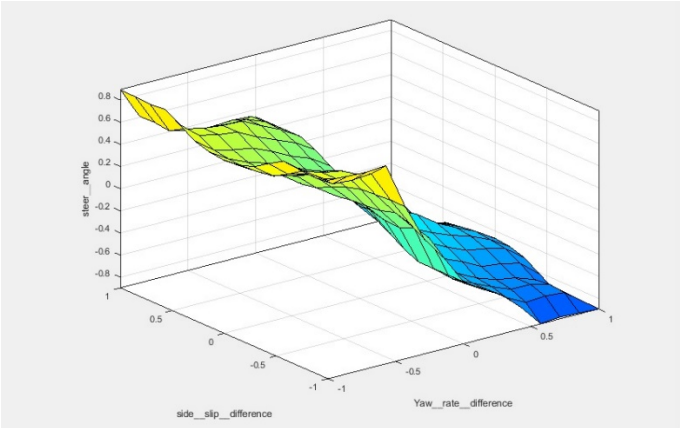

Figure 5-4: surface shape for membership***[124]***

Table 5-1: Fuzzy rules for the membership function of the AFS Fuzzy control system***[124]***

Rule number	Yaw rate difference	Side slip difference	Steer angle
1	PB	NB	NB
2	PB	NS	NB
3	PB	ZE	NM
4	PB	PS	NB
5	PB	PB	NB
6	PS	NB	NB
7	PS	NS	NM
8	PS	ZE	NS
9	PS	PS	NM
10	PS	PB	NS
11	ZE	NB	NS
12	ZE	NS	NS
13	ZE	ZE	ZE
14	ZE	PS	PS
15	ZE	PB	PS
16	NS	NB	PB
17	NS	NS	PM
18	NS	ZE	PS
19	NS	PS	PM
20	NS	PB	PS

21	NB	NB	PB
22	NB	NS	PM
23	NB	ZE	PB
24	NB	PS	PB
25	NB	PB	PB

5.2.5 Defuzzification

The Fuzzy logic control outputs are based on seven sets for each input. The shape for these sets is triangle membership function based on Sun et al. [124]. They are divided into seven primary knowledge-based rules. Figure 5-5[124] shows the Fuzzy set for output steer angle.

- PB positive big,
- PM positive medium,
- PS positive small,
- ZE zero,
- NS negative small,
- NM negative medium,
- NB negative big

The range of the Fuzzy sets determines the output of the Fuzzy controller. The corrective steering angle of the tractor is determined by the scale range [-1,1].

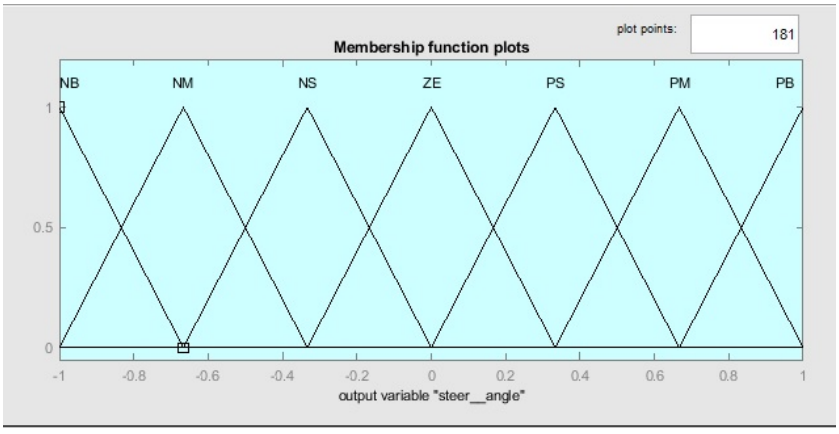

Figure 5-5: Fuzzy set for output steer angle***[124]***

5.3 Integrated control: ESC with AFS

As mentioned in the literature, integrated control should enhance the performance of the vehicle. In this study, the integrated control of electronic stability and the AFS on a multi-body dynamics model is tested. Typically, the integrated control system requires two stages, such as downstream and upstream. These stages are responsible for handling the signals from the two controllers with the system. However, in this study, the two controllers work on the same principle and the same control methodology, which motivates to try different scenarios in combining the two controllers. Thus, after several trials, it was found that the best option for this model is to apply the signals from the two controllers together to enhance the performance.

The final signal from the controllers is multiplied by a factor. One of them is for the front steering control, and the other for the ESC. The front steering control factor, which is 0.5, is used to ensure that the calculated steering angle (the steering angle is measured at the road wheel), which is calculated from the defuzzification, is multiplied by 0.5 and added to the input steering angle and added to the system. Also, to make sure that it is appropriate to the steering angle's input value at the road wheel. The ESC factor is quite different from the brake factor used previously in chapter four; this factor is 0.5. All these factors are obtained from trials and errors.

5.3.1 Results

After adding the AFS to the system, tests were done on four different criteria; the uncontrolled system, the ESC system only, the AFS only and the integrated control. The model runs for 6 seconds with a ramp steering input like the previous test in chapter 4. The main output results are the tractor-trailer Yaw rate, articulation angle, lateral acceleration and the brake torque applied to each wheel. The results from the new ESC and the AFS are ignored. The following

figures compare and show the difference between the uncontrolled simulation model, reference model, old ESC model and integrated control. Tractor-trailer longitudinal velocity is shown in Figure 5-6. The integrated model follows the ESC for the first 1.8 seconds; then it starts to be lower than it by about 0.2m/sec until it reaches the peak value, then the velocity starts to drop until it reaches around 0.6m/sec by the end of the simulation.

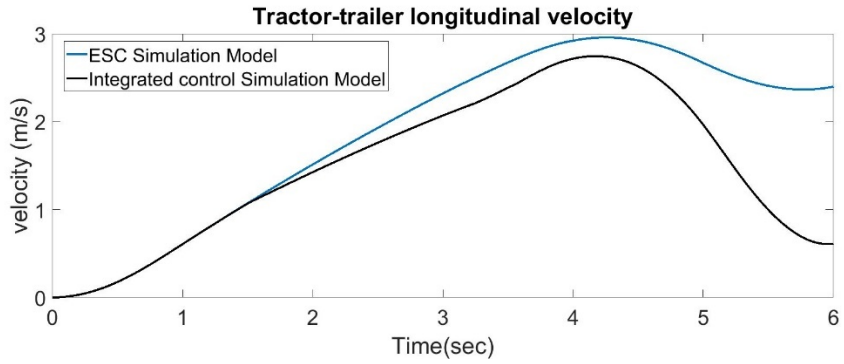

Figure 5-6: tractor-trailer longitudinal velocity comparison for both control systems

Figure 5-7 shows the comparison of the tractor Yaw rate of the two control systems. Overall, the ESC system almost follows the same trend as the reference model, while the integrated model was worse than the uncontrolled model. The simulation shows that the integrated control model starts to deviate from the other curves from 1.5 seconds. First, it was lower than all of them with a slight difference; then it starts to be the highest from around 3.6 seconds. It reaches a 45 deg/sec peak; then, it decreases when it reaches 5 seconds to be lower than the uncontrolled one before the end of the simulation by 0.5 seconds. The other three curves remain the same trend as explained before in the previous chapter.

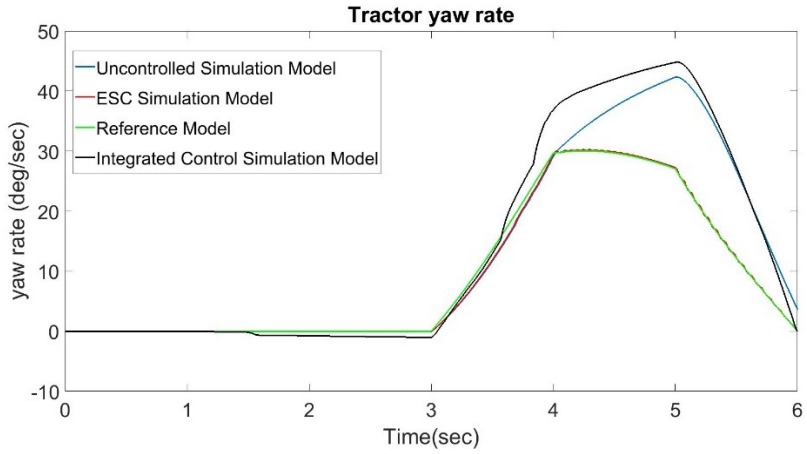

Figure 5-7: tractor Yaw rate comparison for both control systems

Also, the trailer Yaw rate, as shown in Figure 5-8. The same happens with the trailer, but the integrated control curve was smoother than the tractor figure. Again the other two curves follow the same trend from the previous chapter.

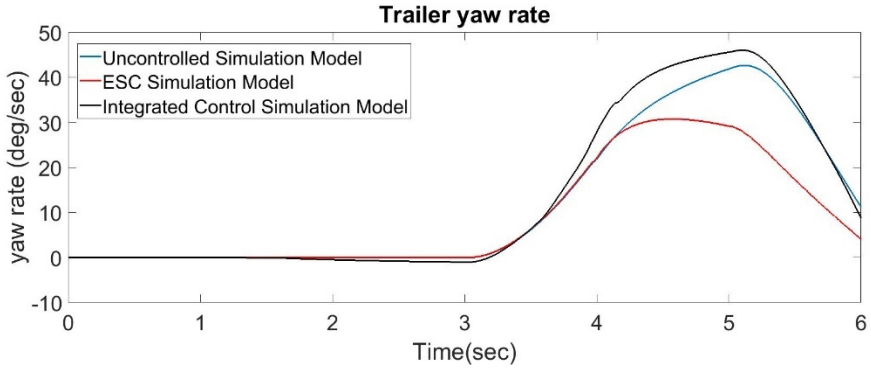

Figure 5-8: trailer Yaw rate comparison for both control systems

The articulation angle is shown in Figure 5-9. The integrated control was lower in its value than the reference model, starts from 1.5 seconds until it reaches the fourth second it starts to be higher and then, it matches with the uncontrolled model from the fifth second until the end of the simulation, with a very slight difference than the uncontrolled model before the end.

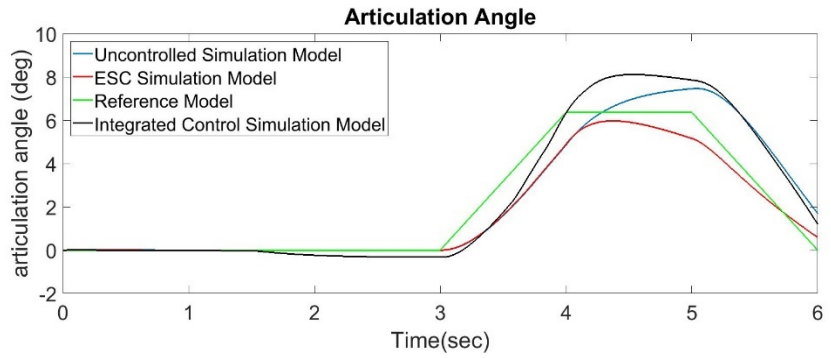

Figure 5-9: tractor-trailer articulation angle comparison for both control systems

Figure 5-10 presents the tractor lateral acceleration. The integrated control curve is higher than the uncontrolled one as well, but it matches the uncontrolled curve when it reaches the fifth second, then it deviates again with a slightly higher value than it.

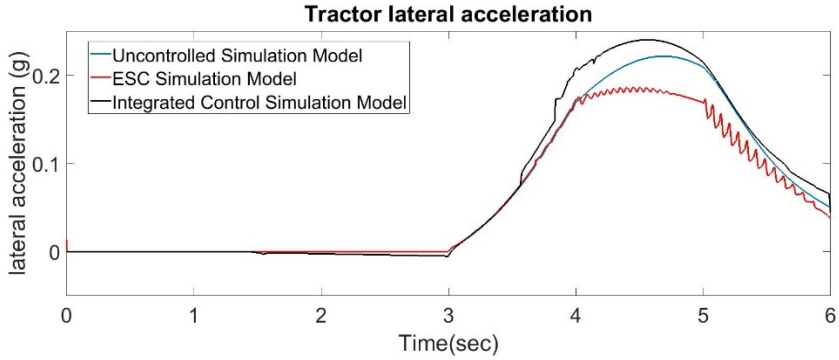

Figure 5-10: tractor lateral acceleration comparison for both control systems

Figure 5-11 shows the trailer lateral acceleration. The trailer curve is different from the tractor one when it reaches 3.5 seconds, but it is the same trend as the tractor one when it reaches the peak but is not matching until the end of the simulation.

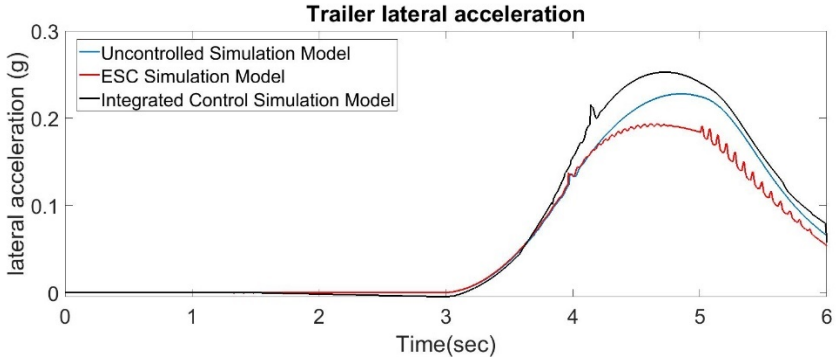

Figure 5-11: trailer lateral acceleration comparison for both control systems

5.3.2 Discussion of results

The performance of the system is changed even with the ESC system. This is because the MSC ADAMS model's co-simulation with MATLAB depends on generating an M file in MSC ADAMS and importing it into MATLAB to define the system matrices. So, by changing the number of degrees of freedom in the model and adding another motion to the steering system, all the matrices and the vehicle's performance are changed. Besides, tuning the new system changes the ESC logic, therefore comparing the different output parameters of the integrated control and the output of the previous ESC is the way out to help in understanding the output performance of changing the degrees of freedom and to measure the effectiveness of the integrated control in this case. These figures prove that changing the degrees of freedom affects the control methodology, which is apparent in the tractor Yaw rate results. Also, the results show that the ESC is much better than the integrated control while the integrated control is even worse than the uncontrolled situation. This means that the development of integrated control makes the vehicle more unstable than the uncontrolled situation. The same occurs with the trailer Yaw rate.

Furthermore, the vehicle speed reduces greatly, as shown in Figure 5-6, which means that the integrated control applies a much bigger brake force on the vehicle, slowing it down almost to a stop. Similar behaviour is observed for the rest of the output performances from the articulation angle, tractor lateral acceleration and trailer lateral acceleration. Thus, using integrated control is not better than using ESC solely.

Finally, the way the integrated control was implemented is by switching both the ESC and the AFS on. However, some studies [100, 101] prefer to establish layers that can govern the two control systems; in this case, the governer can choose which control needs to be on and which ones need to be off according to the state of the vehicle. Therefore it can optimize the performance of the vehicle. Meanwhile, the aim was to test different control schemes rather than optimizing a current one.

Chapter 6: Summary and future work

6.1 Conclusion

This chapter concludes and summarises the complete work that has been done to achieve this study project on “investigation of integrated control of articulated heavy vehicle using scaled multi-body dynamic model”. Besides, this chapter proposes recommendations on future research work that can be done to further progress and expand the current study work for more insights and research findings.

In this study, a literature review highlighted the need to test and develop new control systems for heavy vehicle road safety. To achieve this research's main aim, the fidelity of modelling a scaled model of a tractor semi-trailer using multi-body dynamics software was investigated. Also, to develop new control systems for enhancing heavy vehicle stability, a co-simulation is constructed to test different control schemes to enhance the vehicle's total performance. Thus, it allows the developed control method to be applied in the Full-scale model later on.

Also, referring back to the main objectives, this study has concluded the following points.

- The study of heavy vehicle dynamics using a scaled model can be implemented by developing a detailed complete vehicle handling model using computer software (MSC ADAMS/View) and validating it.
- Developing new control systems through co-simulation can be used for stabilising the vehicle through manoeuvres.

- The performance of heavy vehicle scaled model handling dynamics can be enhanced when equipped with control systems via co-simulation.
- The proposed integrated control systems' performance that merges the ESC with the AFS did not achieve better results than the ESC system alone.

After applying the main objectives, some critical points about the conclusion from the way this study was implemented are summarised.

6.1.1 Simulation model

Building a scaled model on multi-body dynamics software requires measuring the different parts precisely, especially the steering and suspension hardpoints. A small error can cause the model to lock or not work precisely.

The scaled models 1/14 leads to small masses in some parts of the suspension and the steering. Modelling these small masses in multi-body dynamics is not desirable, so to reduce the simulation errors, it is preferable to resize the scaled model to 1/10 from the Full-scale.

MSC ADAMS/View is preferable than using MSC ADMAS/Car as it allows the testing of the system while building it and eliminates the interference of the input/output communicators in MSC ADAMS/Car.

6.1.2 Physical test

When using the Arduino Mega with three ultrasonic sensors and the motion control is around 3 Hz, the sampling rate is inadequate to capture the response with enough resolution, so it is preferred to separate the motion controller from the data collection controller.

The microcontroller has a low buffer size (64 bytes) so using an SD card is a must to record each reading from the accelerometer. Consequently, the maximum sampling rate that can be achieved is 10Hz.

It is recommended to use a high torque servo motor to ensure that the steering system produces a more accurate steering angle because the resolution of the servo motor used is not adequate to overcome the backlash from the steering links. The steering mechanism's tolerance (the backlash) affects the steering angle so that hard links can eliminate it.

The ultrasonic sensor range is up to 4 metres, so a Lidar sensor can be used to give a stopping distance of up to 30 metres in case of high speed.

6.1.3 Control and co-simulation

Using the ESC system, which combines the Traction force and the brake force for the heavy vehicle, can enhance vehicle stability through manoeuvres.

Changing the degrees of freedom for a co-simulated multi-body dynamics model worsens the designed controller.

6.2 Recommendations

Using a scaled model at the beginning of designing a new control system and building a prototype is useful in saving money and implementing the control system in a safe environment. A scaled model built on a multi-body dynamic system software can be controlled by co-simulation and allows tests to be carried out for different control methodologies. However, testing these controllers physically needs a precise microcontroller rather than Arduino controllers because the Arduino memory size is too small.

6.3 Future work

Due to the limitation in facilities and time, the following suggested ideas can help in improving the work in future.

- A scaled model with a ratio of 1/10 could be used to obtain more accurate results, avoid small masses in the multi-body dynamics software, and develop control algorithms to prevent jack-knifing and roll-over.
- A controller capable of a higher sampling rate should also be used to enable a higher response resolution.
- Incorporating a more sophisticated tyre model within the vehicle model.
- Extend the present work considering flexible frames.
- Optimisation of the vehicle suspension system parameters considering flexible links.
- Integrate more chassis control systems such as semi-active suspension or active suspension.
- Run the vehicle outdoor on a broader area and run the physical model in different scenarios.
- Build an entire brake system in the physical model as well as the simulation.
- Consider different control theories and robust methodologies for the chassis control system.
- Change the type of the trailer to be more extensive such as tanker trucks.

References

1. Kassebaum, N.J., et al., *Global, regional, and national levels and causes of maternal mortality during 1990–2013: a systematic analysis for the Global Burden of Disease Study 2013.* The Lancet, 2014. **384**(9947): p. 980-1004.
2. Abubakar, I., T. Tillmann, and A. Banerjee, *Global, regional, and national age-sex specific all-cause and cause-specific mortality for 240 causes of death, 1990-2013: a systematic analysis for the Global Burden of Disease Study 2013.* Lancet, 2015. **385**(9963): p. 117-171.
3. Statistics, C.A.f.P.M.a., *Annual bulletin for automobiles and trains accidents.* 2014. **2014-21121-71**.
4. Centre for Road Safety, T.f.N., *ROAD TRAFFIC CRASHES IN NEW SOUTH WALES.* 2014.
5. Parliament, U., *Automotive Sector Report.*
6. Gillespie, T.D., *Fundamentals of vehicle dynamics*. 1992, SAE Technical Paper.
7. Rumar, K., *A worldwide perspective on future automobile lighting.* 2001.
8. UNECE. *UNECE works on new standards to increase the safety of trucks and coaches*. 2011; Available from: https://www.unece.org/press/pr2011/11trans_p10e.html.
9. Chen, L. and Y. Shieh, *Jackknife prevention for articulated vehicles using model reference adaptive control.* Proceedings of the Institution of Mechanical Engineers, Part D: Journal of Automobile Engineering, 2011. **225**(1): p. 28-42.
10. Brennan, S. and A. Alleyne, *Robust scalable vehicle control via non-dimensional vehicle dynamics.* Vehicle System Dynamics, 2001. **36**(4-5): p. 255-277.
11. Chen, L. and J. Hsu, *Investigation of jack-knife prevention in an articulated scaled vehicle.* Vehicle System Dynamics, 2008. **46**(S1): p. 765-777.
12. Brennan, S. and A. Alleyne. *A scaled testbed for vehicle control: The IRS.* in *Proceedings of the 1999 IEEE International Conference on Control Applications (Cat. No. 99CH36328)*. 1999. IEEE.
13. Huang, H.-H., R.K. Yedavalli, and D.A. Guenther, *Active roll control for rollover prevention of heavy articulated vehicles with multiple-rollover-index minimisation.* Vehicle system dynamics, 2012. **50**(3): p. 471-493.
14. Rath, J.J., M. Defoort, and K.C. Veluvolu, *Rollover index estimation in the presence of sensor faults, unknown inputs, and uncertainties.* IEEE transactions on intelligent transportation systems, 2016. **17**(10): p. 2949-2959.
15. Li, B. and S. Rakheja, *Jackknifing Prevention of Tractor-Semitrailer Combination Using Active Braking Control*. 2015, SAE Technical Paper.
16. He, Y., M.M. Islam, and T.D. Webster, *An integrated design method for articulated heavy vehicles with active trailer steering systems.* SAE International Journal of Passenger Cars-Mechanical Systems, 2010. **3**(2010-01-0092): p. 158-174.
17. Palkovics, L. and A. Fries, *Intelligent electronic systems in commercial vehicles for enhanced traffic safety.* Vehicle System Dynamics, 2001. **35**(4-5): p. 227-289.
18. Zhao, Y., S. Chen, and T. Shim, *Investigation of trailer yaw motion control using active front steer and differential Brake.* SAE International Journal of Materials and Manufacturing, 2011. **4**(1): p. 1057-1067.

19. Talukdar, S. and S. Kulkarni, *A Comparative Analysis of a Rigid Bicycle Model with an Elastic Bicycle Model for Small Trucks*. 2011, SAE Technical Paper.
20. Wong, J., *Theory of Ground Vehicles, New York, John Willey & Sons*. 2001, Inc.
21. Xia, X. and E. Law, *Nonlinear dynamic response of four wheel steering automobiles to combined braking and steering commands in collision avoidance maneuvers.* SAE transactions, 1990: p. 1474-1482.
22. Moldenhauer, P.M. and J.C. Huston, *Lateral stability of recreational vehicles in steady-state turning: an extended bicycle model.* SAE transactions, 1986: p. 164-173.
23. Nguyen, V., *Vehicle handling, stability, and bifurcaiton analysis for nonlinear vehicle models*. 2005.
24. Williams, D., *Multi-axle vehicle dynamics*. 2012, SAE Technical Paper.
25. Williams, D. and A. Nhila, *Handling comparison of vehicles with steerable auxiliary axles.* SAE International Journal of Commercial Vehicles, 2013. **6**(2013-01-2353): p. 281-287.
26. Williams, D. and K.A. Sherwin, *Vehicle Performance Improvement by Steering a Third Axle*. 2010, SAE Technical Paper.
27. Dahlberg, E., *A method determining the dynamic rollover threshold of commercial vehicles.* SAE transactions, 2000: p. 789-801.
28. Choi, B.-L., et al., *The optimization of automotive suspension system considering multidisciplinary design requirements*. 2009, SAE Technical Paper.
29. Hahn, Y., *Kinematics and Compliance (K & C) Simulation Using a Nonlinear Finite Element Model*. 2010, SAE Technical Paper.
30. Oz, Y., B. Ozan, and E. Uyanik, *Steering System Optimization of a Ford Heavy-Commercial Vehicle Using Kinematic & Compliance Analysis*. 2012, SAE Technical Paper.
31. Committee, S.V.D., *Vehicle Dynamics Terminology.* SAE J670e, 1976.
32. Pacejka, H., *Tire and vehicle dynamics*. 2005: Elsevier.
33. Göhring, E. and E. Von Glasner, *The Impact Of Tyre Characteristics On The Braking And Steering Performance Of Commercial Vehicles*. 1988, SAE Technical Paper.
34. Pazooki, A., S. Rakheja, and D. Cao, *Effect of terrain roughness on the roll and yaw directional stability of an articulated frame steer vehicle.* SAE International Journal of Commercial Vehicles, 2013. **6**(2013-01-2366): p. 325-339.
35. Tateishi, Y., et al., *The Effects of the Tire Camber Angle on Vehicle Controllability and Stability*. 1986, SAE Technical Paper.
36. FIALA, F., *Seitenkrafte am rollenden luftreifen.* Z. VDI, 1954. **29**.
37. Blundell, M. and D. Harty, *Multibody systems approach to vehicle dynamics*. 2004: Elsevier.
38. Mastinu, G., et al., *A semi-analytical tyre model for steady-and transient-state simulations.* Vehicle system dynamics, 1997. **27**(S1): p. 2-21.
39. Svendenius, J. and M. Gäfvert, *A semi-empirical tyre model for combined slips including the effects of cambering.* Vehicle System Dynamics, 2005. **43**(sup1): p. 317-328.
40. Pacejka, H.B. and E. Bakker, *The magic formula tyre model.* Vehicle system dynamics, 1992. **21**(S1): p. 1-18.
41. Lapapong, S., et al., *Fidelity of using scaled vehicles for chassis dynamic studies.* Vehicle System Dynamics, 2009. **47**(11): p. 1401-1437.

42. Brennan, S. and A. Alleyne, *The Illinois Roadway Simulator: A mechatronic testbed for vehicle dynamics and control.* IEEE/ASME transactions on mechatronics, 2000. **5**(4): p. 349-359.
43. Altafini, C. *Zero dynamics and off-tracking bounds for the path following problem of wheeled vehicles*. in *Proceedings of the 38th IEEE Conference on Decision and Control (Cat. No. 99CH36304)*. 1999. IEEE.
44. Altafini, C. and A. Speranzon. *Backward line tracking control of a radio-controlled truck and trailer*. in *Proceedings 2001 ICRA. IEEE International Conference on Robotics and Automation (Cat. No. 01CH37164)*. 2001. IEEE.
45. Altafini, C., A. Speranzon, and B. Wahlberg, *A feedback control scheme for reversing a truck and trailer vehicle.* IEEE Transactions on robotics and automation, 2001. **17**(6): p. 915-922.
46. Altafini, C., *Path following with reduced off-tracking for multibody wheeled vehicles.* IEEE transactions on control systems technology, 2003. **11**(4): p. 598-605.
47. Kaneko, T., H. Iizuka, and I. Kageyama, *Steering control for advanced guideway bus system with all-wheel steering system.* Vehicle System Dynamics, 2006. **44**(sup1): p. 741-746.
48. Chen, L.-k., *Jack-Knife Prevention for Articulated Vehicles Using Self-Organizing Fuzzy Control*. 2011, SAE Technical Paper.
49. Patil, C.B., R.G. Longoria, and J. Limroth. *Control prototyping for an anti-lock braking control system on a scaled vehicle*. in *42nd IEEE International Conference on Decision and Control (IEEE Cat. No. 03CH37475)*. 2003. IEEE.
50. Longoria, R.G., A. Al-Sharif, and C.B. Patil, *Scaled vehicle system dynamics and control: a case study in anti-lock braking.* International journal of vehicle autonomous systems, 2004. **2**(1-2): p. 18-39.
51. Travis, W.E., et al. *Using scaled vehicles to investigate the influence of various properties on rollover propensity*. in *Proceedings of the 2004 American Control Conference*. 2004. IEEE.
52. Whitehead, R., B. Clark, and D.M. Bevly. *ESC effectiveness during property variations on scaled vehicles*. in *ASME 2005 International Mechanical Engineering Congress and Exposition*. 2005. American Society of Mechanical Engineers.
53. Chen, L.-k. and S.-y. Hsu. *Investigation of driver-controller interaction in vehicle rollover prevention*. in *2006 IEEE International Conference on Systems, Man and Cybernetics*. 2006. IEEE.
54. Cai, L., A.B. Rad, and W.-L. Chan, *A genetic fuzzy controller for vehicle automatic steering control.* IEEE transactions on vehicular technology, 2007. **56**(2): p. 529-543.
55. Polley, M. and A.G. Alleyne. *Dimensionless analysis of tire characteristics for vehicle dynamics studies*. in *Proceedings of the 2004 American control conference*. 2004. IEEE.
56. Polley, M., A. Alleyne, and E.D. Vries, *Scaled vehicle tire characteristics: dimensionless analysis.* Vehicle System Dynamics, 2006. **44**(2): p. 87-105.
57. Verma, R., D. Del Vecchio, and H.K. Fathy, *Development of a scaled vehicle with longitudinal dynamics of an HMMWV for an ITS testbed.* IEEE/ASME Transactions on Mechatronics, 2008. **13**(1): p. 46-57.
58. Verma, R., D. Del Vecchio, and H.K. Fathy. *Longitudinal vehicle dynamics scaling and implementation on a HIL setup*. in *ASME 2008 Dynamic Systems and Control Conference*. 2008. American Society of Mechanical Engineers Digital Collection.

59. Phanomchoeng, G. and R. Rajamani, *New rollover index for the detection of tripped and untripped rollovers.* IEEE Transactions on Industrial Electronics, 2012. **60**(10): p. 4726-4736.
60. Phanomchoeng, G. and R. Rajamani, *Real-time estimation of rollover index for tripped rollovers with a novel unknown input nonlinear observer.* IEEE/ASME Transactions on Mechatronics, 2013. **19**(2): p. 743-754.
61. Mahyuddin, M.N., et al., *Adaptive observer-based parameter estimation with application to road gradient and vehicle mass estimation.* IEEE Transactions on Industrial Electronics, 2013. **61**(6): p. 2851-2863.
62. Parczewski, K. and H. Wnęk, *Using mobile scaled vehicle to investigate the truck lateral stability.* Eksploatacja i Niezawodność, 2013. **15**.
63. He, W., et al. *A scaled-down traffic system based on autonomous vehicles: A new experimental system for ITS research*. in *2012 15th International IEEE Conference on Intelligent Transportation Systems*. 2012. IEEE.
64. Solmaz, S. and T. COŞKUN, *An automotive vehicle dynamics prototyping platform based on a remote control model car.* Turkish Journal of Electrical Engineering & Computer Sciences, 2013. **21**(2): p. 439-451.
65. Ahn, H., et al. *Experimental testing of a semi-autonomous multi-vehicle collision avoidance algorithm at an intersection testbed*. in *2015 IEEE/RSJ International Conference on Intelligent Robots and Systems (IROS)*. 2015. IEEE.
66. Rosolia, U., S. De Bruyne, and A.G. Alleyne, *Autonomous vehicle control: A nonconvex approach for obstacle avoidance.* IEEE Transactions on Control Systems Technology, 2016. **25**(2): p. 469-484.
67. Goila, A., et al., *ADAS Feature Concepts Development Framework via a Low Cost RC Car*. 2017, SAE Technical Paper.
68. Kuyt, C. and M. Como. *Mixed Kinematics and Camera Based Vehicle Dynamic Sideslip Estimation for an RC Scaled Model*. in *2018 IEEE Conference on Control Technology and Applications (CCTA)*. 2018. IEEE.
69. Sabbioni, E. and F. Cheli, *Analysis of ABS/ESP control logics using a HIL test bench*. 2011, SAE Technical Paper.
70. Schuette, H. and P. Waeltermann, *Hardware-in-the-loop testing of vehicle dynamics controllers–a technical survey.* SAE transactions, 2005: p. 593-609.
71. Liu, C., et al., *Model Integration and Hardware-in-the-Loop (HiL) Simulation Design for the Testing of Electric Power Steering Controllers*. 2016, SAE Technical Paper.
72. Salaani, M.K., et al., *Hardware-in-the-loop pneumatic braking system for heavy truck testing of advanced electronic safety interventions.* SAE International journal of passenger cars-mechanical systems, 2016. **9**(2016-01-1648): p. 912-923.
73. Lozoya-Santos, J.d.-J., R. Morales-Menendez, and R.A. Ramirez-Mendoza, *Evaluation of on–off semi-active vehicle suspension systems by using the hardware-in-the-loop approach and the software-in-the-loop approach.* Proceedings of the Institution of Mechanical Engineers, Part D: Journal of Automobile Engineering, 2015. **229**(1): p. 52-69.
74. Datar, M.V., *Uncertainty quantification in ground vehicle dynamics through high fidelity co-simulation*. 2009, University of Wisconsin--Madison.
75. Limroth, J., T. Kurfess, and E.H. Law, *Co-Simulation of Heavy Truck Tire Dynamics and Electronic Stability Control Systems (Phase A).* 2009.

76. Rao, S.J., *Vehicle modeling and Adams-Simulink co-simulation with integrated continuously controlled electronic suspension (CES) and electronic stability control (ESC) models*. 2009, The Ohio State University.
77. Li, S.-q. and L. He, *Co-simulation study of vehicle ESP system based on ADAMS and MATLAB.* Journal of Software, 2011. **6**(5): p. 866-872.
78. Lin, X., et al., *High speed optimal yaw stability of tractor-semitrailers with active trailer steering*. 2014, SAE Technical Paper.
79. Zhao, Y., et al., *Study on the ride performance of a semi-active air suspension vehicle under complex models based on co-simulation*. 2015, SAE Technical Paper.
80. Joshi, A., *Powertrain and Chassis Hardware-in-the-Loop (HIL) Simulation of Autonomous Vehicle Platform*. 2017, SAE Technical Paper.
81. ; Available from: https://www.truckingtruth.com/cdl-training-program/page48/driving-combination-vehicles.
82. Hwang, T., et al. *Development of HILS systems for active brake control systems*. in *2006 SICE-ICASE International Joint Conference*. 2006. IEEE.
83. Ferguson, S.A., *The effectiveness of electronic stability control in reducing real-world crashes: a literature review.* Traffic injury prevention, 2007. **8**(4): p. 329-338.
84. Trigell, A.S., et al., *Advanced vehicle dynamics of heavy trucks with the perspective of road safety.* Vehicle system dynamics, 2017. **55**(10): p. 1572-1617.
85. LATEEF, M. and M.K. RAO, *HYDRO PNEUMATIC SUSPENSION SYSTEM FOR TRACTOR IMPLEMENT*.
86. Crosby, M. and D.C. Karnopp, *The active damper—a new concept for shock and vibration control.* Shock and Vibration Bulletin, 1973. **43**(4): p. 119-133.
87. Ahmadian, M., *Integrating Electromechanical Systems in Commercial Vehicles for Improved Handling, Stability, and Comfort.* SAE International Journal of Commercial Vehicles, 2014. **7**(2014-01-2408): p. 535-587.
88. Agrawal, H. and J. Gustafsson, *Investigation of active anti-roll bars and development of control algorithm*. 2017.
89. Mulla, A.A. and D.R. Unaune. *Active suspensions future trend of automotive suspensions*. in *International Conference on Emerging Trends in Technology*. 2013.
90. Chen, Y., A.W. Peterson, and M. Ahmadian, *Achieving anti-roll bar effect through air management in commercial vehicle pneumatic suspensions.* Vehicle system dynamics, 2019. **57**(12): p. 1775-1794.
91. Gillespie, T.D., *Fundamentals of vehicle dynamics*. Vol. 400. 1992: Society of automotive engineers Warrendale, PA.
92. Kumar, E.A., D. Dinesh, and N. Kamble, *An overview of active front steering system.* International Journal of Scientific & Engineering Research, 2012. **3**(6): p. 556-565.
93. Kim, K.-i., et al., *Active steering control strategy for articulated vehicles.* Frontiers of Information Technology & Electronic Engineering, 2016. **17**(6): p. 576-586.
94. Chung, S. and H. Lee. *Estimating desired yaw rate and control strategy analysis on developed air ESC system for performance evaluation*. in *2015 15th International Conference on Control, Automation and Systems (ICCAS)*. 2015. IEEE.
95. Yang, X., J. Song, and J. Gao, *Fuzzy logic based control of the lateral stability of tractor semitrailer vehicle.* Mathematical Problems in Engineering, 2015. **2015**.
96. Shi, X. and J. Bao. *An improved vehicle rollover prediction algorithm*. in *2013 International Conference on Computational and Information Sciences*. 2013. IEEE.
97. Czechowicz, M.P. and G. Mavros, *Analysis of vehicle rollover dynamics using a high-fidelity model.* Vehicle System Dynamics, 2014. **52**(5): p. 608-636.

98. Chen, C. and M. Tomizuka, *Lateral control of commercial heavy vehicles.* Vehicle System Dynamics, 2000. **33**(6): p. 391-420.
99. HOSSEINIAN AHANGARNEJAD, A., *Integrated control of active vehicle chassis control systems.* 2018.
100. Zhu, B., Y. Chen, and J. Zhao, *Integrated chassis control of active front steering and yaw stability control based on improved inverse Nyquist array method.* The Scientific World Journal, 2014. **2014**.
101. Vivas-Lopez, C.A., et al., *Global chassis control system using suspension, steering, and braking subsystems.* Mathematical Problems in Engineering, 2015. **2015**.
102. Wang, Y.-Y. and F.-N. Yang. *Integrated control to improve vehicle handling and stability based on the control authority of chassis key electronic controller*. in *2017 International Conference on Circuits, Devices and Systems (ICCDS)*. 2017. IEEE.
103. John, S. and J.O. Pedro. *A comparative study of two control schemes for anti-lock braking systems*. in *2013 9th Asian Control Conference (ASCC)*. 2013. IEEE.
104. Van Putten, B., M. Traineeship, and I.I. Besselink, *Design of an Electronic Stability Program for vehicle simulation software.* DCT 2008.138, 2008.
105. Oraby, W., et al., *Improvement of vehicle lateral dynamics by active front steering control.* SAE transactions, 2004: p. 1101-1110.
106. Noh, T., et al., *A control strategy to compensate the reaction torque of active front steering system*. 2007, SAE Technical Paper.
107. Zhao, W., H. Zhang, and Y. Li, *Displacement and force coupling control design for automotive active front steering system.* Mechanical Systems and Signal Processing, 2018. **106**: p. 76-93.
108. Ding, X., et al. *A comparative study of control algorithms for active trailer steering systems of articulated heavy vehicles*. in *2012 American Control Conference (ACC)*. 2012. IEEE.
109. Wang, Q., S. Zhu, and Y. He, *Model reference adaptive control for active trailer steering of articulated heavy vehicles*. 2015, SAE Technical Paper.
110. Ahmadian, M., *Semiactive fuzzy logic control for heavy truck primary suspensions: Is it effective?* 2005, SAE Technical Paper.
111. Hwang, T., et al., *Design of integrated chassis control logics for AFS and ESP.* International Journal of Automotive Technology, 2008. **9**(1): p. 17-27.
112. Fergani, S., O. Sename, and L. Dugard. *A LPV suspension control with performance adaptation to roll behavior, embedded in a global vehicle dynamic control strategy*. in *2013 European Control Conference (ECC)*. 2013. IEEE.
113. Wang, C., et al., *Chassis Tuning Study of a Commercial Vehicle*. 2015, SAE Technical Paper.
114. Lomada, B., R. Jayaganthan, and V. Vijaykumar, *Optimisation of Steering System Geometry of Longer FOH Commercial Vehicles*. 2015, SAE Technical Paper.
115. Hou, Y. and M. Ahmadian, *Effects of Commercial Truck Configuration on Roll Stability in Roundabouts*. 2015, SAE Technical Paper.
116. Yang, X., R. Zhu, and J. Gao, *Handling-Stability Oriented Parameter Optimization for a Tractor Semi-Trailer Vehicle*. 2015, SAE Technical Paper.
117. Ibrahim, I., D. Crolla, and D. Barton, *Effect of frame flexibility on the ride vibration of trucks.* Computers & Structures, 1996. **58**(4): p. 709-713.
118. Sill, J., et al., *Roll stability control for torsionally compliant vehicles*. 2010, SAE Technical Paper.

119. Geller, B. and T. Bradley, *Quantifying Uncertainty in Vehicle Simulation Studies.* SAE International Journal of Passenger Cars-Mechanical Systems, 2012. **5**(2012-01-0506): p. 381-392.
120. Katriniok, A., *Optimal vehicle dynamics control and state estimation for a low-cost GNSS-based collision avoidance system*. 2014: VDI Verlag.
121. Hashemi, E., *Full vehicle state estimation using a holistic corner-based approach.* 2017.
122. Wang, L., et al., *Vehicle Mass Estimation for Heavy Duty Vehicle*. 2015, SAE Technical Paper.
123. Sensortec, B., *Intelligent 9-axis absolute orientation sensor.* BNO055 datasheet, November, 2014.
124. Sun, T., et al., *Study on integrated control of active front steering and direct yaw moment based on vehicle lateral velocity estimation.* Mathematical Problems in Engineering, 2013. **2013**.

Appendix A: Tyre property File

```
$----------------------------------------------------------------------MDI_HEADER
[MDI_HEADER]
 FILE_TYPE     =  'tir'
 FILE_VERSION  =  2.0
 FILE_FORMAT   =  'ASCII'
{COMMENTS}
{comment_string}
 Tire      - XXXXXX'
 Pressure  - XXXXXX'
 Test Date - XXXXXX'
 Test tire'
 New File Format v2.1'
$----------------------------------------------------------------------------units
[UNITS]
 LENGTH              = 'mm'
 FORCE               = 'newton'
 ANGLE               = 'degree'
 MASS                = 'kg'
 TIME                = 'sec'
$-----------------------------------------------------------------------------model
[MODEL]
   use mode    1   2
   -------------------------
   smoothing       X

 PROPERTY_FILE_FORMAT    = 'FIALA'
 USE_MODE                = 1.0
$--------------------------------------------------------------------------dimension
[DIMENSION]
 UNLOADED_RADIUS         = 41.5
 WIDTH                   = 20
 ASPECT_RATIO            = 0.78
$-------------------------------------------------------------------------parameter
[PARAMETER]
 VERTICAL_STIFFNESS      = 873
 VERTICAL_DAMPING        = 10.0
 ROLLING_RESISTANCE      = 0.1
 CSLIP                   = 30000
 CALPHA                  = 400
 CGAMMA                  = 0.0
 UMIN                    = 0.7
 UMAX                    = 0.8
$----------------------------------------------------------------------------shape
[SHAPE]
{radial width}
 1.0    0.0
 1.0    0.2
 1.0    0.4
 1.0    0.5
 1.0    0.6
 1.0    0.7
 1.0    0.8
 1.0    0.85
 1.0    0.9
 0.9    1.0
```

Appendix B: Microcontroller programme used

B.1. Arduino Mega Sketch for controlling the motion

```
#include <SoftwareSerial.h> // for the serial
#include <Servo.h> // for the servo motors
#include <Wire.h> // for I2C
#define trigpin1 8 // the transmitting pin connection for the front sensor
#define echopin1 9 // the receiving pin connection for the front sensor
#define trigpin2 10 // the transmitting pin connection for the right sensor
#define echopin2 11 // the receiving pin connection for the right sensor
#define trigpin3 12 // the transmitting pin connection for the left sensor
#define echopin3 13 // the receiving pin connection for the left sensor
const byte M1CWPin = 4; // INA: Clockwise Input
const byte M1CCWPin = 5; // INB: Counter-clockwise Input
const byte M1PWMPin = 6; // PWM Input
const byte M1CurrentSensePin = A14; // CS: Current sense ANALOG Input
const byte M1EnablePin = A15; // EN: Status of switches output (Analog pin)
int i=0;
Servo mysteerservo; // create servo object to control a servo
Servo myshiftservo;
int steer = 100; // variable to store the servo position
int shift = 90;
int pos = 0; // variable to store the servo position
long
time_front,distance_front,minimum_front,distance_left,minimum_left,time_left,distance_righ
t,minimum_right,time_right;
void setup() {
  Serial.begin (9600);
```

```
pinMode(trigpin1, OUTPUT);
pinMode(echopin1, INPUT);
pinMode(trigpin2, OUTPUT);
pinMode(echopin2, INPUT);
pinMode(trigpin3, OUTPUT);
pinMode(echopin3, INPUT);
mysteerservo.attach(34); // attaches the servo on pin 34 to the servo object
  myshiftservo.attach(35); // attaches the servo on pin 35 to the servo object
 mysteerservo.writeMicroseconds(1600);
 myshiftservo.write(shift); /////// chech angle
  pinMode(M1CWPin, OUTPUT);
  pinMode(M1CCWPin, OUTPUT);
  pinMode(M1PWMPin, OUTPUT);
  digitalWrite(M1CWPin, LOW);
  digitalWrite(M1CCWPin, LOW);
  delay(5000);
  }
void loop() {
digitalWrite(M1CWPin, HIGH);
digitalWrite(M1CCWPin, LOW);
analogWrite(M1PWMPin, 255);
mysteerservo.writeMicroseconds(1600);
  if(millis()>12000)
 {
  digitalWrite(M1CWPin, LOW);
  digitalWrite(M1CCWPin, LOW);
  analogWrite(M1PWMPin, 0);
  }
```

```
if(millis()<9000)
{
  mysteerservo.writeMicroseconds(1600);
  }
if(millis()>9000)
 {
  mysteerservo.writeMicroseconds(2000);
// for (pos = 180; pos >= 100; pos -= 90) { // goes from 180 degrees to 0 degrees
// mysteerservo.write(pos); // tell servo to go to position in variable 'pos'
// delay(1500); // waits 15ms for the servo to reach the position
// }
}
if(millis()>10000)
 {
  mysteerservo.writeMicroseconds(1400);
// for (pos = 100; pos <= 180; pos += 90) { // goes from 180 degrees to 0 degrees
// mysteerservo.write(pos); // tell servo to go to position in variable 'pos'
// delay(1500); // waits 15ms for the servo to reach the position
// }
  }
//if(millis()>11000)
// {
// mysteerservo.writeMicroseconds(1400);
// }
}
```

B.2. Arduino Uno Sketch for recording the sensor reading on SD card

```
#include <SD.h>
#include <SPI.h>
#include <Wire.h>
#include <Adafruit_Sensor.h>
#include <Adafruit_BNO055.h>
#include <utility/imumaths.h>
#define BNO055_SAMPLERATE_DELAY_MS (10)
#define CSpin 3
String dataString = ""; // holds the data to be written to the SD card
File sensorData;
String dataString1 = ""; // holds the data to be written to the SD card
File sensorData1;
float longacc;
float longaccold = 0;
float longaccnew;
float latacc;
float lataccold = 0;
float lataccnew;
float vertacc;
float vertaccold = 0;
float vertaccnew;
float pitch;
float pitchold = 0;
float pitchnew;
float roll;
float rollold = 0;
```

```
float rollnew;
float Yaw;
float yawold = 0;
float yawnew;
float
float heading;
float headingold = 0;
float headingnew;
Adafruit_BNO055 myIMU = Adafruit_BNO055();
void setup() {
  Serial.begin(115200);
Serial.print("Initialising SD card...");
pinMode(CSpin, OUTPUT);
// see if the card is present and can be initialised:
if (!SD.begin(CSpin)) {
Serial.println("Card failed, or not present");
// don't do anything more:
return;
}
Serial.println("card initialised.");
myIMU.begin();
delay(1000);
int8_t temp = myIMU.getTemp();
myIMU.setExtCrystalUse(true);
}
void loop() {
 imu::Vector<3>                                    acc                                    =
myIMU.getVector(Adafruit_BNO055::VECTOR_ACCELEROMETER);
imu::Vector<3> gyro = myIMU.getVector(Adafruit_BNO055::VECTOR_GYROSCOPE);
```

```
imu::Vector<3> mag = myIMU.getVector(Adafruit_BNO055::VECTOR_MAGNETOMETER);
longacc = (acc.y()/9.807);
longaccnew = (.9*longaccold+.1*longacc);
latacc = (acc.x()/9.807);
lataccnew = (.9*lataccold+0.1*latacc);
vertacc = (acc.z()/9.807);
vertaccnew = (.9*vertaccold+.1*vertacc);
pitch = (gyro.x());
pitchnew = (.9*pitchold+.1*pitch);
roll = (gyro.y());
rollnew = (.9*rollold+.1*roll);
Yaw = (gyro.z());
yawnew = (.9*yawold+.1*Yaw);
heading = atan2(mag.x(), mag.y()) * (180 /PI);
headingnew=(.9*headingold+.1*heading);
//Serial.print(millis());
//Serial.print(",");
//Serial.print(acc.x()/9.807);
//Serial.print(",");
Serial.println(longaccnew);
Serial.print(",");
//Serial.println((-longaccnew)-0.12);
//Serial.print(acc.z()/9.807);
//Serial.print(",");
//Serial.print(gyro.x());
//Serial.print(",");
//Serial.print(gyro.y());
```

```
//Serial.print(",");
//Serial.print(gyro.z());
//Serial.print(",");
//Serial.println(heading);
  float A = millis();
 float B = (longaccnew);
 float C = lataccnew;
 float D = vertaccnew;
 float E = rollnew;
 float F = pitchnew;
 float G = yawnew;
 float H = headingnew;
 float I = (longacc);
 float j = latacc;
 float k = vertacc;
 float l = roll;
 float m = pitch;
 float n = Yaw;
 float o = heading;
  dataString = String(A) + "," + String(B) + "," + String(C) + "," + String(D) + "," + String(E)
+ "," + String(F) + "," + String(G)+ "," + String(H);
 dataString1 = String(A) + "," + String(I) + "," + String(j) + "," + String(k) + "," + String(l) +
"," + String(m) + "," + String(n)+ "," + String(o);
 saveData(); // save to SD card
 saveData1(); // save to SD card
longaccold=longaccnew;
lataccold=lataccnew;
vertaccold=vertaccnew;
pitchold=pitchnew;
```

```
rollold=rollnew;
yawold=yawnew;
headingold=headingnew;
delay(BNO055_SAMPLERATE_DELAY_MS);
}
void saveData()
{
if(SD.exists("data.csv")){ // check the card is still there
// now append new data file
sensorData = SD.open("data.csv", FILE_WRITE);
if (sensorData){
sensorData.println(dataString);
sensorData.close(); // close the file
}
}
else{
Serial.println("Error writing to file!");
}
}
void saveData1()
{
if(SD.exists("data1.csv")){ // check the card is still there
// now append new data file
sensorData1 = SD.open("data1.csv", FILE_WRITE);
if (sensorData1){
sensorData1.println(dataString1);
sensorData1.close(); // close the file
}
```

```
}
else{
Serial.println("Error writing to file!");
}
}
```

Appendix C: Steps for Co-simulation

This appendix shows steps to export the ADAMS/View model and connect with Simulink

Step 1: Select the system element tap as shown in Figure C- 1.

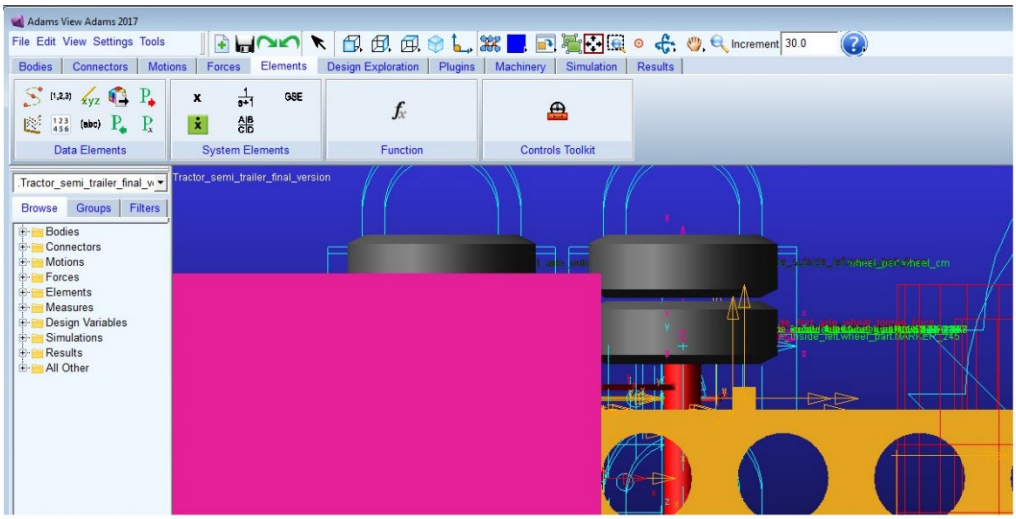

Figure C- 1: ADAMS/View model

Step 2: define the system element for the user-defined function as shown in Figure C- 2.

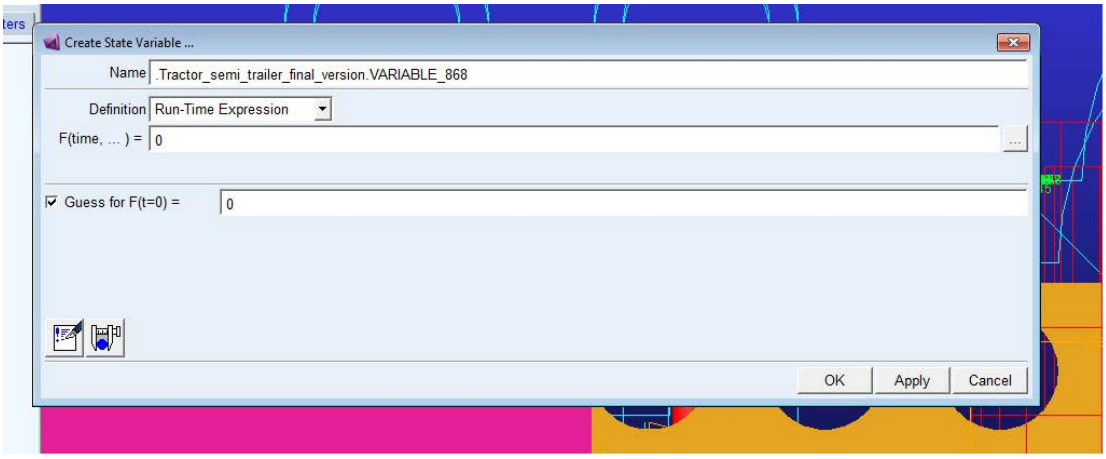

Figure C- 2: ADAMS/View state variable window for run-time expression

Step 3: define the system element for the user-written subroutine, as shown in Figure C- 3.

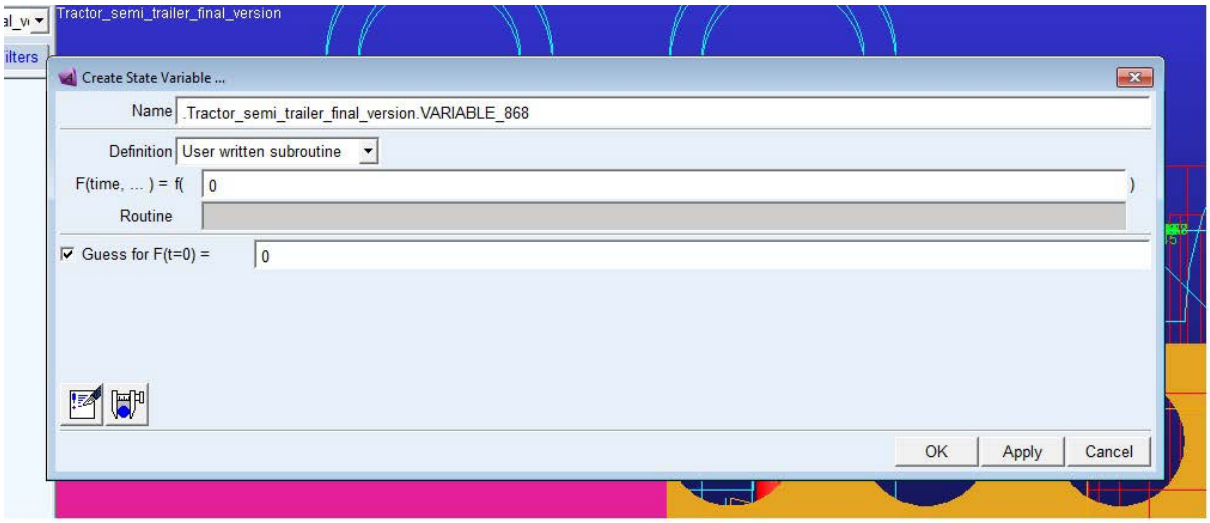

Figure C- 3: ADAMS/View state variable window for user-written subroutine

Step 4: Select the control tap from the plugin, as shown in Figure C- 4.

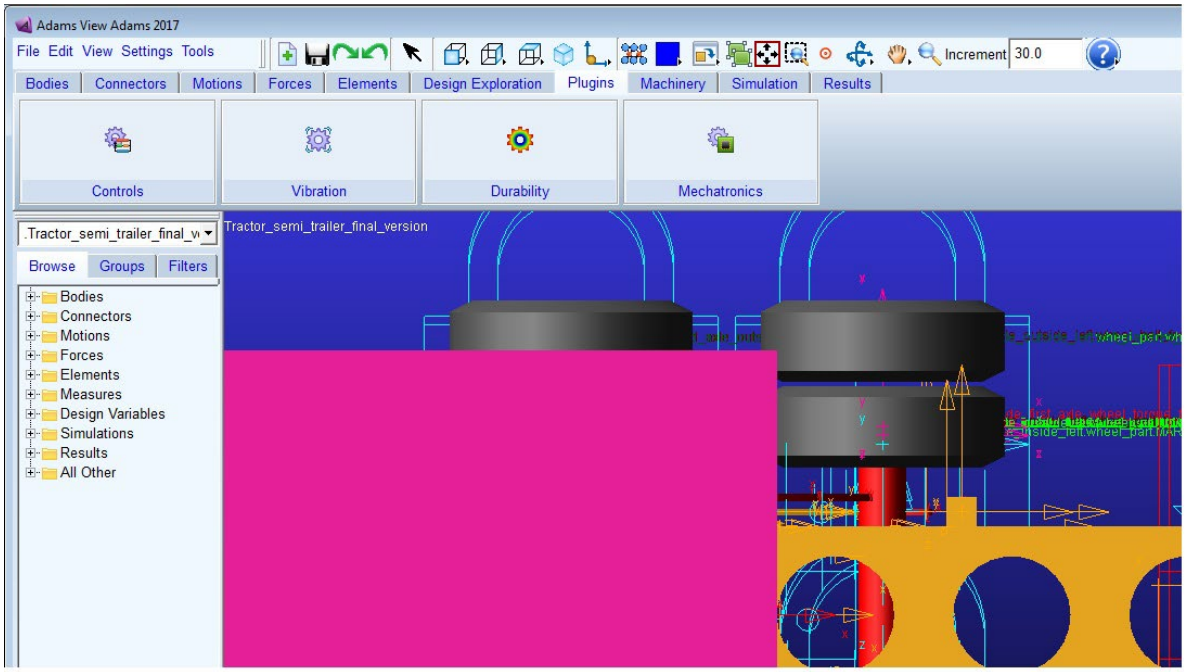

Figure C- 4: ADAMS/View control tab

Step 5: select the plant export from the control tab, as shown in Figure C- 5.

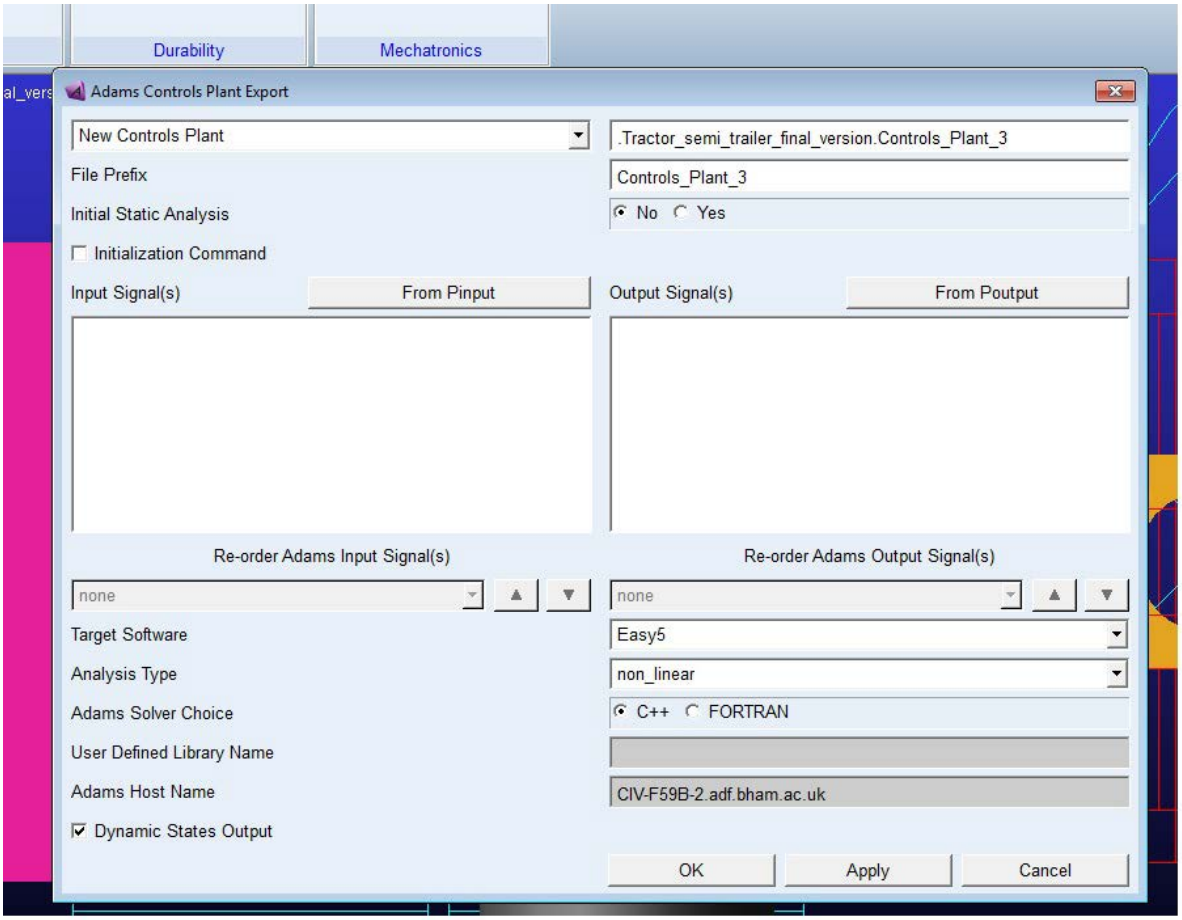

Figure C- 5: ADAMS/View control plant for Input and output parameters

Step 6: right-click in the Input signal area to enter the Input system element and the same step for the output signals, as shown in Figure C- 6.

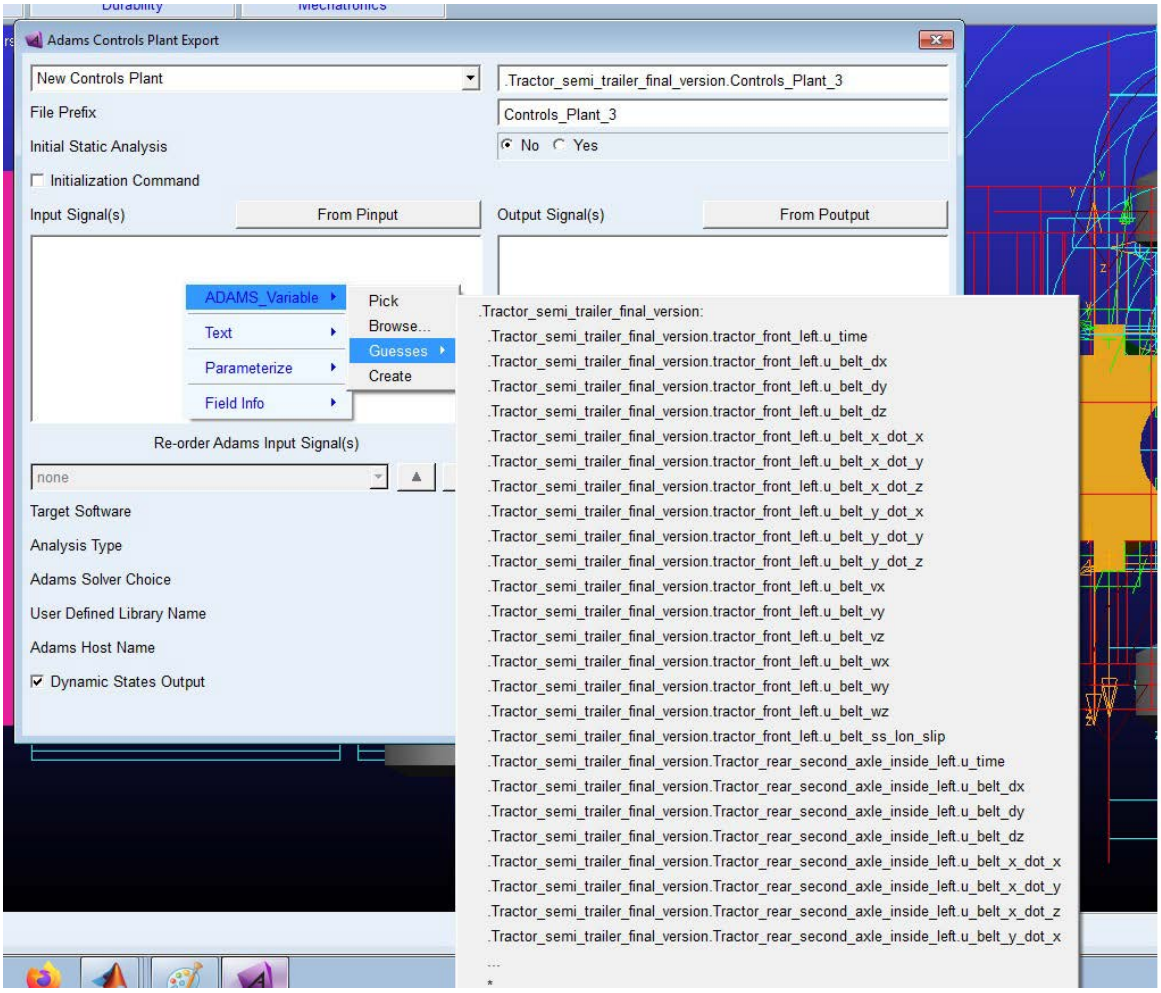

Figure C- 6: ADAMS/View importing inputs signals

Step 7: import the m file into the MATLAB editor, as shown in Figure C- 7.

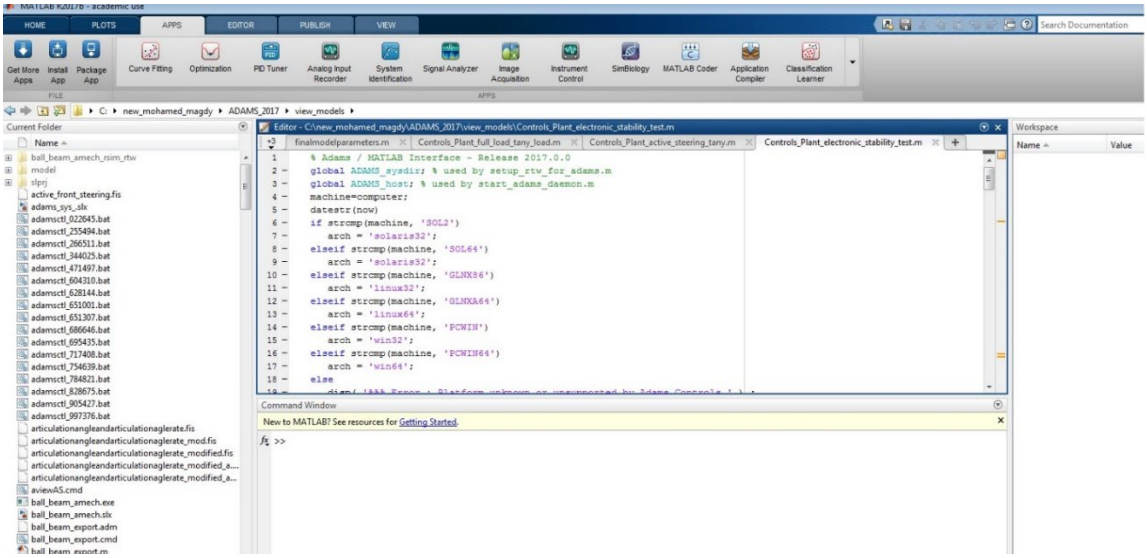

Figure C- 7: ADAMS/View m file in MATLAB

Step 8: run the m file and identify the Input and output signals in the command window shown in Figure C- 8.

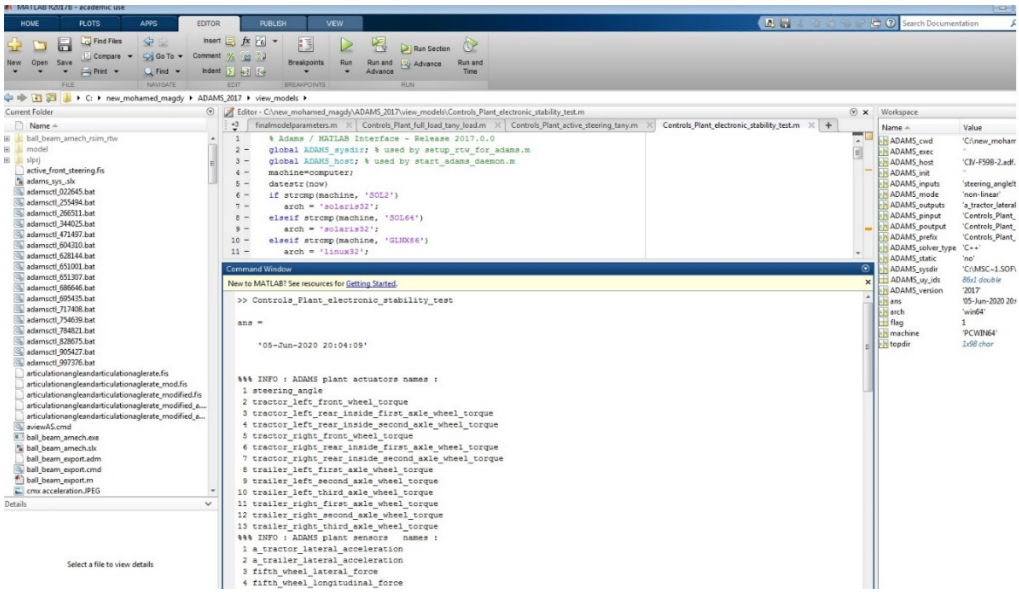

Figure C- 8: defining Input/output parameters for ADAMS/View plant

Step 9: type the syntax “adams_sys” in the command window to open the ADAMS block, as shown in Figure C- 9.

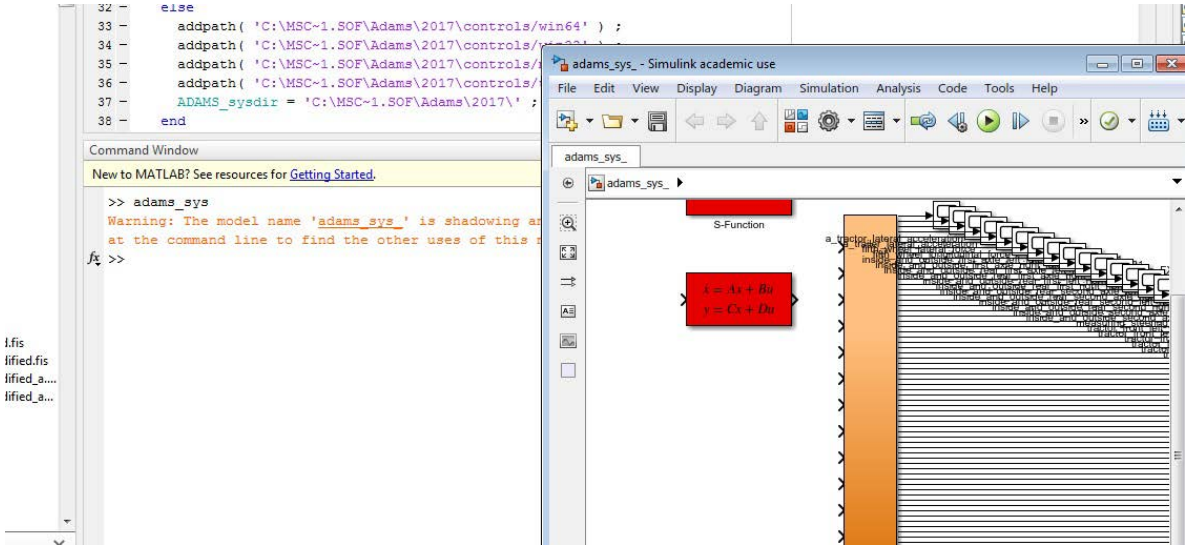

Figure C- 9: opening the ADAMS plant Simulink block

Step 10: copy the ADAMS block and paste it into the Simulink model and connect signals shown in Figure C- 10.

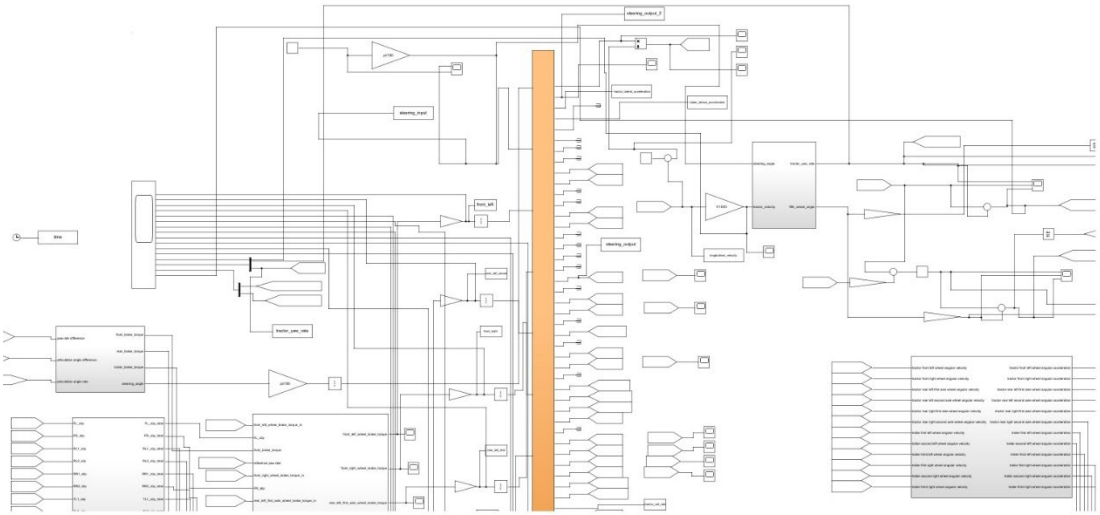

Figure C- 10: Co-simulation control model